MR No. L5I12b

NATIONAL ADVISORY COMMITTEE FOR AERONAUTICS

WARTIME REPORT

ORIGINALLY ISSUED
October 1945 as
Memorandum Report L5I12b

AN INVESTIGATION OF THE RANGER V-770-8 ENGINE INSTALLATION FOR THE EDO XOSE-1 AIRPLANE

II - AERODYNAMICS

By Mark R. Nichols and John S. Dennard

Langley Memorial Aeronautical Laboratory
Langley Field, Va.

NACA

WASHINGTON

MR No. L5I12b

NATIONAL ADVISORY COMMITTEE FOR AERONAUTICS

MEMORANDUM REPORT

for the

Bureau of Aeronautics, Navy Department

AN INVESTIGATION OF THE RANGER V-770-8 ENGINE INSTALLATION FOR THE EDO XOSE-1 AIRPLANE

II - AERODYNAMICS

By Mark R. Nichols and John S. Dennard

SUMMARY

An investigation has been conducted in the Langley propeller-research tunnel to determine the cowling and cooling requirements of the Ranger V-770-8 engine installation for the Edo XOSE-1 airplane. The present report summarizes the aerodynamic data obtained in the testing.

Extensive model changes including alternate baffles, exhaust stacks, cooling-air exits, and oil-cooler ducts were tested in attempts to increase the cooling capacity of the cowling and to reduce the drag. Final cowl configurations possessed sufficient engine and oil-cooler pressure drops in the critical normal-power climb condition to cool the cylinders and the oil below the specified temperature limits with any of the three baffle configurations tested. Drag clean-up tests indicated minor changes which will result at sea level in approximate increases of 5 miles per hour in high speed, 34 feet per minute in rate of climb, and 7 percent in maximum range. The indicated critical Mach number of the cowling was found to be 0.70 as determined by the pressures on the lower lip of the inlet.

Pressure data are presented for wide ranges of exit area, angle of attack, and thrust disk-loading coefficient. Sample applications of the data to the estimation of the required exit area are shown.

INTRODUCTION

At the request of the Bureau of Aeronautics, Navy Department, an investigation of the aerodynamic and cooling characteristics of the Ranger V-770-8 engine installation for the Edo XOSE-1 airplane has been conducted in the Langley propeller-research tunnel. The objects of the investigation were (1) to determine the cooling characteristics and requirements of the engine, (2) to determine the aerodynamic characteristics of the cowling, and (3) to develop a cowling with adequate cooling-pressure drop and low drag. The present report, part II, summarizes air flow, pressure, and force data obtained in tests of a number of model configurations; part I, reference 1, presents corresponding temperature data and engine cooling correlations.

The Edo XOSE-1 airplane is a single-engine scout-observation seaplane with a normal gross weight of 5200 pounds, a wing area of 238 square feet, and a wing span of 38 feet. As estimated by the manufacturer, the high speed of this airplane at sea level with military power is 192 miles per hour and the rate of climb at this altitude and power is 1460 feet per minute at a climbing speed of 108 miles per hour. Because of these low flight speeds, special emphasis has been directed toward the reduction of the pressure drops required to cool and increasing the pressure drops available.

The wind-tunnel investigation included propeller-removed and propeller-operating measurements to determine drag and cooling-air-flow characteristics. Changes to the original configuration included alternate baffles, exhaust stacks, cooling-air exits, and modifications to the oil-cooler ducts. For the more promising configurations, extensive pressure surveys were made in the internal flow and on the external cowl surface over wide ranges of cooling-exit area, angle of attack, and thrust disk-loading coefficient.

The flow-resistance characteristics of the engine, the oil cooler, the cowl leakage area, the generator, and the generator blast tube were determined from ground-stand calibration tests.

SYMBOLS

a	speed of sound, feet per second
A	cross-sectional area of duct, square feet
C_D	drag coefficient, $\frac{\text{Drag}}{q_o S}$
ΔC_D	increment of drag coefficient
C_{D_i}	coefficient of internal drag, $\frac{\text{Internal drag}}{q_o S}$
D	propeller diameter, 9 feet
g	acceleration due to gravity, 32.2 feet per second per second
H	total pressure, pounds per square foot or inches of water
ΔH	increment of total pressure, inches of water
M_{cr}	critical Mach number, V_{cr}/a
n	rotational speed, revolutions per second
p	static pressure, pounds per square foot or inches of water
ΔP_c	cooling-air pressure drop across oil cooler $(\overline{H_f} - \overline{p_r})$, pounds per square foot or inches of water
ΔP_e	cooling-air pressure drop across individual engine cylinder $(\overline{H_f} - \overline{p_r})$, pounds per square foot or inches of water
q	dynamic pressure, pounds per square foot
Q	volume rate of flow, cubic feet per minute
S	wing area, 238 square feet
T	effective thrust, pounds

T_c thrust disk-loading coefficient, $\frac{T}{\rho_o V_o^2 D^2}$

V velocity, feet per second

V_{cr} free-stream velocity at which local surface velocity reaches speed of sound, feet per second

W weight rate of flow, pounds per hour or per minute

α angle of attack of thrust axis, degrees

β propeller blade angle at 0.75 radius, degrees

δ cooling-air flap angle from flush position, degrees

θ design angle of propeller blade element, degrees

ρ mass density of air, slugs per cubic foot

σ relative density of air, $\rho/0.002378$

Subscripts:

b at front of cylinder barrels

c oil cooler

e engine

f at front face of oil cooler or between fins of cylinder heads

i at cowl inlet

ic at inlet of oil-cooler duct

o in free stream

r at rear of oil cooler or engine

x at cooling-air exit

Double subscripts indicate that both apply. A bar above a symbol is used to denote an arithmetic average.

MODEL, POWER-PLANT INSTALLATION, AND INSTRUMENTATION

The model consisted of a complete power-plant installation mounted on a mock-up of the forward part of the airplane. A 15.21-foot stub wing was fitted to the mock-up; the tail surfaces and floats were not installed. The general arrangement and principal dimensions of the model are presented in figure 1; general views of the model are shown in figure 2. The various model configurations are identified and assigned symbols in table I. (As received, the model was in the configuration designated Ia.) Significant duct areas are listed in table II.

The Ranger V-770-8 engine (fig. 3) is a 12-cylinder inverted-V-type air-cooled engine with a propeller gear ratio of 3:2. It has a normal power rating of 500 horsepower at 3150 rpm from sea level to 8000 feet and a military rating of 550 horsepower at 3300 rpm from sea level to 4500 feet. The propeller used for these tests, a two-blade, 9-foot-diameter, constant-speed, Hamilton Standard propeller (blade number 6101A-12), is described in figure 4.

Sketches and photographs of the baffles tested on the engine are presented as figures 5 and 6, respectively. The conventional baffles were installed on the outboard side of the barrels. The turbulent-flow baffles were installed on both sides of the heads and barrels and had several turbulence strips extending from the baffle shell to the cylinder fins. The NACA designed baffles, installed on the barrels only, fitted tightly against the barrel fins over an arc of about 300° and had inlets alined with the flow and diffuser-tail exits designed to reduce pressure losses at the baffle exit. A more complete discription of the baffles is contained in reference 1.

Exhaust-stack details are shown in figures 7 through 10. The stacks were manifolded in groups of three except for the mocked-up individual stacks of configuration IVc. All stacks except those used in configurations IVb, IVd, and IVe were equipped with shrouds intended to reduce heating of the engine and oil-cooler air. Shroud cooling was effected by cooling air which entered at the top of the shrouds and exhausted at the

surface of the cowl. (See fig. 9.) External configuration variables for the manifolded stacks included "vertical" and "horizontal" fishtail-type flame dampers, short stacks, and flush stacks. The mock-up individual stacks were equipped with horizontal fishtail flame dampers. The flame dampers were not used extensively in the power-on testing because of recurring structural failure (fig. 10).

Views of the inlet duct configuration and coordinates of the inlet lips are presented in figure 3 and table III, respectively. All cooling and charge air was taken into the triangular-shaped main inlet. Oil-cooling and carburetor air was taken from the back of the inlet section by ducts below the left cam cover and between the exhaust stacks, respectively. The engine cooling air was exhausted from the cylinder exits into the exit and accessory compartment which extended from the spinner bulkhead to the firewall and was open to the rear of both banks of cylinders.

A specially built United Aircraft Products elliptical oil cooler, designated U-840713, was installed in the model. (See fig. 11.) It had 0.21-inch-diameter tubes, a face area of 74 square inches, and a core depth of 9 inches. Configurations of the oil-cooler duct are shown in figure 12. Installation variables included exit ducts, exit flaps, and guide vanes. (See fig. 13.)

A photograph of the carburetor duct is presented as figure 14; installation details are shown in figure 8(b). The hot-air door in the bottom of the duct closed off the passage to the pressure box when opened and caused all the carburetor air to be taken from the accessory compartment.

Cooling-air exit details are shown in figures 15 through 17. A flow-directing vane was used in the oil-cooler-exit duct of configuration Ic; two vanes were used in each of the engine-cooling-air exits of all configurations except IVe; an NACA designed fairing strip (fig. 17) was installed in the accessory compartment exit of configurations Ia and Ib. Cooling-air shutter and flap dimensions were as follows:

Cooling-air duct	Type of exit control	Height (in.)	Length (in.)
Engine	Shutter	17.56	9.40
Engine	Flap	17.75	11.94
Oil cooler	Shutter	12.87	4.25
Oil cooler	Flap	13.31	7.38

Variations of the cooling-air exit area with shutter or flap opening are shown in figure 18.

A $1\frac{1}{2}$-inch-diameter blast tube (fig. 8(b)) was used to supply cooling air to the generator located at the top of the engine. Configurations were tested in which the inlet was located at the top of the cowl inlet (fig. 19), at the rear wall of the pressure box beneath the right cam cover (fig. 8(b)), at the rear wall of the pressure box above the carburetor duct, and in the oil-cooler inlet duct just upstream of the oil cooler (fig. 13). From 3 to 5 feet of tubing and a number of bends were required in each of the above configurations.

The engine panel incorporated remote indicating instruments and an electric actuator system for operating the engine controls and flaps. Forces were read on the six-component wind-tunnel balance system. Pressures were measured by the total and static tubes itemized in table IV. Methods and instrumentation for obtaining temperatures and other engine operating data are discussed in reference 1.

GROUND-STAND CALIBRATIONS

Ground-stand flow-resistance calibrations of several components of the installation were made as a preliminary to the analysis of the wind-tunnel test results. Experimental setups are shown in figures 20 and 21. Special instrumentation consisted of the calibrated venturi in the former setup and the calibrated contraction cone and grids of total pressure tubes at both ends of the blast tube of the latter setup.

Engine-baffle combinations and oil cooler.- Propeller-removed cooling-air-flow calibrations of the three engine-baffle combinations are presented in figure 22; corresponding comparisons of the average pressure drops across the left and right banks are shown in figure 23. Effective orifice areas, $\frac{W}{g\sqrt{2\rho\Delta P_e}}$ (expressed in foot-pound-second units), were about 0.75, 0.68, and 0.73 square foot for the conventional, turbulent-flow, and diffuser-baffle installations, respectively. The latter value is for an installation with diffuser baffles on all cylinders.

A propeller-removed cooling-air-flow calibration of the oil cooler is presented as figure 24. The effective orifice area and the pressure-drop coefficient $\left(\frac{\Delta P}{q_f}\right)$ for the cooler were approximately 0.26 square foot and 4.0, respectively.

It is emphasized that the above calibrations are for the cold condition only; the pressure drop must be corrected for cooling-air-density changes due to heat dissipation and altitude before being applied to power-on operation. The necessary corrections are discussed extensively in references 2 through 4. Reference 4 indicates that a very close approximation of the engine-cooling-air flow in altitude operation may be obtained from a cold calibration by basing σ on the density of the cooling air just downstream of the engine.

Leakage.- The combined leakage through the exhaust-stack shrouds and the pressure-box seams for the calibration condition is presented as a function of the engine front pressure and the engine pressure drop in figure 25. At a baffle pressure drop of 8 inches of water, the leakage flow is about 6000 pounds per hour or approximately 15 percent of the cooling-air flow through the engine. Attention is called to the fact that these data are of a strictly qualitative nature as the external surface pressures, the oil-cooler flow, and the charge-air flow for the flight conditions were not duplicated; the actual leakage flow would probably be greater for the high-speed condition and less for the climb and cruising conditions.

The leakage through the cowl seams downstream of the engine (with respect to the cooling-air flow) and from the gap between the cowling and the firewall (figs. 16(b) and 17) for the flush-flap calibration condition is shown in figure 26 as a function of the engine rear pressure. Although these data are also of a qualitative nature, they indicate that the leakage was a large percentage of the exit flow for the high-speed flight condition. The clearance gap between the cowl and the spinner was found to be the source of a large amount of additional leakage.

Generator and blast tube.- An air-flow calibration of the generator is presented in figure 27. The pressure drop across the generator is shown to be a more important variable than the rotational speed in determining the cooling-air flow; the built-in fan appears to be relatively ineffective at large flow quantities. At the rated engine speed of 3150 rpm a pressure drop of approximately 3.3 inches of water was sufficient to supply the 75 cubic feet of cooling air per minute specified by the engine manufacturer. Navy specifications (reference 5), however, are not based on the pressure drop but stipulate that the ram at the generator flange shall be at least 6 inches of water in flight at the best climb speed at sea level. As the accessory compartment pressure is below atmospheric pressure in the climb condition this requirement is conservative.

A pressure-drop calibration of the generator blast tube is presented as figure 28. Large increases in the pressure losses occurred when either the tube length or the bend angle were increased. At the air flow required for generator cooling (75 cubic feet per minute) the loss through a typical installation with a 56.5-inch blast tube having a total bend angle of 270° would be between 7 and 8 inches of water. This large loss could most easily be reduced in the present installation by using a larger diameter blast tube.

TUNNEL TESTS

The initial portion of the tunnel testing consisted of propeller-removed pressure and drag studies at a tunnel speed of about 100 miles per hour directed toward the development of a cowling with adequate cooling pressure drop and low drag. Propeller-installed tests of the

best cowl arrangement were then conducted to determine the cooling characteristics of the several engine-baffle configurations and those of the oil-cooler (reference 1), and the available cooling pressure over the range of flight conditions. Several final configurations were checked at the end of the test program.

The estimated sea-level flight conditions used as a basis for the propeller-installed tests were as follows:

Flight condition	Horse-power	Engine (rpm)	β (deg)	T_c	α (deg)	V_o (ft/sec)
High speed:						
Normal power	500	3150	22	0.057	-1.3	274
Military power	550	3300	22	.062	-1.6	282
Maximum-endurance-cruise at 30.6 percent normal power	153	1800	24.5	.15	11.2	132
Climb:						
Normal power	500	3150	17.5	.26	7.5	158
Military power	550	3300	16.5	.28	7.5	159

The climb and maximum-endurance-cruise conditions were approximately duplicated in the tunnel at the proper airspeed; military power could not be quite attained in most cases because of losses in manifold pressure occasioned by the charge-air measuring venturi installed in the carburetor duct (reference 1). The high-speed condition was simulated at a tunnel speed of 100 miles per hour by duplicating the flight value of V_o/nD with the flight blade angle of 22°.

TUNNEL TEST RESULTS

The results of the tunnel tests are presented in sections which deal with cowl development, internal flow, required exit area, drag, and surface pressures. The types of data presented for each model configuration along with the configuration identifications are listed in table I.

Modifications to Installation

Preliminary propeller-removed pressure surveys indicated that the available pressure drops across the engine, oil cooler, and generator of the original configuration (Ia) would be either marginal or insufficient for cooling in the normal-power climb condition. Testing of this configuration was discontinued immediately and a series of modifications to the cowling were investigated.

Engine and oil-cooler ducts.- A summary of comparative data pertinent to the development of the engine and oil-cooler ducts is presented in table V. The available engine and oil-cooler pressure drops at $\alpha = 7.5$ and with propeller removed were increased $0.21q_o$ and $0.54q_o$, respectively, by substituting the flapped exits for the shutter exits. (Compare results for configurations Ie and IIa.) For the normal-power climb condition, removing the exhaust-stack shrouds (configurations IVa and IVb) increased the engine and oil-cooler pressure drops by $0.08q_o$ and $0.09q_o$, by reducing leakage and removing obstructions from the pressure box, but also increased the cooling-air and carburetor-air temperatures by 8° F. For the same test condition, removing the vanes from the engine-cooling-air exits and sealing the accessory-compartment exit gap (configurations IVb and IVe) decreased the engine pressure drop by only $0.04q_o$ but increased the accessory-compartment temperature by 15° F. The flapped exits, the exhaust-stack shrouds, and the unsealed accessory-compartment exit gap were components of the series II and series III configurations tested most extensively and for which cooling adequacy was established. (See reference 1.)

Generator blast tube.- Generator cooling-pressure data for four blast-tube inlet locations are summarized in table VI. The highest pressure recovery for the climb-at-normal-power condition, $0.58q_o = 3.3$ inches of water, was obtained with the blast-tube inlet located at the rear wall of the pressure box above the carburetor duct. The pressure drop for this configuration, 4 inches of water, is shown by figure 28 to be more than sufficient to furnish the 75 cubic feet of cooling air per minute specified by the engine manufacturer.

Internal Flow

Extensive pressure surveys were conducted in the series II and series III configurations, considered to be most promising, to determine the available cooling pressures and the effects of the several flight and model variables on the internal flow.

Pressure distributions.- Pressures measured throughout basic configuration IIa are presented in figure 29 for the high-speed and climb attitudes with propeller removed. These data indicate excellent flow into the cowling with pressure recoveries in the inlet and at the end of the diffuser (beneath cylinders 6R and 6L) nearly equal to $1.0q_o$. Recoveries at the front of the cylinder barrels varied between $0.91q_o$ and $0.99q_o$; but corresponding pressures at the front of the cylinder heads were much lower due in part to flow obstructions presented by the ignition harness (fig. 3). Pressures measured between the fins of the cylinder heads (used as the front pressures in the determination of the cylinder pressure drops) were approximately equal to those measured in front of the heads. Recoveries at the face of the oil cooler were about $0.95q_o$ and $0.76q_o$ for the high-speed and climb attitudes, respectively.

Typical propeller-operating pressures (fig. 30) show substantial increases in ram over those obtained in the propeller-removed tests. At the inlet, total pressures reached maximum values of $1.30q_o$ and $2.33q_o$ in the high-speed and climb conditions, respectively. The occurrence of these peak pressures in the lower and right parts of the inlet are indicative of increased loading of the propeller-blade sections in front of these regions due, in the former case, to the increased propeller radius and more effective airfoil section and, in the latter case, to the pitched attitude of the propeller. Pressure recoveries at the left-bank cylinders and in the left side of the pressure box were higher than corresponding pressures in the right half of the cowling because of slipstream rotation. Pressure distributions at the rear of the engine, at the oil-cooler face, and at the carburetor deck were nearly uniform.

The ram in the carburetor duct with both normal and alternate inlets is shown in figure 31. These data,

taken in the maximum-endurance condition, indicate that the flow at the carburetor deck was uniform with either inlet configuration; the average ram with the alternate inlet, however, was approximately $1.2q_o$ below that with the normal inlet.

Cylinder pressure and pressure-drop distributions for model configurations with the three types of baffles are shown in figures 32 and 33 for the propeller-removed and propeller-operating conditions, respectively. The front pressures varied by as much as $0.5q_o$ between individual cylinders; but, as previously noted, the rear pressures were nearly uniform. The lowest front pressures and consequently the smallest pressure drops were consistently measured at the forward cylinders of each bank. Substituting the NACA designed diffuser baffles for the turbulent-flow baffles on the left-bank cylinders increased the pressure drop across these cylinders and caused substantial reductions in outboard barrel temperatures (reference 1), but at the same time caused small reductions in the pressure drops across the right cylinders.

Average duct pressures.- Pressure data obtained in the flight-simulation tests are summarized in table VII. The ram pressure in the inlet for the II and III series configurations averaged $1.30q_o$ in the normal-power high-speed condition and $2.14q_o$ in the normal-power climb condition. Rams at the carburetor deck for these flight conditions and configurations ($1.35q_o$ and $2.01q_o$, respectively) correspond to airplane critical altitudes of 9900 feet and 9000 feet based on the engine critical altitude of 8000 feet. It should be noted that the engine charge-air flow was not simulated exactly for the high-speed condition as this air flow is not proportional to T_3. For the normal-power climb condition (configurations IIc and IIIa), static pressures in the engine and oil-cooler cooling-air exits were about $-0.43q_o$ and $-0.28q_o$; corresponding engine and oil-cooler pressure drops averaged $1.54q_o$ and $1.86q_o$ and were sufficient to cool the engine and the oil below the specified temperature limits. Pressure drops for the series IV configurations with the mixed baffles were of the same order and were likewise adequate for cooling in this critical flight condition. It is noted that the measured thrust coefficients for the climb condition tests were consistently less at military power than at normal power possibly because of efficiency losses incurred by the high Mach

number and high loading of the propeller tips or by the decrease in V_o/nD; increasing the gear ratio or modifying the propeller might result in overall increases in airplane performance at military power.

The average pressures in the engine and oil-cooler ducts are presented in figures 34 and 35 as functions of V_i/V_o and α for the propeller-removed tests and as a function of T_c for the propeller-installed tests. Variations of the exit total pressure are omitted from the figures as these pressures were very nearly equal to and conflicted with the presentation of the rear pressures. Some of the rear pressures, in turn, have been omitted from the central portions of the figures for the sake of clarity. Propeller-removed data are used as the end points of the curves in which T_c is the independent variable because the model with propeller installed was not tested at this condition.

Inlet total pressures for the propeller-removed condition were nearly unity over the complete V_i/V_o and α ranges tested. Propeller operation increased these pressures to a much greater extent than would be expected from consideration of the simple momentum theory (from which the inlet pressure rise would be $\frac{\delta}{\pi}T_c$). Analysis of the propeller-operating conditions indicates that this result was attributable to the increased loading of the propeller cuff sections caused by reduction of the effective V_o/nD in the low velocity field in front of the inlet.

Pressure losses between the inlet and the front of either the engine or oil-cooler (figs. 34 and 35) increased appreciably between the limiting propeller-removed test inlet velocity ratios of 0.4 and 0.7 and were essentially independent of angle of attack, propeller removed. Attention is called to the fact that the slopes of the curves of front, rear, and exit pressures versus T_c are influenced by the changes in V_i/V_o which accompany increases in T_c as these curves are presented for constant outlet configurations.

Static pressures at the rear of the engine or oil cooler and in the cowl exits generally decreased with increases in α, propeller removed. With propeller installed, the exit static pressure increased with T_c with undeflected exit flaps but decreased with T_c with fully extended flaps.

The pressure losses ahead of the engine and oil cooler are shown in figure 36 as a function of inlet-velocity ratio. The continuity of the curves for the propeller-removed and propeller-installed conditions indicates that losses caused by misalinement of the inlet with the incoming flow were small for the propeller-installed condition. The greater losses with the turbulent-flow baffles than with the conventional baffles were probably caused by the obstructions to the flow in the vee presented by the inboard parts of the turbulent-flow baffles. The magnitude of the losses at the higher inlet-velocity ratios emphasize the need for large inlets for installations of this engine in low-speed aircraft. Losses ahead of the oil cooler could be reduced by using larger ducts.

Ducting efficiency.- The ducting efficiency of the cowling expressed as the relationship of the pressure drop across the heat exchanger $(\overline{\Delta P})$ to the pressure drop across the cowling $(\overline{H_i} - \overline{H_x})$ is shown in figure 37 for ranges of engine and oil-cooler pressure drop. Configurations Ie, IIa, and IIc with the conventional baffles had maximum engine/duct pressure-drop ratios of about 0.85 compared to 0.78 for configuration IIIa with the turbulent-flow baffles. The maximum oil-cooler-duct pressure-drop ratio was approximately 0.95.

Outlet effectiveness.- The static pressure depressions in the cowl exits caused by opening the flaps and shutters are shown in figure 38. Opening the engine and oil-cooler flaps reduced the exit static pressures by approximately $0.57q_o$ and $0.65q_o$, respectively. The advantage of using a flapped exit is shown by comparisons of the flapped-exit and shutter-exit curves; at the maximum shutter-exit areas the static pressures in the flapped engine and oil-cooler exits with the same areas were $0.26q_o$ and $0.21q_o$ less than the corresponding pressures in the shutter exits. The increased effectiveness of the flapped exits is further indicated (fig. 39) by the larger inlet-velocity ratio for any given outlet area. The rapid increase in inlet-velocity ratio with T_c is noted in this figure.

Charts for Predicting Exit Areas

To facilitate application of the pressure data, engine and oil-cooler pressure drops are presented in figures 40 and 41 as functions of A_x, α, and T_c.

All available propeller-installed data were plotted in the right portions of the figures regardless of angle of attack as this variation was obviously of second-order importance; the lines shown were faired through the $\alpha = 7.5^\circ$ points and would be shifted up or down by changes in α, but would not be changed appreciably in slope. The exit areas and flap angles required for engine and oil cooling in the steady flight conditions of this airplane may be estimated from these figures by the following method as indicated on figure 40:

1. Locate the value of $\frac{\overline{\Delta P}}{q_o}$ required for cooling at the T_c for the flight condition in the right-hand portion of the figure and determine $\frac{\overline{\Delta P}}{q_o}$ at $T_c = 0$ by constructing a straight line through this point parallel to the two test lines or through this point and the intersections of these lines.

2. Locate the above-obtained value ($\frac{\overline{\Delta P}}{q_o}$ for $T_c = 0$) at the flight angle of attack and determine $\frac{\overline{\Delta P}}{q_o}$ for $\alpha = 7.5^\circ$ by constructing a line through this point parallel to adjacent test lines.

3. From the value of $\frac{\overline{\Delta P}}{q_o}$ for $\alpha = 7.5^\circ$ read the flap angle and exit area from the curves in the left portion of the figure. As indicated on the charts, allowance must be made for loss in flap effectiveness caused by deflection of flaps ahead of or behind the outlet under consideration.

Estimates of the required flap angles and exit areas based on the cooling-requirement predictions presented in reference 1 are shown in table VIII. It is noted that with the auto-rich mixture setting, flap deflections of 6° or less will be sufficient to cool the engine cylinders with either type of baffling in the high-speed, climb, and cruise conditions; opening the flaps will produce sufficient additional pressure drop to cool the conventionally baffled engine with the auto-lean mixture. The negative engine-cooling-air exit areas shown for the maximum-endurance-cruise condition indicate that leakage through the cowl joints will be more than adequate to cool the engine at this low power.

Drag

Drag studies based on force and pressure measurements were conducted throughout the investigation to assist in the development of an optimum engine installation.

Force measurements.- A summary of the propeller-removed force data, table IX, shows that substantial reductions in drag for the high-speed attitude may be realized by minor modifications to the installation. (Figures illustrating the test conditions of the model are listed in the table.) With the exhaust stack shrouds sealed drag coefficient increments chargeable to the installation of the individual and manifolded exhaust stacks with horizontal flame dampers were 0.0021 and 0.0015, respectively, compared to 0.0007, 0.0004, and 0.0003 for the manifolded stacks with vertical flame dampers, the manifolded short stacks, and the manifolded flust stacks. Leakage from the external pressure-box and cowl joints and from the accessory-compartment exit gap at the cowl-firewall juncture increased the drag coefficient by 0.0005. Removing the NACA designed fairing strip from the accessory-compartment exit gap (fig. 17) increased the drag coefficient by 0.0006 thereby indicating the effectiveness of this fairing in reducing and directing the accessory-compartment flow. Substituting the flap exits for the shutter exits decreased the drag coefficient by 0.0007 in the fully closed condition without decreasing the pressure drops across the engine or oil cooler; this drag increment is attributed in part to the more effective seals around the edges of the flaps and in part to the elimination of the recessed surface at the shutters.

From the preceding items it appears that an overall reduction in drag coefficient of approximately 0.0033 can be obtained in the high-speed condition by: substituting the short exhaust stacks for the individual stacks, sealing all external cowl joints except that at the firewall, installing the fairing strip in the accessory-compartment exit, and substituting the flapped exits for the shutter exits. This reduction in drag coefficient corresponds to an increase in high speed of 5 miles per hour at sea level; reductions at angles of attack of $7\frac{1}{2}^{\circ}$ and 3° correspond respectively to an increase in the rate of climb of approximately 3/4 feet per minute and an increase in maximum range, according to Diehl's

range formula, of about 7 percent. As indicated by the calibration results, sizeable additional drag reductions can probably be obtained by sealing the front bulkhead of the cowl to eliminate the large amount of leakage from the clearance between the spinner and the cowl.

With the flush flapped exits, the short exhaust stacks, all seals removed, and the firewall fairing strip removed, the over-all drag coefficient increments above the sealed and faired condition were 0.0022, 0.0029, and 0.0025 for configurations IIc, IIIa, and IVa with the conventional, turbulent-flow, and mixed baffles, respectively. With open flaps corresponding over-all increments were 0.0068, 0.0073, and 0.0071. Since the available engine pressure drops for the three baffle configurations were of the same order, the selection of the baffles for this airplane should be based exclusively on cooling considerations.

Internal drag.- Internal cooling drag coefficients (fig. 42) were computed from the total pressure loss through the cowling and the weight flow of cooling air by the following expression rearranged from a form presented in reference 6:

$$C_{D_i} = \frac{WV_o}{gq_oS}\sqrt{\frac{\overline{H_1} - p_o}{q_o}}\left[1 - \sqrt{1 - \frac{(\overline{H_1} - \overline{H_x})}{(\overline{H_1} - p_o)}}\right]$$

The differences in over-all pressure losses for the three baffle configurations were counterbalanced to such an extent by changes in the internal flow that only one line could be faired through the calculated points. At the high-speed condition, $T_c = 0.057$, the internal drag coefficients for the engine and oil-cooler ducts were 0.0021 and 0.0002, respectively. Corresponding internal drag coefficients at the climb condition, $T_c = 0.26$, were 0.0112 and 0.0031. It is interesting to note that the sum of the calculated internal drag coefficients for the closed-flap condition (0.0023) was of the same order as the propeller-removed differences in drag coefficient between the complete installations and the sealed and faired basic shape.

Comparisons of the measured and calculated drag increments caused by opening the exits to increase the cooling-air pressure drops are presented in figure 43. The calculated internal drag coefficients were somewhat higher than the measured over-all increments partly because of the decrease in leakage which took place as the internal static pressures decreased with increases in the internal flow. For a given increase in pressure drop, the increase in drag coefficient was nearly the same for exits equipped with shutters or flaps.

Surface Pressures

Surface pressures were measured at the right side and at the inlet of the cowling primarily to obtain data on the air loads and on the static pressures at the cooling-air exits. Extrapolations of the pressures to high Mach numbers were made by use of the von Kármán relationship given in reference 7.

Pressures measured along the right side of the sealed and faired cowling are presented in figure 44. The static pressure at the engine-cooling-air exit was less than the free-stream static pressure whereas at the oil-cooler air exit, it was equal to or slightly greater than this pressure. Changing the angle of attack from -1.5° to 11.2° caused little change in the pressures at the exits. Moving the wing 20 inches forward to conform with a design change made subsequent to construction of the model would cause only small changes in the static pressures at the exits and consequently would not affect the application of the test results.

Surface pressure distributions at the cowl inlet with propeller removed are shown as figure 45; indicated critical Mach numbers corresponding to these data are presented in figure 46. Peak negative pressures on the lips decreased with increases in both inlet-velocity ratio and angle of attack. Pressure peaks on section C-C reached a maximum of $-1.05q_o$ at $\alpha = -4.5^\circ$ with $V_i/V_o = 0.46$ but were only $-0.51q_o$ for the high-speed attitude, $\alpha = -1.5^\circ$, $V_i/V_o = 0.54$. These pressures correspond to critical Mach numbers of 0.57 and 0.70 and critical speeds in sea-level standard air of 442 and 533 miles per hour, respectively. Such high indicated critical speeds show that the cowl lip shape (table III) might be applied successfully to a high-speed airplane.

The effects of propeller operation on the surface pressures at the cowl inlet for the closed-flap condition are shown in figure 47. Positive pressure peaks increased with T_c and also moved toward the right side of the airplane. Negative pressure peaks on the right and bottom sides of the inlet decreased with increases in T_c partly because of the pressure rise through the propeller but mainly because of the attendent increase in V_i/V_o. A comparison in figures 45(c) and 47 of the pressures on critical section C-C (for the high-speed inlet velocity ratio of 0.54) shows that propeller operation did not result in pressure changes large enough to alter the critical Mach number as predicted from the propeller-removed tests.

SUMMARY OF RESULTS

The more important results of the investigation are summarized as follows:

1. Available pressure drops across the engine and oil cooler of original cowl configuration Ia were insufficient for adequate cooling in the normal-power climb condition. Final cowl configurations of the II, III, and IV series, however, possessed ample engine and oil-cooler pressure drops (about $1.5q_o$ and $1.9q_o$) for cooling in this critical flight condition with each of the three baffle configurations tested therein.

2. The flap-flush exit area was sufficient to cool the engine in the high-speed condition in any configuration tested; leakage alone would furnish adequate cooling in the maximum-endurance-cruise condition.

3. The rams at the carburetor deck of the series II configurations were $1.35q_o$ and $2.01q_o$ for the normal-power, high-speed, and climb conditions, respectively; corresponding critical altitudes of the airplane in standard air are about 9900 feet and 9000 feet based on the engine critical altitude of 8000 feet.

4. The flapped exits produced higher pressure drops and had lower drags at equal pressure drops than the shutter exits.

5. In the normal-power climb condition (flaps open):

(a) Removing the exhaust-stack shrouds increased the engine and oil-cooler pressure drops by $0.08q_o$ and $0.09q_o$, respectively, but increased both the charge-air and cooling-air temperatures by 8° F.

(b) Sealing the accessory-compartment exit gap at the firewall increased the accessory-compartment temperature by 15° F.

(c) Removing the vanes from the engine-cooling-air exits caused little, if any, decrease in engine pressure drop.

6. A ram of 3.3 inches of water at the generator blast-tube flange was attained in the climb-at-normal-power condition by locating the blast-tube inlet at the rear of the pressure box above the carburetor duct. Although this ram was less than the Navy requirement, the pressure drop across the generator furnished air flow in excess of that specified by the engine manufacturer.

7. As indicated by ground-stand calibrations, leakage from the external cowl joints in the high-speed flight condition would be a large percentage of the engine cooling-air flow.

8. At $\alpha = -1.5°$, a propeller-removed drag-coefficient increment of 0.0011 was caused by leakage through the pressure-box joints, the cowl joints, and the cowl-firewall clearance. This increment was reduced to 0.0005 by an NACA designed fairing strip which blocked part of the flow and directed the remainder more nearly parallel to the fuselage.

9. At $\alpha = -1.5$ and with the exhaust-stack shrouds sealed, the drag coefficients for exhaust stacks with individual and manifolded horizontal-fishtail-type flame dampers were 0.0021 and 0.0015 compared to 0.0004 for manifolded short stacks and 0.0007 for manifolded stacks equipped with vertical-fishtail-type flame dampers.

10. Minor model modifications indicated by the drag tests would result at sea level in approximate increases of 5 miles per hour in high speed, 3/4 feet per minute in rate of climb, and 7 percent in maximum range.

11. The over-all drag coefficient was essentially independent of baffle configuration.

12. In the propeller-removed condition at $\alpha = -1.5^{\circ}$, the drag coefficients for configurations IIc, IIIa, and IVa with closed flaps, short exhaust stacks, and no seals were 0.0022 to 0.0029 greater than that for the sealed and faired basic shape. These increments were of the same order as those for the calculated internal drags.

13. Measured thrust coefficients for the climb condition tests were consistently less at military power than at normal power possibly because of propeller tip losses or the decrease in V_o/nD. Increases in the propeller gear ratio or modifications to the propeller might result in over-all increases in airplane performance at military power.

14. For the high-speed condition, the indicated critical Mach number of the installation as determined by the negative peak pressure on the lower lip of the inlet was 0.70.

Langley Memorial Aeronautical Laboratory
National Advisory Committee for Aeronautics
Langley Field, Va.

REFERENCES

1. Conway, Robert N.,and Emmons, M. Arnold, Jr.: An Investigation of the Ranger V-770-8 Engine Installation for the Edo XOSE-1 Airplane. I - Cooling. NACA MR No. L5I12, 1945.

2. Becker, John V., and Baals, Donald D.: The Aerodynamic Effects of Heat and Compressibility in the Internal Flow Systems of Aircraft. NACA ACR, Sept. 1942.

3. Becker, John V.,and Baals, Donald D.: Simple Curves for Determining the Effects of Compressibility on Pressure Drop through Radiators. NACA ACR No. L4I23, 1944.

4. Williams, David T.: High Altitude Cooling. II - Air-Cooled Engines. NACA ARR No. L4I11a, 1944.

5. Anon.: Specification for the Measurement of Engine Installation Temperatures. NAVAER E-59c, Bur. Aero., July 7, 1943.

6. McHugh, James G.,and Pepper, Edward: The Propeller and Cooling-Air-Flow Characteristics of a Twin-Engine Airplane Model Equipped with NACA D_8-Type Cowlings and with Propellers of NACA 16-Series Airfoil Sections. NACA ACR No. L4I20, 1944.

7. von Kármán, Th.: Compressibility Effects in Aerodynamics. Jour. Aero. Sci., vol. 8, no. 9, July 1941, pp. 337-356.

TABLE I.- KEY TO MODEL CONFIGURATION AND DATA PRESENTED

Configuration		Symbol	Distinctive engine and cowling components installed		[a]Data presented	
				Substituted components	Pressure	Force
I	a		Conventional baffles Shutter exits Exhaust stacks with horizontal flame dampers and shrouds Original oil-cooler ducts		----	X
	b	◺		Exhaust stacks with vertical flame dampers and shrouds	X	X
	c			Modified oil-cooler-exit duct	X	X
	d			Modified oil-cooler-exit duct with vane omitted	X	----
	e	○		Modified oil-cooler-exit duct, vanes installed in oil-cooler-inlet duct	X	X
II	a	□	Conventional baffles Flapped exits Exhaust stacks with vertical flame dampers and shrouds Vaned oil-cooler-inlet duct		X, Y	X, Y
	b			Flush exhaust stacks with shrouds	----	X
	c	△		Short exhaust stacks with shrouds	Y	Y
III	a	X	Turbulent flow baffles Flapped exits Short exhaust stacks with shrouds Vaned oil-cooler-inlet duct		X, Y	X, Y
IV	a	◇	Turbulent flow baffles on right bank mixed NACA-designed baffles on left bank baffles Flapped exits Short exhaust stacks with shrouds Vaned oil-cooler-inlet duct		X, Y	X, Y
	b	+		Short exhaust stacks without shrouds	Y	Y
	c			Individual stacks with horizontal flame dampers and shrouds	----	X
	d			Exhaust stacks with vertical flame dampers and without shrouds	----	X
	e	▽		Short exhaust stacks without shrouds Flapped engine-cooling-air exits without vanes	Y	Y

[a]X Propeller removed.
Y Propeller installed.

TABLE II.- SUMMARY OF DUCT AREAS.

(Measured perpendicular to flow)

Item	Area (sq ft)
Cowl inlet	1.480
Carburetor-duct inlet	0.222
Carburetor deck	.219
Oil-cooler-duct inlet	.357
Oil-cooler face	.514
Oil-cooler-duct exit:	
(a) Original shutter exit (configurations Ia, Ib)	
shutter closed	.006
shutter open	.253
(b) Modified shutter exit (configurations Ic, Id, Ie)	
shutter closed	.019
shutter open	.200
(c) Flapped exit (configurations II, III, IV)	
flap closed	.050
flap open	.410
Engine-cooling air exits:	
(a) Shutter exits (configuration I)	
shutters closed	.400
shutters open	1.420
(b) Flapped exits (configurations II, III, IV)	
flaps closed	.440
flaps open	1.690

L-562

TABLE III.- ORIFICE LOCATIONS AND COWL CONTOURS AT INLET.

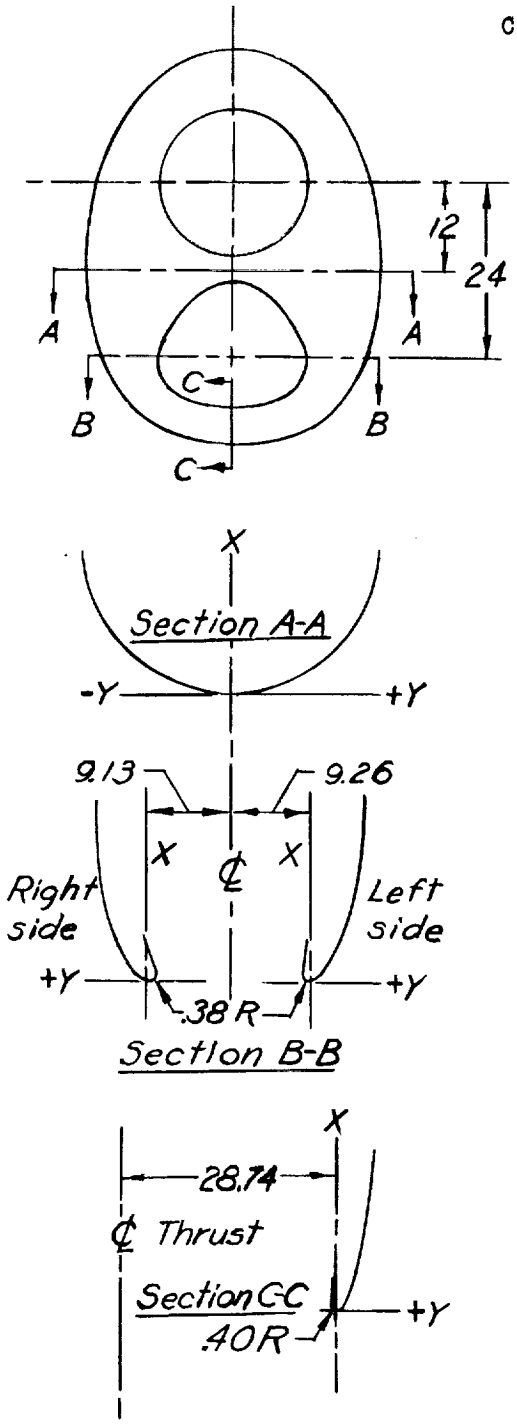

Section A-A	
X	Y
22.92	18.43
16.21	16.82
13.87	15.97
11.96	15.05
7.72	12.88
6.02	11.94
4.38	10.79
2.94	9.49
1.68	7.87
.76	6.12
.20	4.19
0	2.19
0	.17
0	-1.82
.14	-3.84
.75	-5.77
1.69	-7.51
2.96	-9.09
4.42	-10.35
6.13	-11.40
7.89	-12.35
11.26	-13.88
13.24	-14.74
15.53	-15.65
22.21	-17.15

Section B-B (left side)	
X	Y
1.89	-0.17
.98	-.31
.40	-.39
.17	-.31
.01	-.04
.11	-.26
.34	.63
1.04	1.38
1.76	2.03
2.61	2.62
4.42	3.59
6.32	4.34
7.76	4.74
12.41	5.74
16.54	6.29

Section B-B (right side)	
X	Y
1.82	0.07
.93	-.21
.45	-.36
.15	-.29
.01	-.06
.08	.34
.30	.78
.93	1.59
1.65	2.29
2.47	2.89
4.25	3.91
6.06	4.70
7.99	5.30
11.83	6.14
15.76	6.78

Section C-C	
X	Y
1.63	-0.15
.63	-.39
.15	-.35
.02	-.14
.02	.08
.33	.54
.69	.85
1.05	1.10
1.41	1.30
1.92	1.55
2.35	1.75
3.26	2.08
5.21	2.58
7.19	2.93
11.66	3.59
15.88	4.12
19.40	4.42

Note: All dimensions in inches. Each coordinate locates a pressure tube.

NATIONAL ADVISORY COMMITTEE FOR AERONAUTICS

TABLE IV.- PRESSURE TUBE INSTRUMENTATION

Location	Number of tubes	Type of pressure tube	Reference figures and table
cowl inlet	19	shielded total	3(a), 19, 29
	9	static	Do.
	6	surface orifice	Do.
pressure box (in plane of number 6 cylinders)	28	total	3(a), 29
engine vee (in front of barrels and heads)	24	-do-	3(b), 6(B), 29
between head fins	14	-do-	5, 29
behind barrel baffles	14	total facing baffle	5, 6, 29
engine-cooling-air exits	18	shielded total	16(c), 29
	12	total	29
	38	static	16(c), 29
	6	surface orifice	Do.
generator-blast tube flange	1	total	21
carburetor-duct inlet	12	-do-	3(b), 14, 29
	3	static	Do.
	6	surface orifice	Do.
carburetor screen	16	total	Do.
oil cooler:			
duct inlet	15	-do-	3(b), 29
	3	static	Do.
	6	surface orifice	Do.
front face	16	total	11, 29
rear face	8	open end facing rear	Do.
duct exit	9	total	16(c), 29
	3	static	Do.
	6	surface orifice	Do.
inlet lips	71	-do-	table III, 45
right flank of cowl	31	-do-	44

TABLE V.- SUMMARY OF COMPARATIVE DATA PERTINENT TO THE DEVELOPMENT OF THE ENGINE AND OIL-COOLER DUCTS. $\alpha = 7.5^\circ$.

Configuration	Model Description	Ref. fig.	Test condition	Type of exits	Flap or shutter position		$\frac{\overline{\Delta P_e}}{q_o}$	$\frac{\overline{\Delta P_c}}{q_o}$	$^a\Delta C_D$	REMARKS
					Engine	Oil cooler				
Ib	Same as Ia except that vertical flame dampers were substituted for horizontal flame dampers (See table I)	7	propeller removed	shutter	closed	open	--	0.49	--	--
Ic	Same as Ib except that modified oil cooler exit duct incorporating a vane and more gradual exit fairing was installed.	12	-do-	-do-	-do-	-do-	--	.38	-0.0004	--
Id	Same as Ic except that vane was removed from oil-cooler-exit duct	-do-	-do-	-do-	-do-	-do-	--	.40	--	--
Ie	Same as Id except that cascade vanes were installed in oil-cooler inlet duct	12	-do-	-do-	-do-	-do-	0.48	.41	--	A
		13			open	closed	.69	.09	--	--
IIa	Same as Ie except that flapped exits were substituted for shutter exits	15	-do-	flap	closed	open	.49	.95	.0004	A
		16			open	closed	.90	.20	.0020	
		12			-do-	open	.86	.91	--	
IVa	See table I	--	normal-power climb	flap	open	open	1.54	1.86	--	--
IVb	Same as IVa except that exhaust stack shrouds were removed	9	-do-	-do-	-do-	-do-	1.62	1.95	---	B
IVe	Same as IVb except that vanes were removed from engine-cooling air exit and accessory-compartment exit gap at firewall was sealed	16(c)	-do-	-do-	-do-	-do-	1.58	1.94	--	C
		17								

[a]Increment of drag coefficient caused by the modification.

A - Modification adopted for all succeeding configurations.

B - Modification undesirable as air temperature was increased 8° F at the rear of the engine vee, at the carburetor, and at the face of the oil cooler.

C - Vane removal is considered desirable as smallness of decrease in pressure drop is attributed to increased effectiveness of exit. Accessory compartment exit-gap seal is undesirable as accessory compartment temperature was increased 15° F by the modifications.

TABLE VI.- SUMMARY OF GENERATOR COOLING-PRESSURE DATA

Location of blast-tube inlet	Reference figure	Operating condition	α (deg)	Flap or shutter position	Pressure recovery at generator $\frac{\bar{H} - p_o}{q_o}$	Downstream pressure $\frac{\overline{p_{re}} - p_o}{q_o}$	Generator pressure drop $\frac{\bar{H} - \overline{p_{re}}}{q_e}$	Generator pressure drop $\bar{H} - \overline{p_{re}}$ at flight speed (in. water)
At top of cowl inlet, configuration Ia	19	propeller removed	-1.5	closed	0.71	0.46	0.25	----
		-do-	7.5	-do-	.73	.48	.25	----
		-do-	-1.5	open	.30	.17	.13	----
		-do-	7.5	-do-	.32	.18	.14	----
At right-rear wall of pressure box, configurations IIa and IIc	8b	-do-	-1.5	closed	.61	.47	.14	----
		-do-	7.5	-do-	.62	.47	.15	----
		-do-	-1.5	open	.23	-.04	.27	----
		-do-	7.5	-do-	.21	-.08	.29	----
		high speed at normal power	-1.5	closed	.66	.55	.11	1.89
		maximum endurance cruise at 30.6 percent normal power	11.2	-do-	.80	.59	.21	.84
		climb at normal power	7.5	open	.28	-.02	.30	1.71
At rear wall of pressure box above carburetor-duct inlet, configuration IIIa	--	propeller removed	-1.5	closed	.57	.39	.18	----
		-do-	7.5	-do-	.53	.39	.14	----
		-do-	-1.5	open	.25	-.09	.34	----
		-do-	7.5	-do-	.22	-.10	.32	----
		high speed at normal power	-1.5	closed	.74	.45	.29	4.98
		maximum endurance cruise at 30.6 percent normal power	11.2	-do-	1.38	.65	.73	2.91
		climb at normal power	7.5	open	.58	-.12	.70	4.00
At downstream end of oil-cooler inlet duct, configurations IVc and IVe	19	propeller removed	7.5	closed	.50	.44	.06	----
		climb at normal power	7.5	open	.36	-.05	.41	2.34

NATIONAL ADVISORY
COMMITTEE FOR AERONAUTICS

TABLE VII

SUMMARY OF PROPELLER-INSTALLED PRESSURE DATA FOR FLIGHT SIMULATION CONDITIONS

Flight condition	Model configuration	bhp (from engine specifications)	Baffles	Flap angle δ (deg)		V_o	σ_o	q_o	T_c	α	$\frac{V_i}{V_o}$	$\frac{H_i - p_o}{q_o}$	Engine duct				Oil-cooler duct				Carburetor duct		$\frac{\overline{\Delta p_e}}{q_o}$	$\frac{\overline{\Delta p_o}}{q_o}$
				Engine	Oil cooler	(ft/sec)		(lb/sq ft)		(deg)			$\frac{\overline{H_f - p_o}}{q_o}$	$\frac{\overline{p_f - p_o}}{q_o}$	$\frac{\overline{p_x - p_o}}{q_o}$	$\frac{\overline{H_x - p_o}}{q_o}$	$\frac{\overline{H_f - p_o}}{q_o}$	$\frac{\overline{p_f - p_o}}{q_o}$	$\frac{\overline{p_x - p_o}}{q_o}$	$\frac{\overline{H_x - p_o}}{q_o}$	$\frac{H_i - p_o}{q_o}$	$\frac{H_d - p_o}{q_o}$		
High-speed normal power	IIa	a	Conventional	0	0	149	0.908	24.1	0.054	-1.5	0.51	1.27	1.18	0.55	0.28	0.50	1.27	1.03	0.69	0.99	1.36	1.35	0.63	0.24
	IIIa	a	Turbulent flow	0	0	147	0.951	24.2	0.055	-1.5	0.46	1.32	1.12	0.45	0.31	0.46	1.28	1.06	0.66	1.03	----	----	0.67	0.22
High-speed military power	IIa	a	Conventional	0	0	149	0.908	23.9	0.059	-1.5	0.52	1.38	1.20	0.53	0.28	0.50	1.29	1.04	0.64	1.00	1.40	1.39	0.67	0.25
	IIIa	a	Turbulent flow	0	0	146	0.938	23.7	0.063	-1.5	0.46	1.35	1.14	0.46	0.30	0.43	1.29	1.07	0.66	1.03	----	----	0.68	0.22
Maximum endurance cruise	IIc	148	Conventional	0	0	129	0.908	17.9	0.134	11.2	0.63	1.77	1.53	0.59	0.33	0.60	1.66	1.38	1.01	1.39	1.78	1.77	0.94	0.28
	IIIa	145	Turbulent flow	0	0	119	0.900	15.0	0.141	11.2	0.56	1.99	1.65	0.65	0.40	0.62	1.86	1.50	1.04	1.55	----	----	1.00	0.36
Climb normal power	IIc	500	Conventional	27.7	30.6	156	0.900	25.9	0.258	7.5	0.98	2.14	1.53	-0.02	-0.47	-0.02	1.68	-0.12	----	0.20	2.05	2.01	1.55	1.80
	IIIa	500	Turbulent flow	27.7	30.6	158	0.900	26.6	0.251	7.5	0.85	2.14	1.41	-0.12	-0.39	-0.07	1.66	-0.26	-0.28	0.21	----	----	1.53	1.92
	IVa	500	Mixed	27.7	30.6	157	0.900	26.5	0.251	7.5	0.90	2.18	Left 1.56 / Right 1.39	Left -0.04 / Right -0.08	-0.44	-0.05	1.61	-0.25	-0.27	0.08	----	----	Left 1.60 / Right 1.47	1.86
	IVb	500	Mixed	27.7	30.6	158	0.900	26.7	0.249	7.5	0.92	2.17	1.62	1.45	-0.09	-0.06	-0.37	-0.09	1.70	-0.25	-0.33	0.09	----	----	1.71	1.53	1.95
	IVe	500	Mixed	27.7	30.6	157	0.880	26.1	0.250	7.5	0.91	2.23	1.62	1.43	-0.04	-0.06	-0.41	-0.13	1.68	-0.26	-0.32	0.07	----	----	1.66	1.49	1.94
Climb military power	IIc	[b]530	Conventional	27.7	30.6	159	0.879	26.4	0.250	7.5	0.99	2.18	1.51	-0.07	-0.45	-0.01	1.65	-0.24	----	0.15	2.14	2.08	1.58	1.89
	IIIa	[b]508	Turbulent flow	27.7	30.6	157	0.911	26.8	0.233	7.5	0.86	2.15	1.43	-0.11	-0.40	-0.08	1.65	-0.25	-0.31	0.18	----	----	1.54	1.90
	IVa	[b]522	Mixed	27.7	30.6	157	0.911	26.7	0.240	7.5	0.89	2.16	1.55	1.37	-0.07	-0.08	-0.43	-0.06	1.45	-0.22	-0.30	0.08	----	----	1.62	1.45	1.67

[a]Simulation condition power; T_c was duplicated using a propeller blade angle of 22°.

[b]Highest power obtainable with auxiliary venturi in carburetor duct.

NATIONAL ADVISORY
COMMITTEE FOR AERONAUTICS

TABLE VIII.- ESTIMATIONS OF THE FLAP ANGLES AND FLUSH EXIT AREAS REQUIRED FOR COOLING IN NAVY AIR

Assumed flight conditions						[a] Required pressure drop				Required flap angles, degrees				Required flush exit area, sq ft			
Nominal condition	Horsepower	Altitude (feet)	V_o miles/hour	T_c	α (deg)	[b] Auto - rich $\frac{\overline{\Delta P_e}}{q_o}$	[b] Auto - rich $\frac{\overline{\Delta P_c}}{q_o}$	[b] Auto - lean $\frac{\overline{\Delta P_e}}{q_o}$	[b] Auto - lean $\frac{\overline{\Delta P_c}}{q_o}$	Auto - rich δ_e	Auto - rich δ_c	Auto - lean δ_e	Auto - lean δ_c	Auto - rich A_{xe}	Auto - rich A_{xc}	Auto - lean A_{xe}	Auto - lean A_{xc}
Configuration IIc (Conventional baffles)																	
High-speed	550	0 10,000	192 203	0.064 .072	-1.6 -1.0	0.39 .42	0.53 .43	0.53 .57	0.53 .43	0 0	8 3	0 0	8 3	0.16 .16	0.155 .090	0.31 .32	0.16 .09
Climb	550	0 9,000	108 122	.281 .275	7.5 7.9	1.18 1.09	1.46 1.17	1.62 1.55	1.46 1.17	0 0	14 9	18 13	14 9	.24 .17	[d] ---- [d] ----	1.30 1.10	[d] -- [d] --
Maximum-endurance cruise	153	1,500	90	.147	11.8	----	----	.25	.17	---	--	0	0	----	----	[c] -.10	.01
Configuration IIIa (Turbulent-flow baffles)																	
High-speed	550	0 10,000	192 203	0.064 .072	-1.6 -1.0	0.46 .57	0.53 .43	0.60 .71	0.53 .43	0 0	8 3	0 2	8 3	0.22 .31	0.155 .090	0.40 .51	0.16 .09
Climb	550	0 9,000	108 122	.281 .275	7.5 7.9	1.42 1.49	1.46 1.17	1.84 1.89	1.46 1.17	3 6	14 9	d-- d--	14 9	.59 .75	d---- d----	d--- d---	d--- d---
Maximum-endurance cruise	153	1,500	90	.147	11.8	----	----	.39	.17	---	--	0	0	----	----	[c] -.03	.01

[a] Obtained from cooling predictions in reference 1.

[b] Carburetor mixture settings.

[c] Negative exit area indicates that leakage through cowl joints is sufficient to cool engine.

[d] Value of $\overline{\Delta P}/q_o$ is too far above test range to permit extrapolation.

NATIONAL ADVISORY COMMITTEE FOR AERONAUTICS

TABLE IX.- SUMMARY OF PROPELLER-REMOVED DRAG DATA.

(Measured at a Reynolds number of 5.3×10^6 based on the mean aerodynamic chord)

Successive modifications to model	Configuration	Illustrative figures	[a] ΔC_D			
			$\alpha = -1.5^\circ$ (High-speed attitude)	$\alpha = 3^\circ$	$\alpha = 7.5^\circ$ (climb attitude)	$\alpha = 11.2^\circ$ (Max. endurance cruise attitude)
Model completely sealed and faired (conventional baffles on cylinders)	--	2(a)	----	----	----	----
Inlet opened and seals removed from engine-cooling-air exits (shutter type)	--	3(a) 16(a)	0.0008	0.0009	0.0010	0.0011
Seals removed from oil-cooler exit (shutter type)	--	16(a)	.0000	.0000	.0001	.0002
Exhaust stacks with horizontal flame dampers installed	Ia	8(a)	.0015	.0009	.0007	.0005
Exhaust stacks with vertical flame dampers installed	Ib	8(b)	-.0008	-.0003	-.0002	.0000
Seals between exhaust stacks and shrouds removed	--	9	.0002	.0001	.0000	.0000
Seals removed from external pressure-box joints	--	8(a)	.0001	.0001	.0000	.0000
Seals removed from external cowl joints except at spinner, firewall, and edges of shutters	--	2(a)	.0002	.0001	.0001	.0001
Seal between cowl and firewall removed	--	16(b), 17	.0002	.0002	.0001	.0001
Fairing strip removed from firewall clearance	--	17	.0006	.0006	.0005	.0004
Oil-cooler-exit shutter opened (Seals removed from edges)	--	15	.0004	.0004	.0005	.0004
Modified oil-cooler-exit duct installed with shutter open	Ic	12	-.0003	-.0003	-.0004	-.0004
Vane removed from oil-cooler-exit duct, vanes installed in oil-cooler-inlet duct, seals removed from edges of engine-air shutters, oil-cooler shutter closed	Ie	12, 13	.0004	.0002	.0001	.0001
All shutters opened	Ie	15	.0017	.0018	.0016	.0014
Flapped exits installed (flaps closed)	IIa	16(b)	-.0007	-.0006	-.0003	-.0003
All flaps opened	IIa	16(c)	.0046	.0046	.0045	.0045
Flush exhaust stacks installed, flaps closed	IIb	7	-.0004	-.0004	-.0003	-.0003
Model restored to original condition, turbulent-flow baffles installed on cylinders	--	2(a), 5, 6	----	----	----	----
Inlet opened, all seals removed except at spinner and exhaust stacks, firewall fairing strip removed	--	9, 17	.0023	.0019	.0019	.0021
Short exhaust stacks installed, shroud seals removed	IIIa	8(c)	.0006	.0006	.0006	.0006
All flaps opened	IIIa	16(c)	.0044	.0042	.0039	.0039
NACA-designed diffuser baffles installed on left bank cylinders, exhaust-stack shrouds sealed, flaps closed	IVa	6(d), 6(e)	-.0006	-.0004	-.0004	-.0004
All flaps opened	IVa	16(c)	.0046	.0044	.0043	.0043
Mocked-up individual stacks with horizontal flame dampers installed, flaps closed	IVc	8(d)	.0017	.0017	.0017	.0015
Exhaust stacks with vertical flame dampers installed	IVd	7, 8(b)	-.0014	-.0014	-.0015	-.0013

[a] Non-indented values are the drag coefficient increments between successive non-indented model conditions. Indented values are based on the respective preceding model conditions.

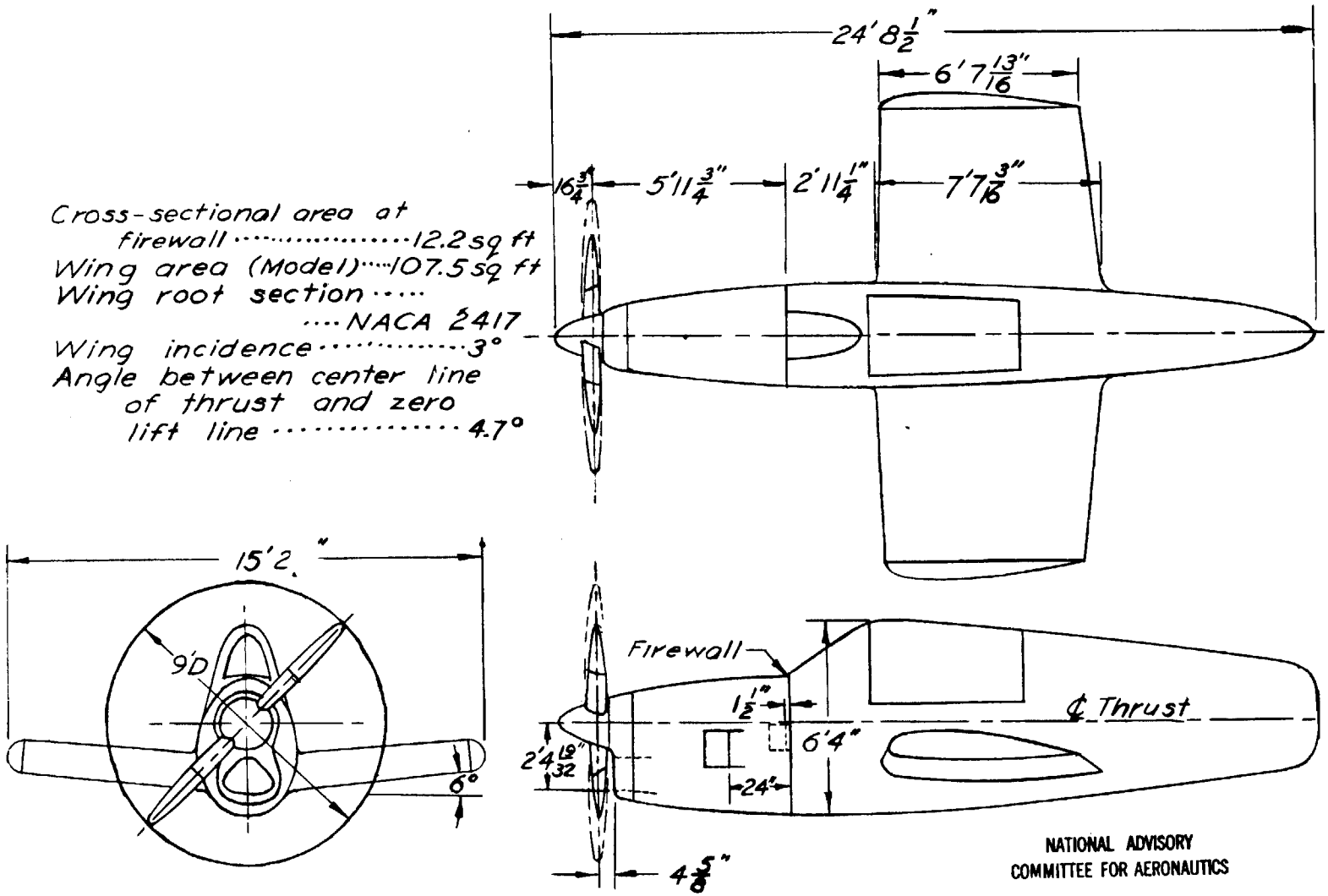

Figure 1 .- General arrangement and principal dimensions of model.

NACA MR No. L5112b

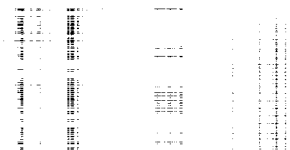

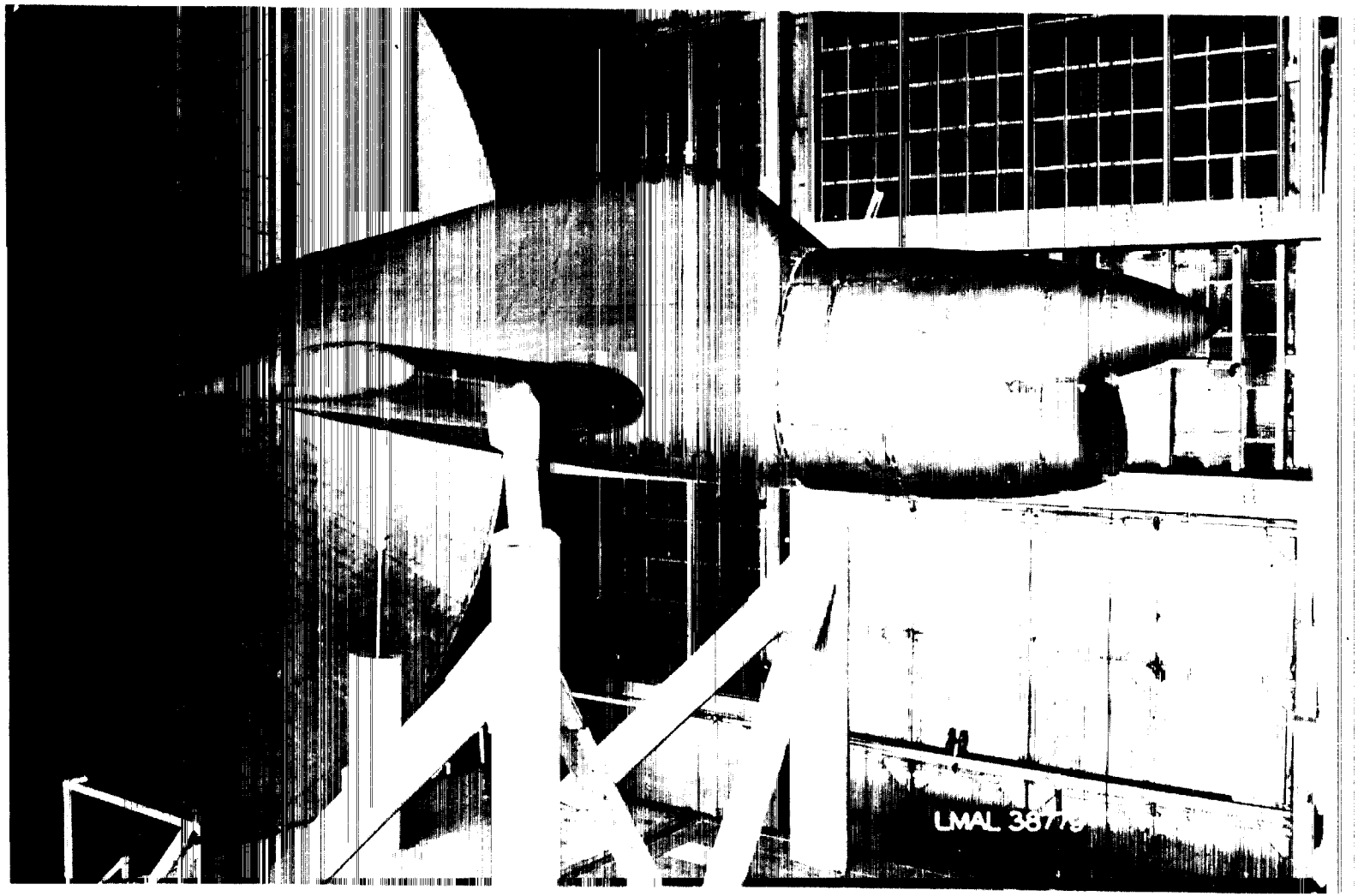

(a) Side view; sealed and faired condition.

Figure 2.- General views of model

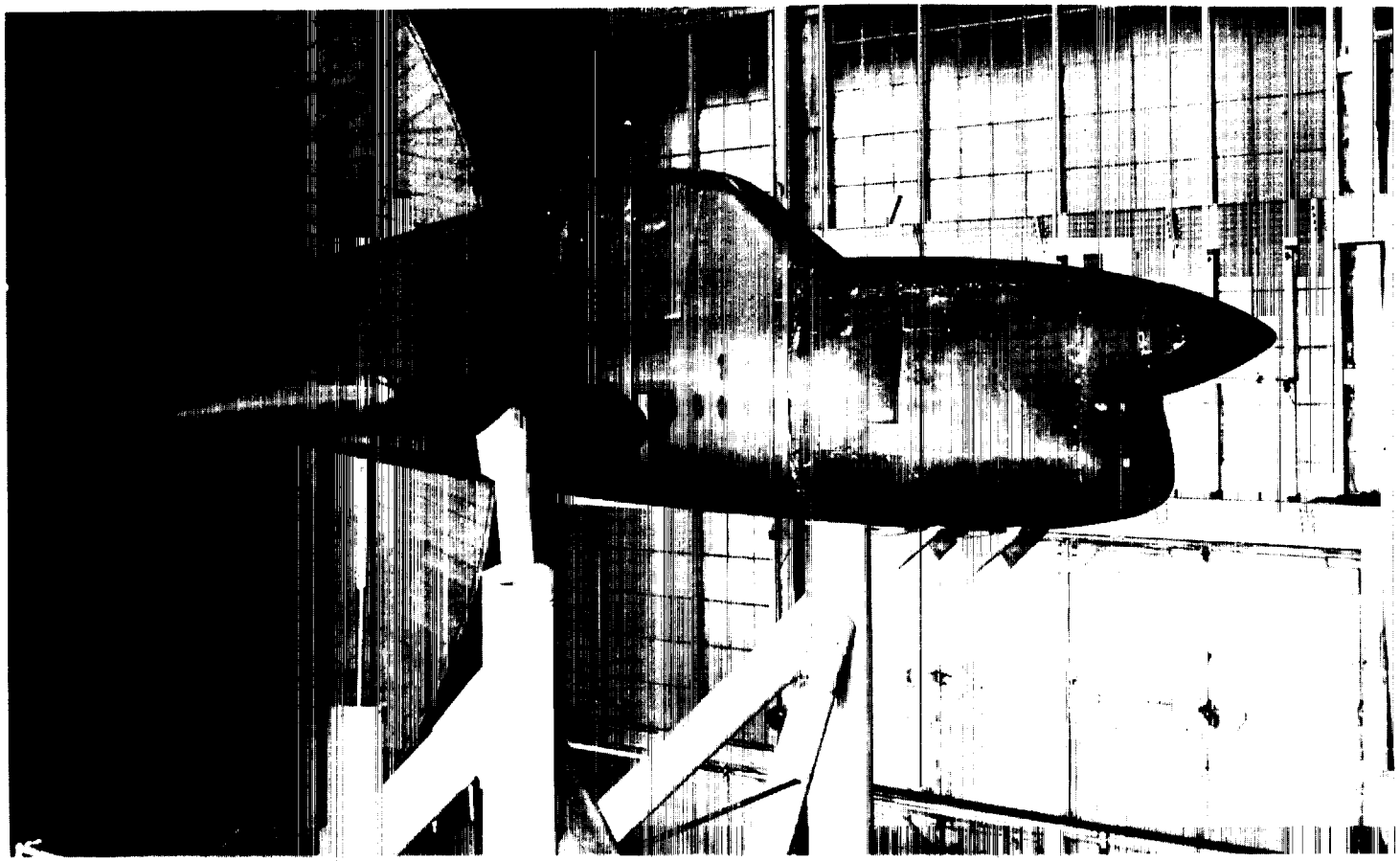

(b) Side view of configuration Ib; shutter exits and vertical-flame-damping exhaust stacks installed.

Figure 2.- Continued.

L562

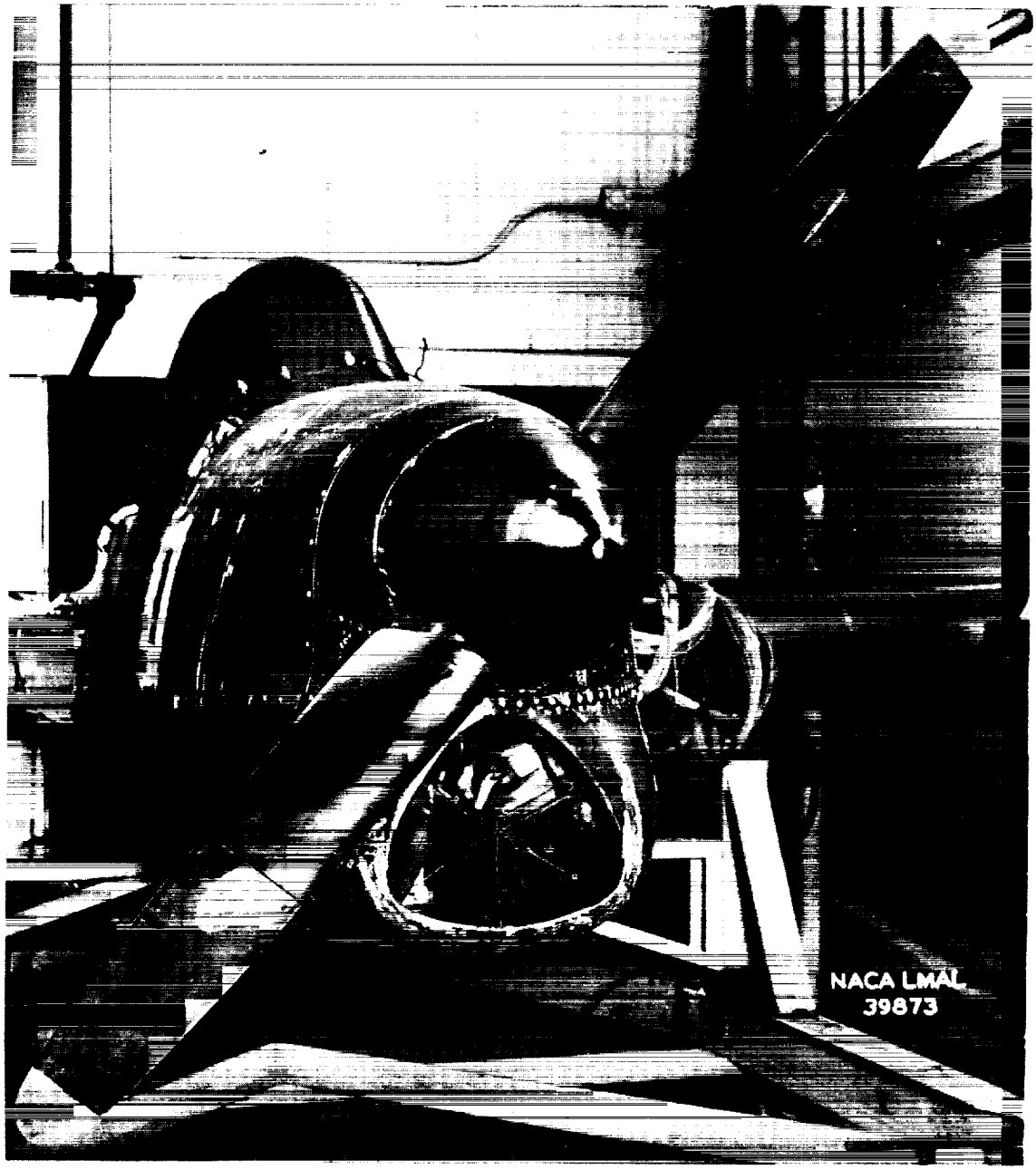

(c) Front view; propeller installed.

Figure 2.- Concluded.

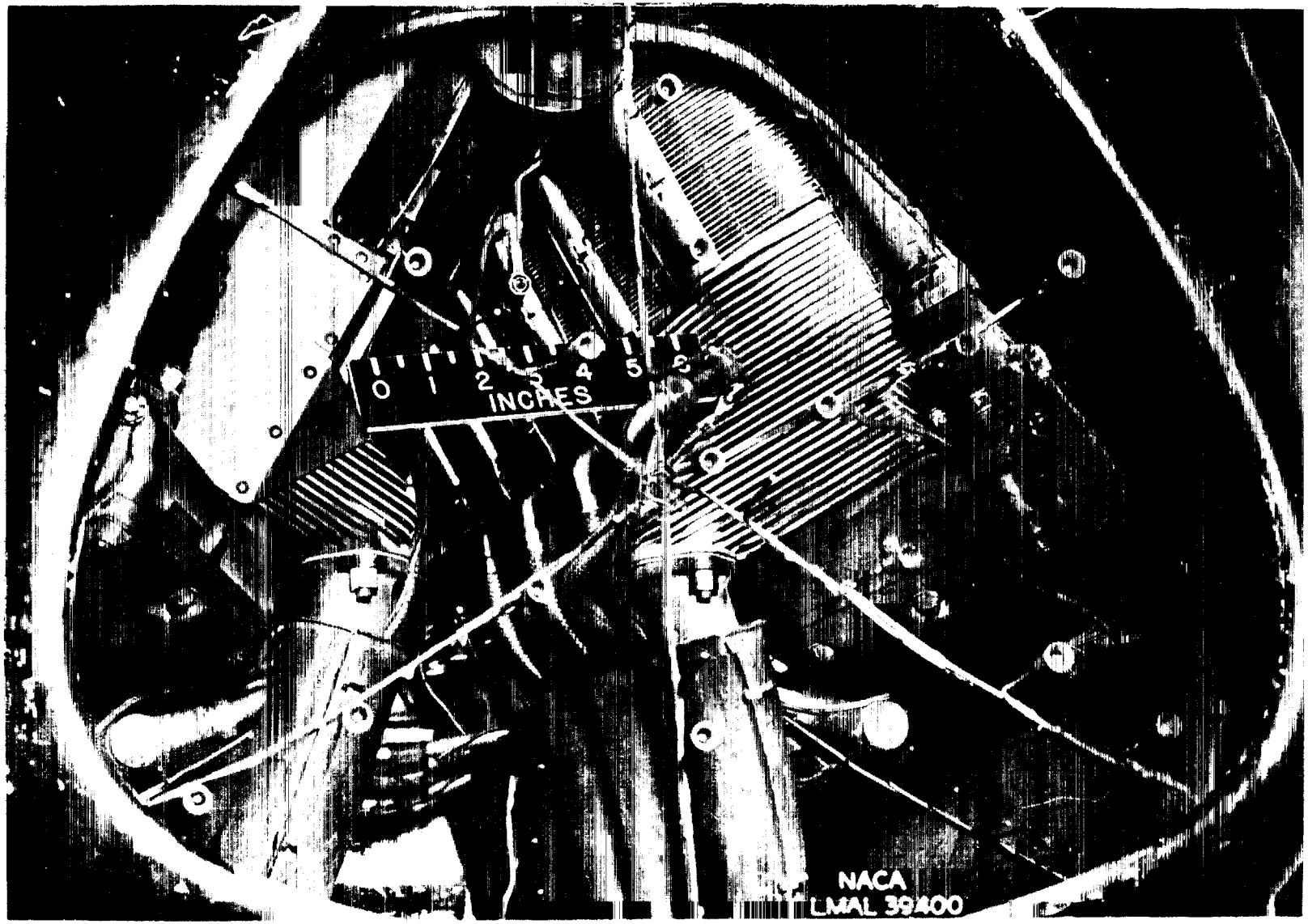

(a) As tested in configurations IVa and IVc.

Figure 3.- Engine and inlet duct.

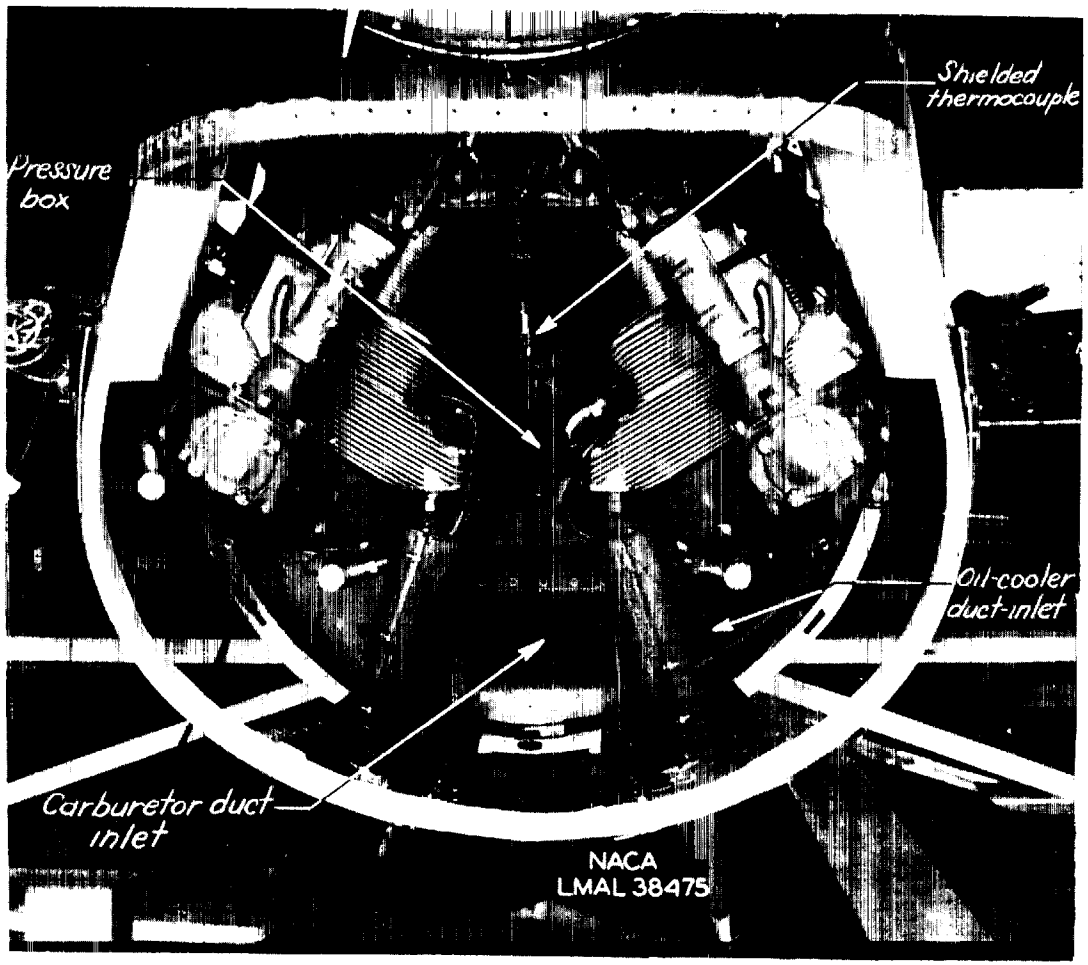

MR No. L5I12b

(b) Inlet lips and skin removed.

Figure 3.- Concluded.

L-562

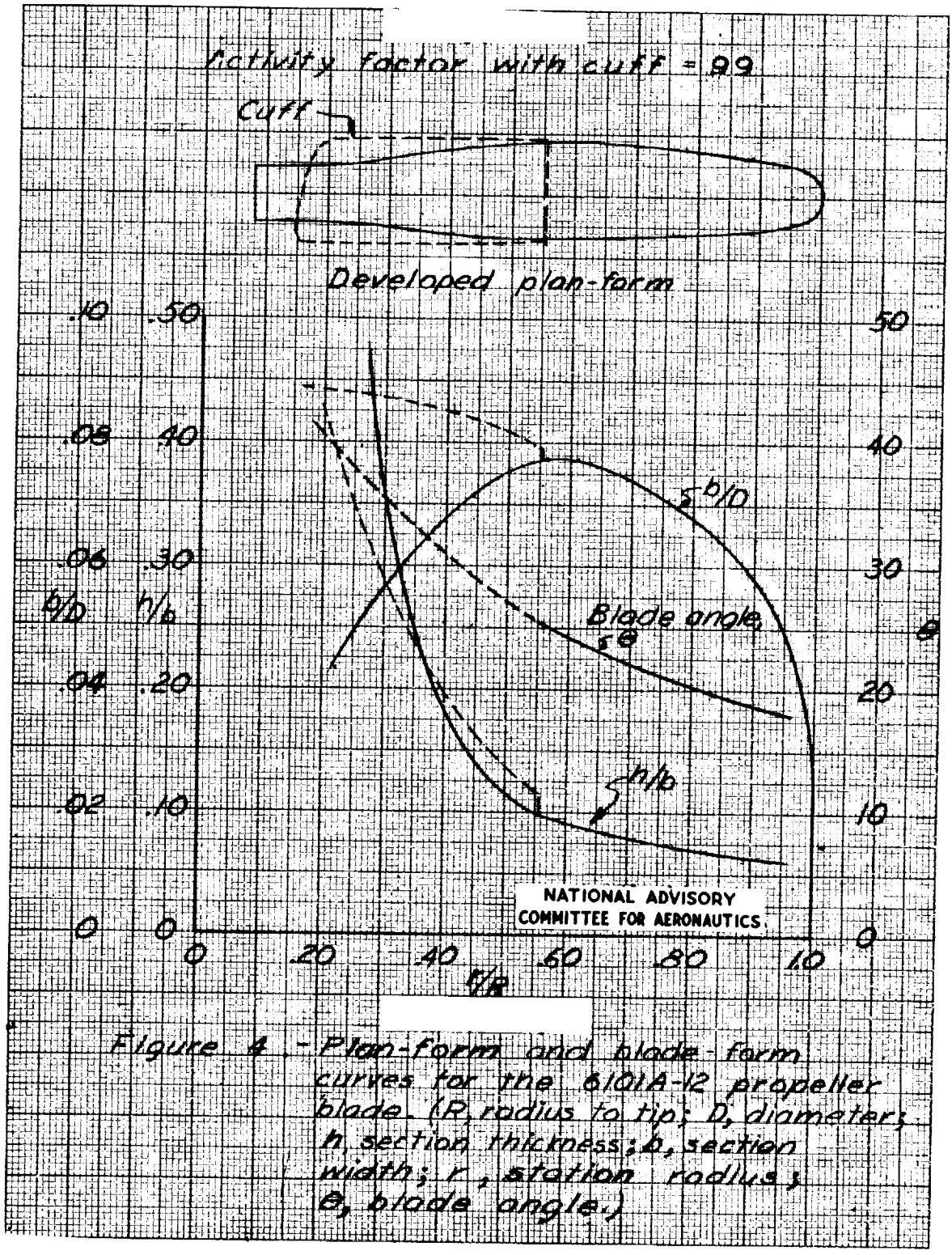

Figure 4. - Plan-form and blade-form curves for the 6101A-12 propeller blade. (R, radius to tip; D, diameter; h, section thickness; b, section width; r, station radius; θ, blade angle.)

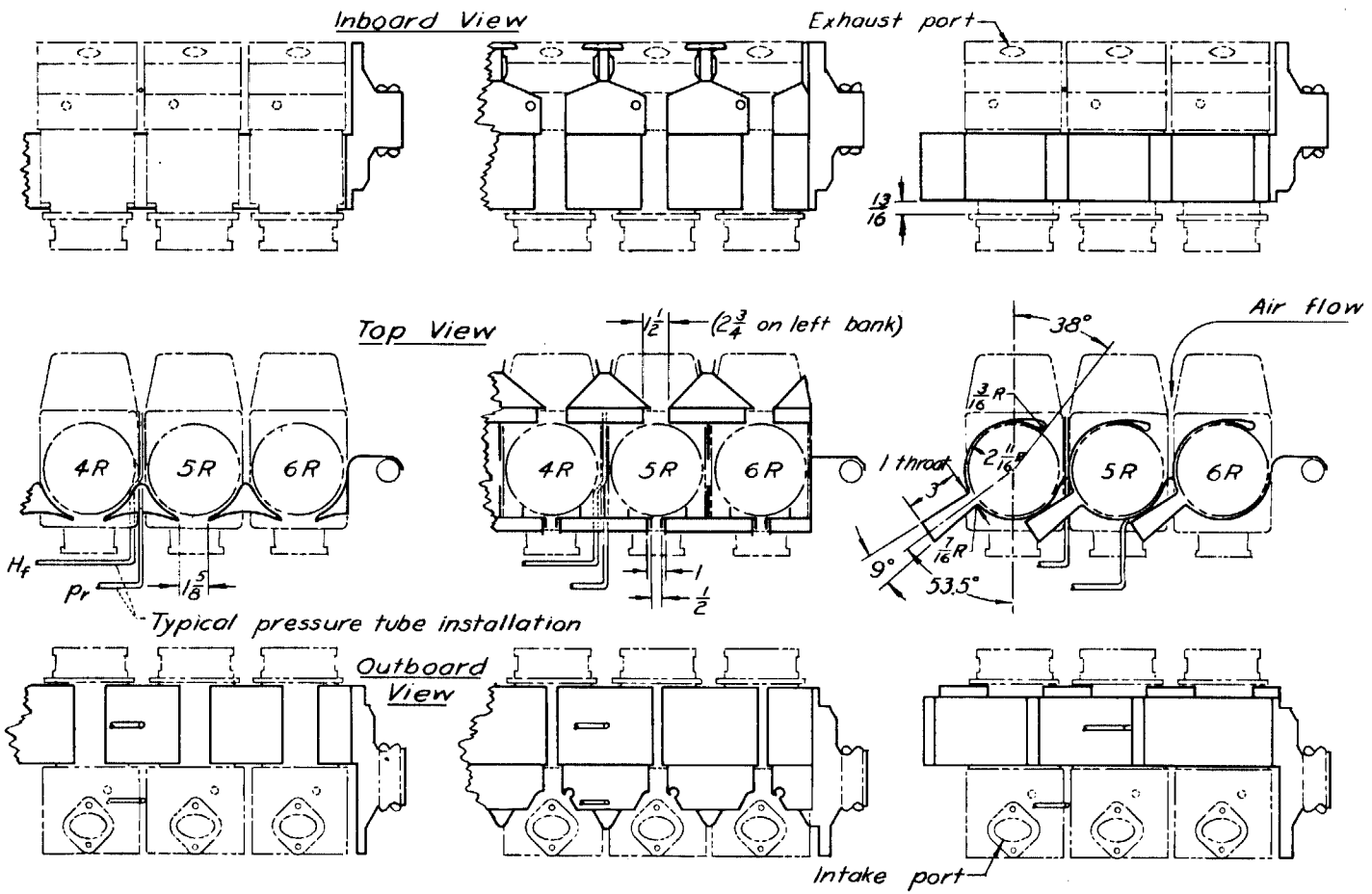

Figure 5 .- Typical baffle and pressure tube installations. Linear dimensions in inches.

NATIONAL ADVISORY COMMITTEE FOR AERONAUTICS

L-562

L562

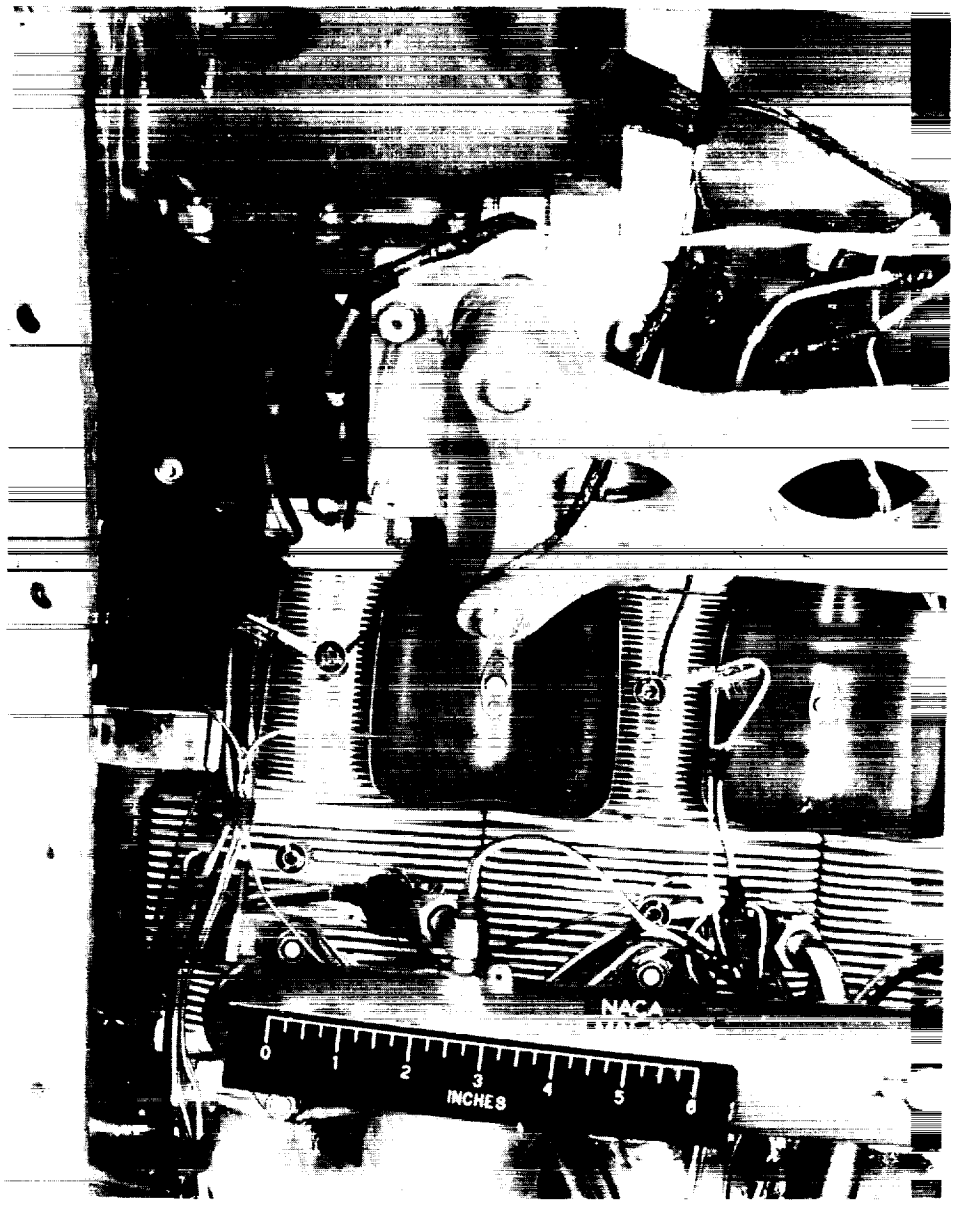

(a) Conventional baffles (installed on outboard side of cylinder only).

Figure 6.- Baffle installations.

(b) Turbulent-flow baffles, inboard view.

Figure 6.- Continued.

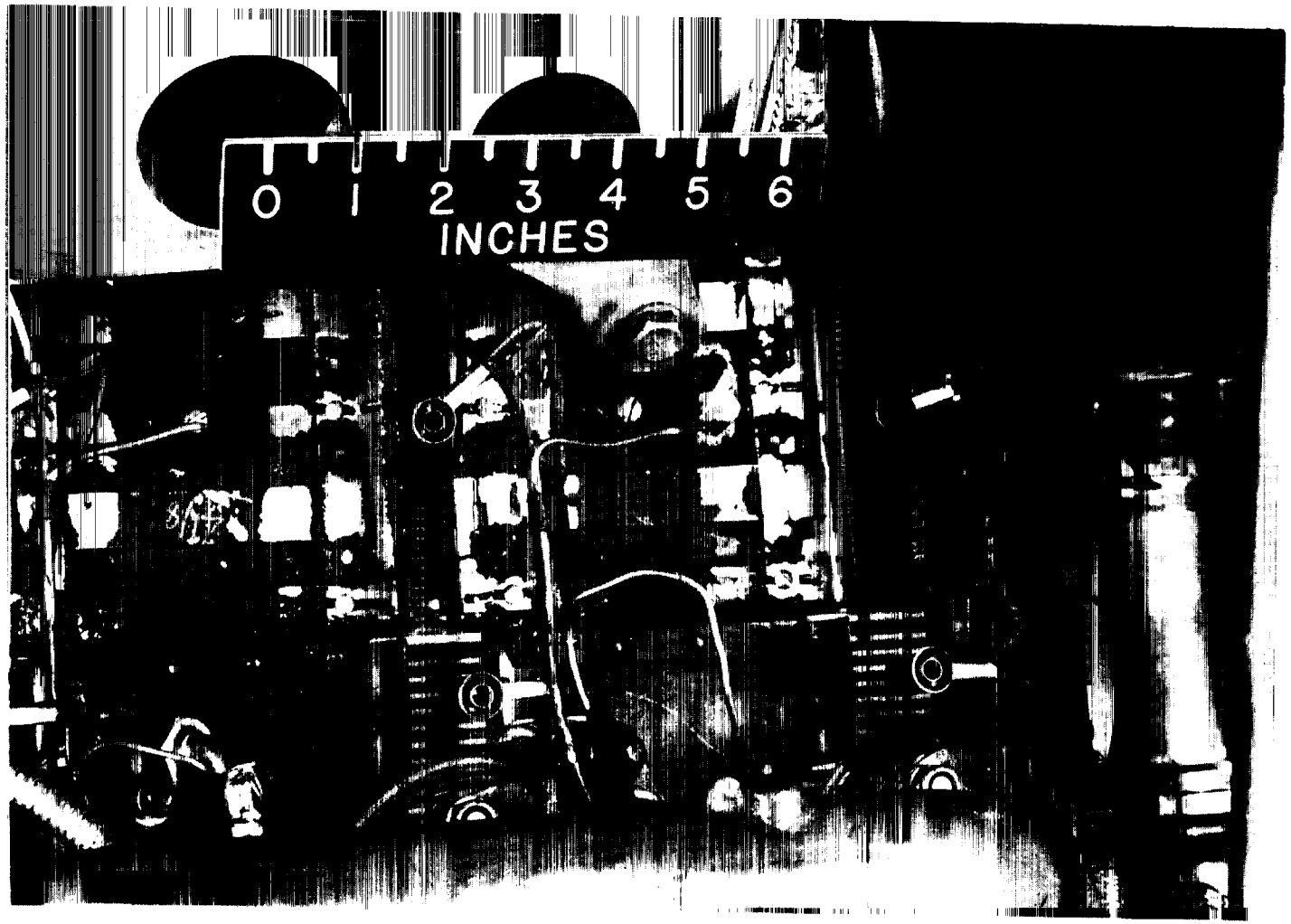

(c) Turbulent-flow baffles, outboard view.

Figure 6.- Continued.

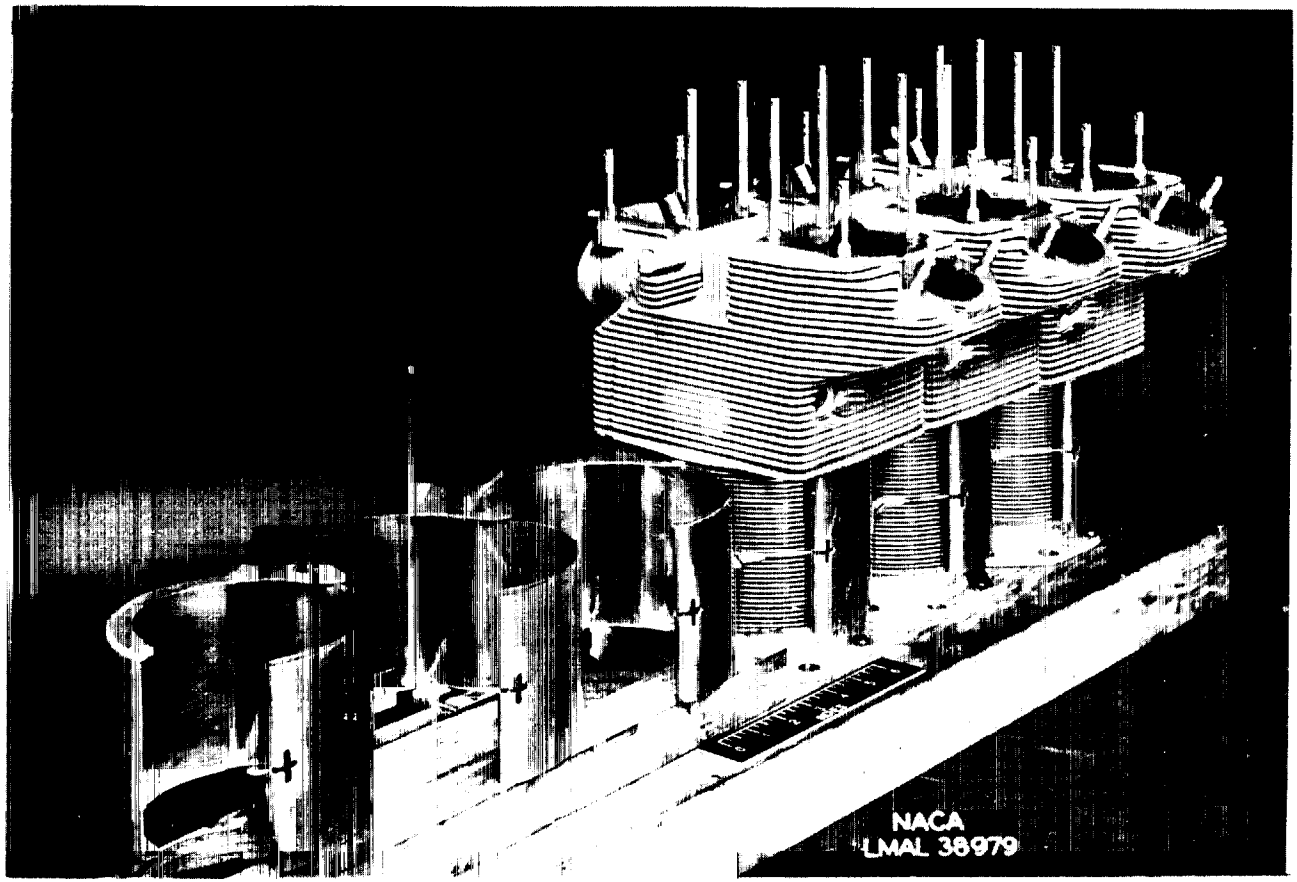

(d) NACA-designed diffuser baffles, inboard view.

Figure 6.- Continued.

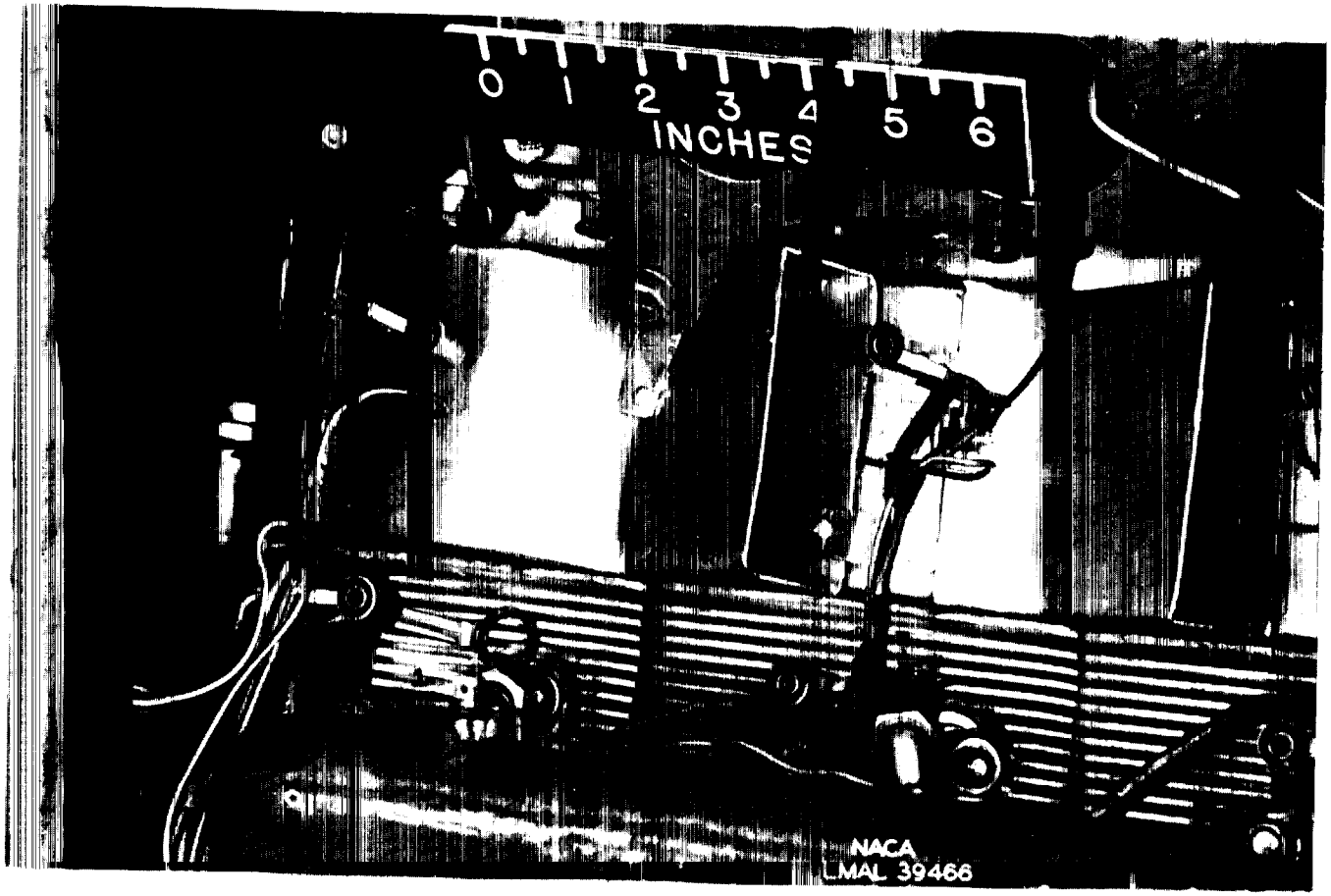

(e) NACA-designed diffuser baffles, outboard view.

Figure 6.- Concluded.

L-562

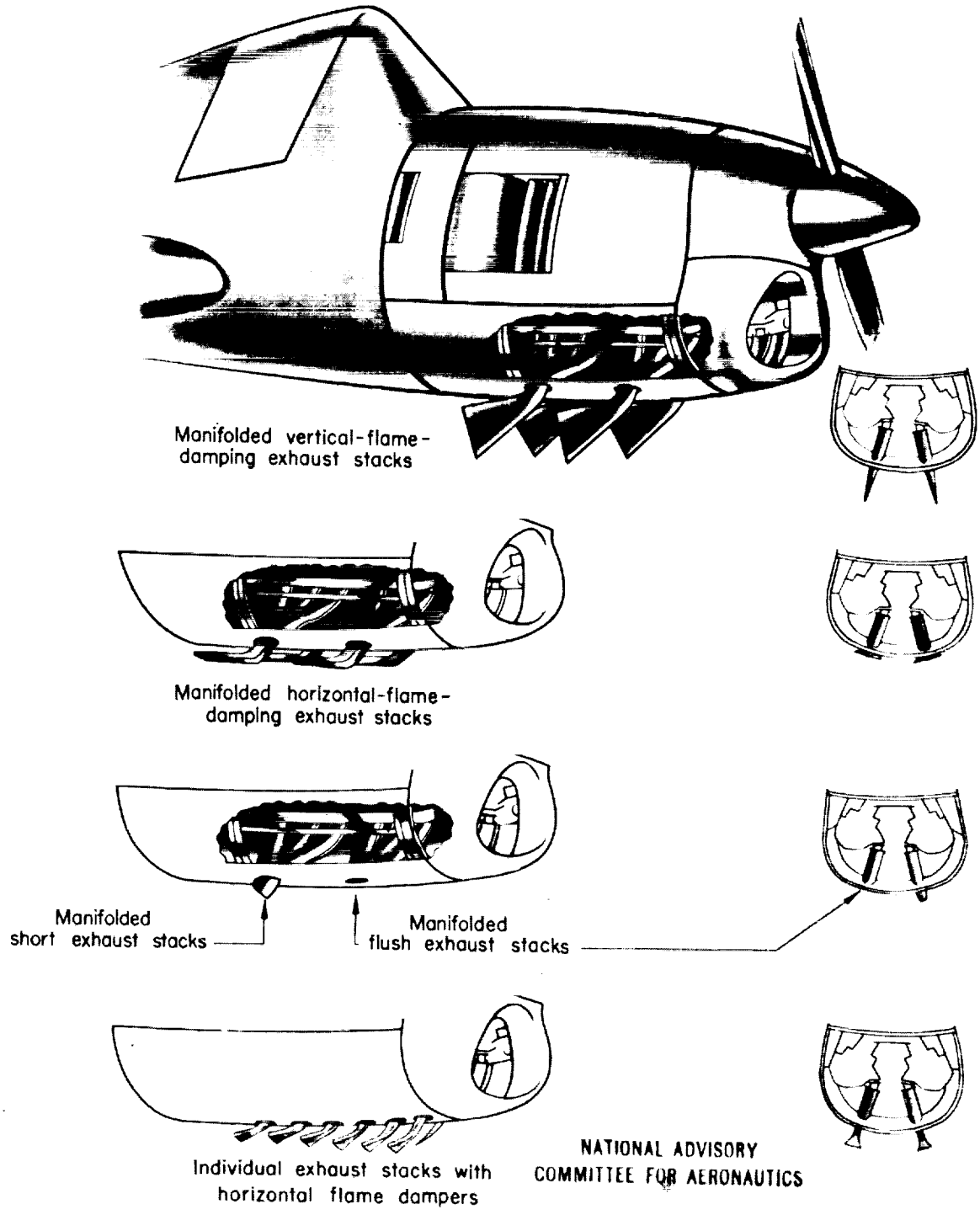

FIGURE 7. – EXHAUST STACK CONFIGURATIONS

(a) Manifolded horizontal-flame-damping exhaust stacks.

Figure 8.- Exhaust stack details.

(b) Manifolded vertical-flame-damping exhaust stacks.

Figure 8.- Continued.

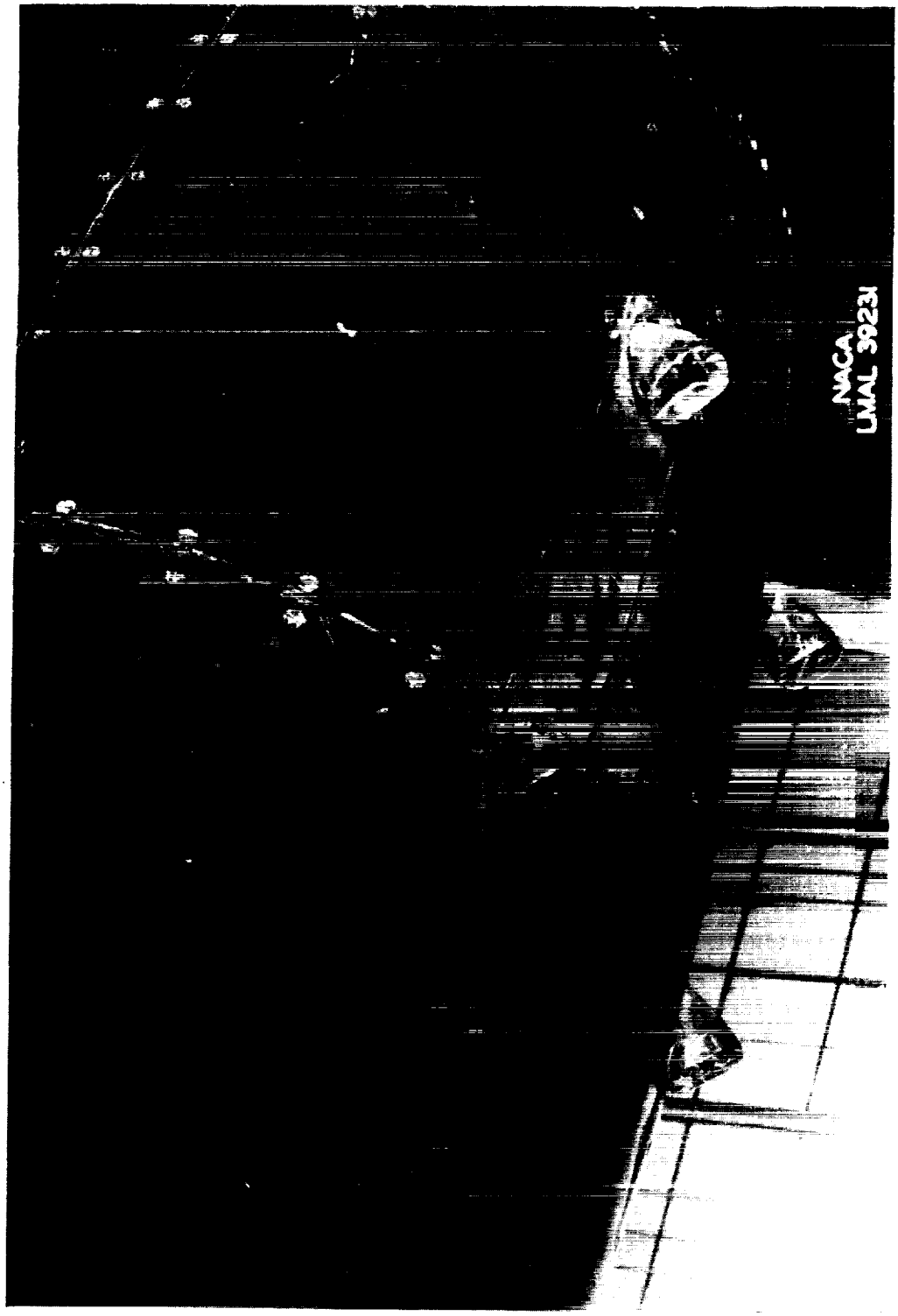

(c) Manifolded short exhaust stacks.

Figure 8.- Continued.

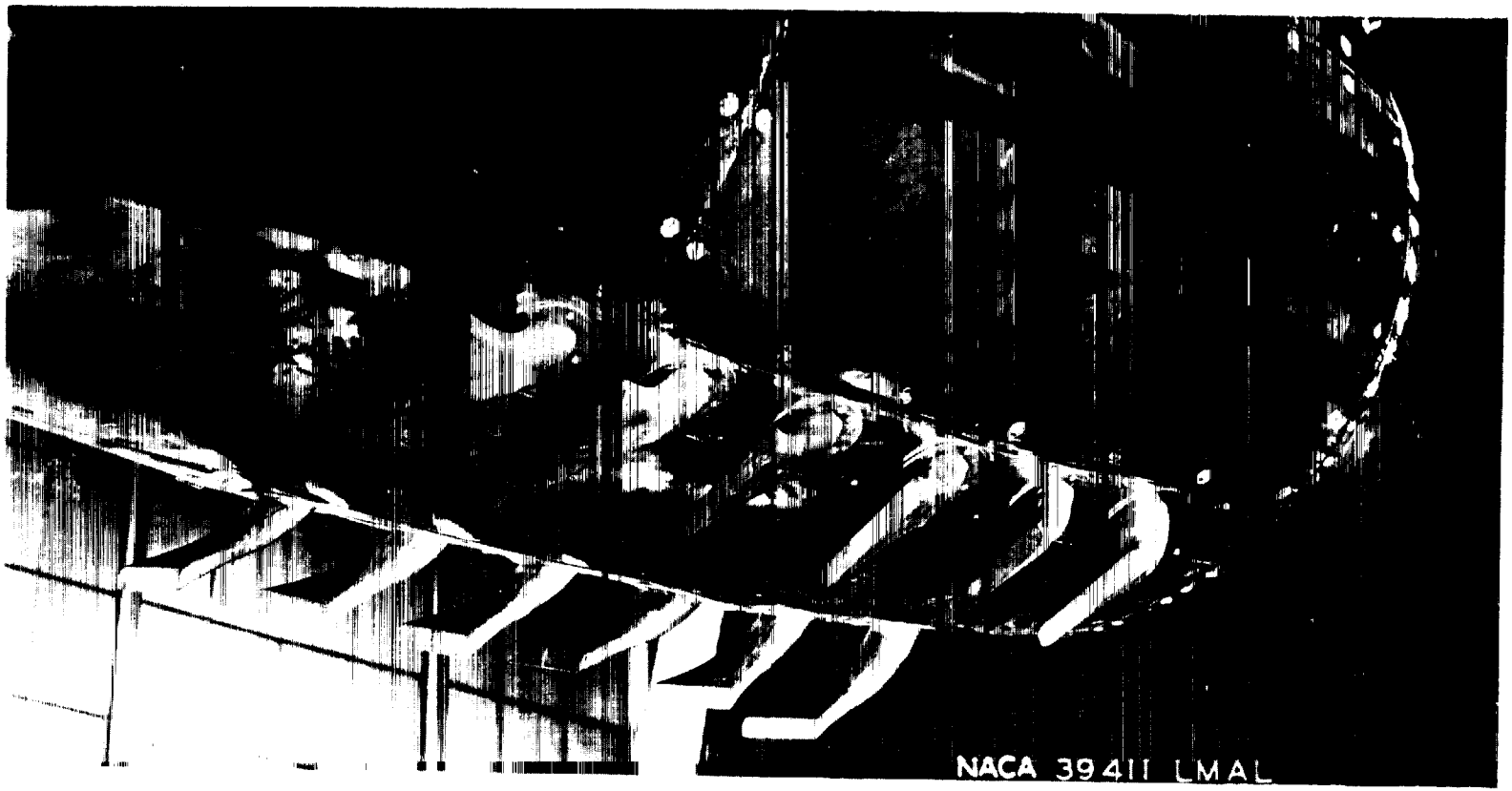

(d) Mocked-up individual exhaust stacks with horizontal flame dampers.

Figure 8.- Concluded.

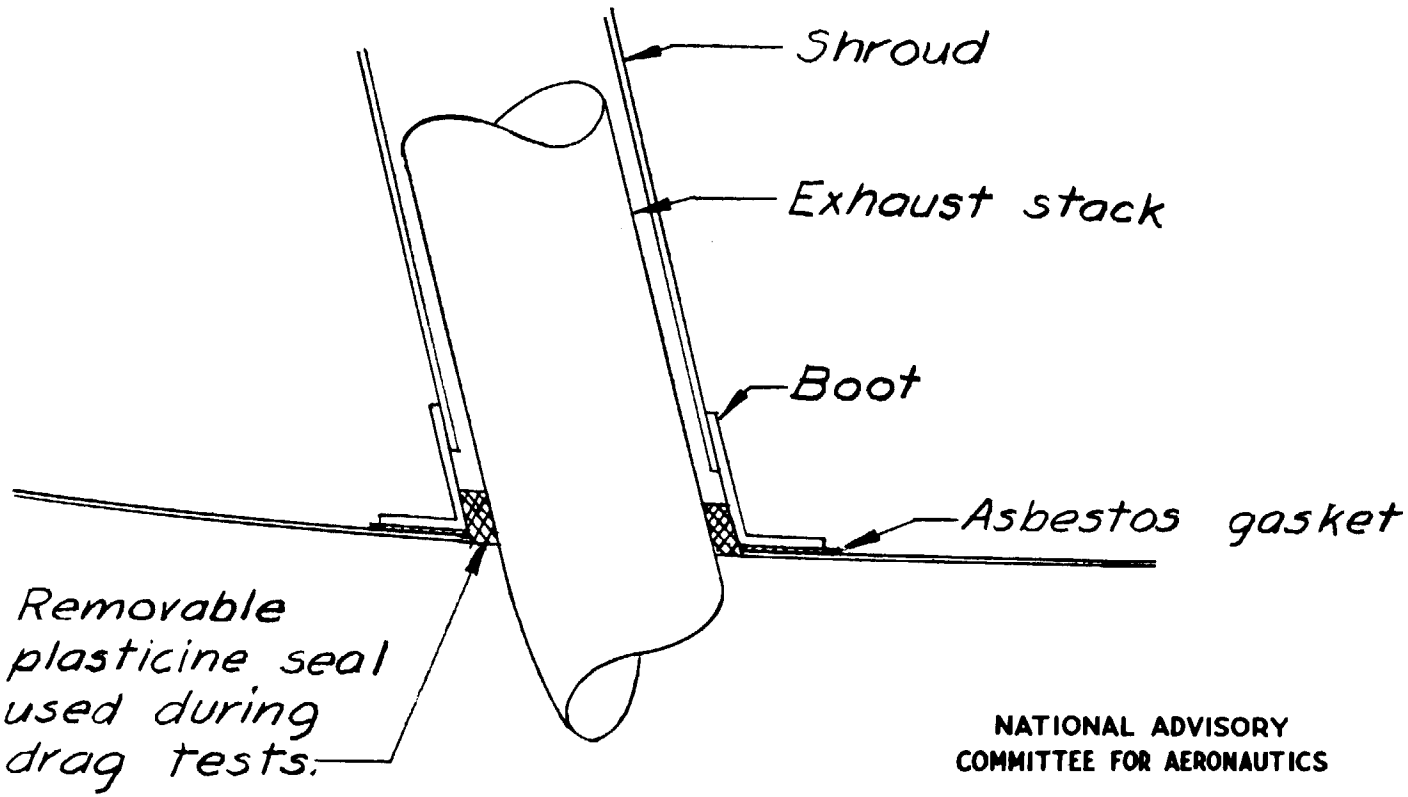

Figure 9. —Details of exhaust-stack-shroud exit.

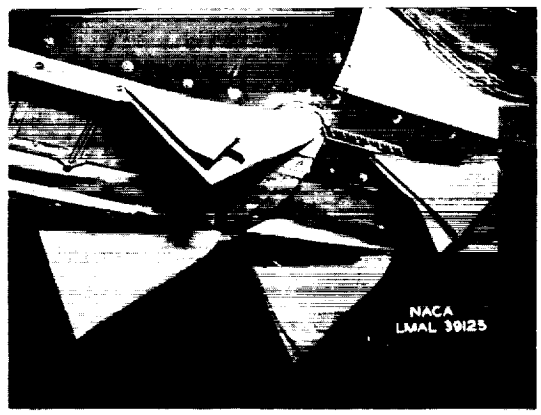

(a) Mild-steel stacks.

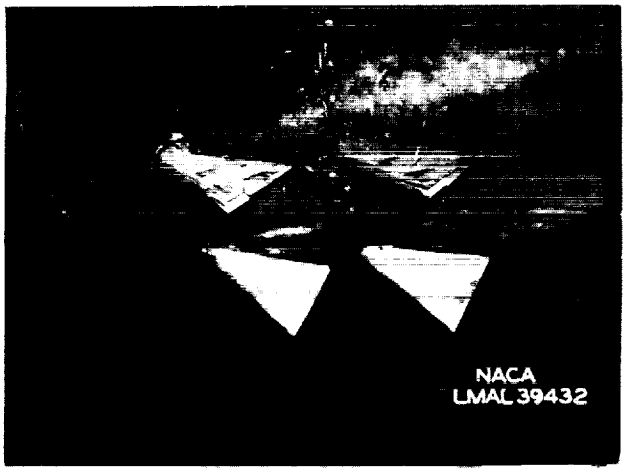

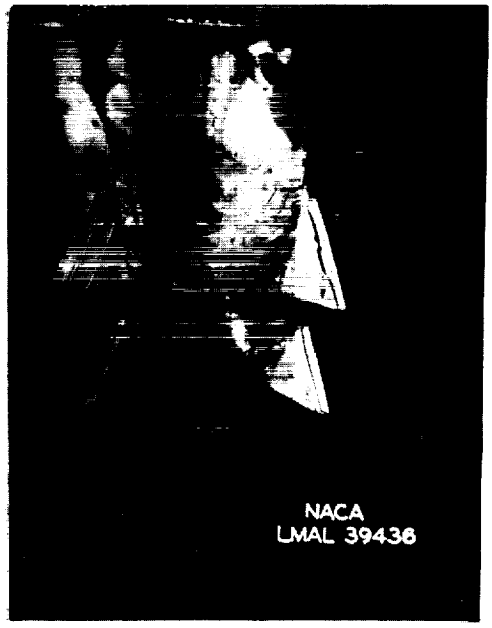

(b) Stainless-steel stacks; flame dampers stiffened with beads and braced by cross struts.

Figure 10.- Views of vertical flame dampers which failed during testing.

L-562

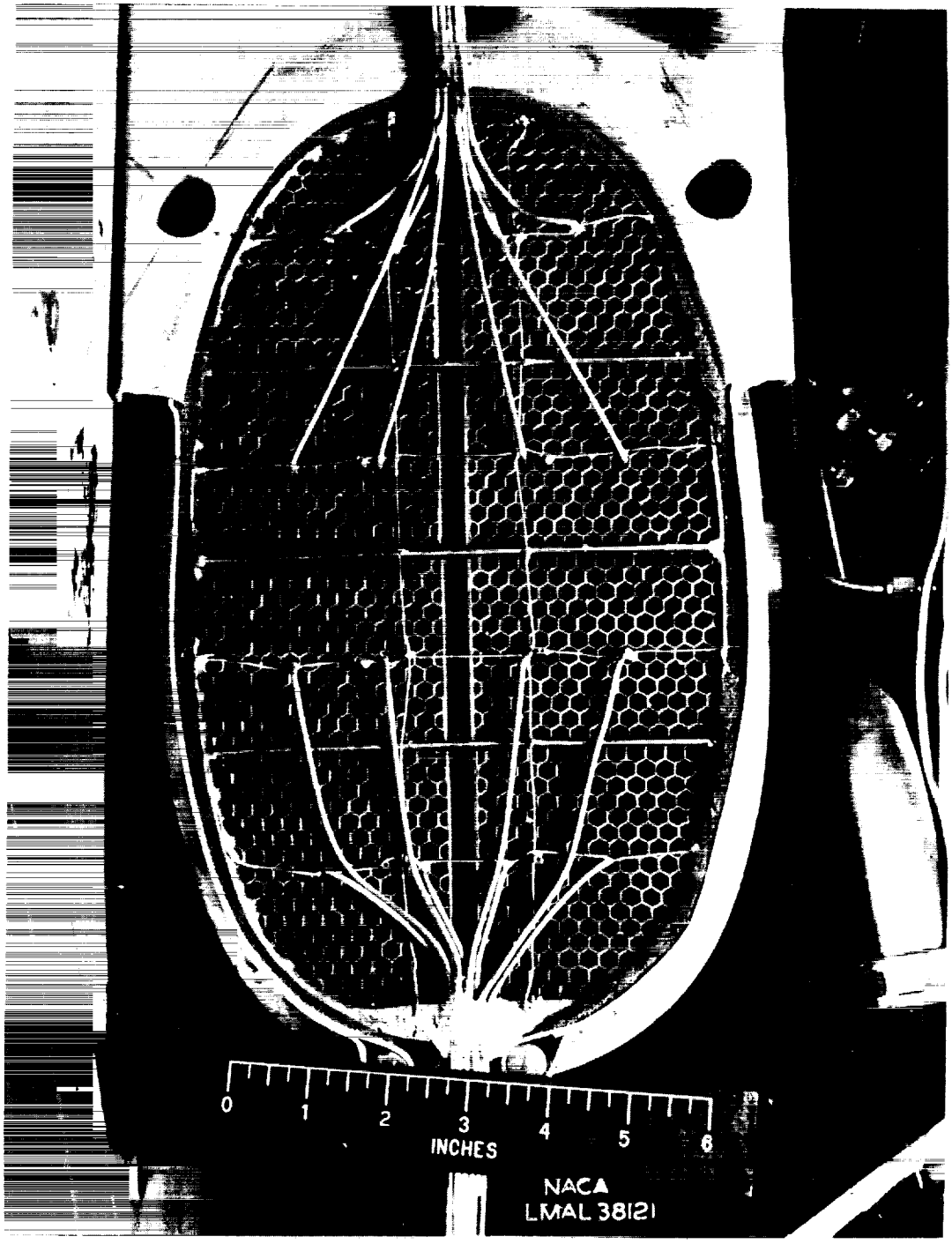

Figure 11.- View of rear face of oil cooler.

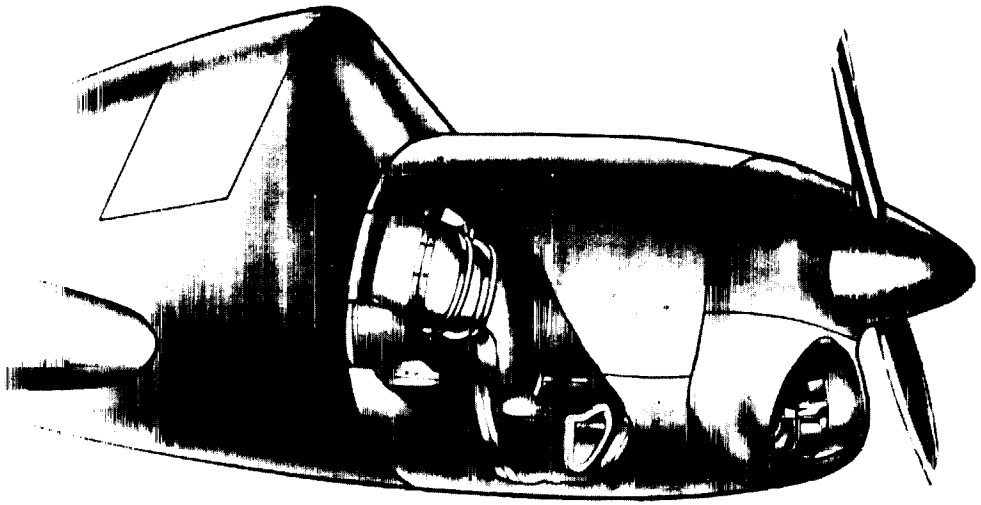

Oil cooler installation

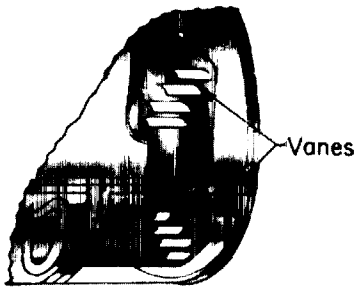

Oil cooler inlet duct

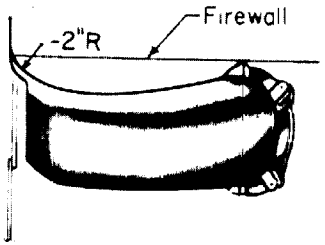

Original duct for shutter exit

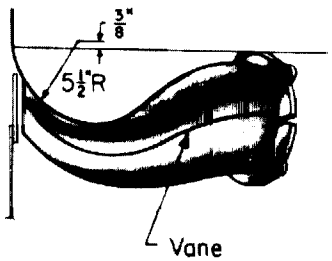

Modified duct for shutter exit

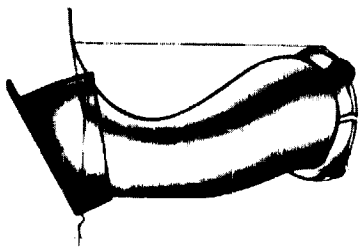

Duct for flap exit

FIGURE 12 - OIL-COOLER DUCT CONFIGURATIONS

NATIONAL ADVISORY
COMMITTEE FOR AERONAUTICS

MR No. L5I12b

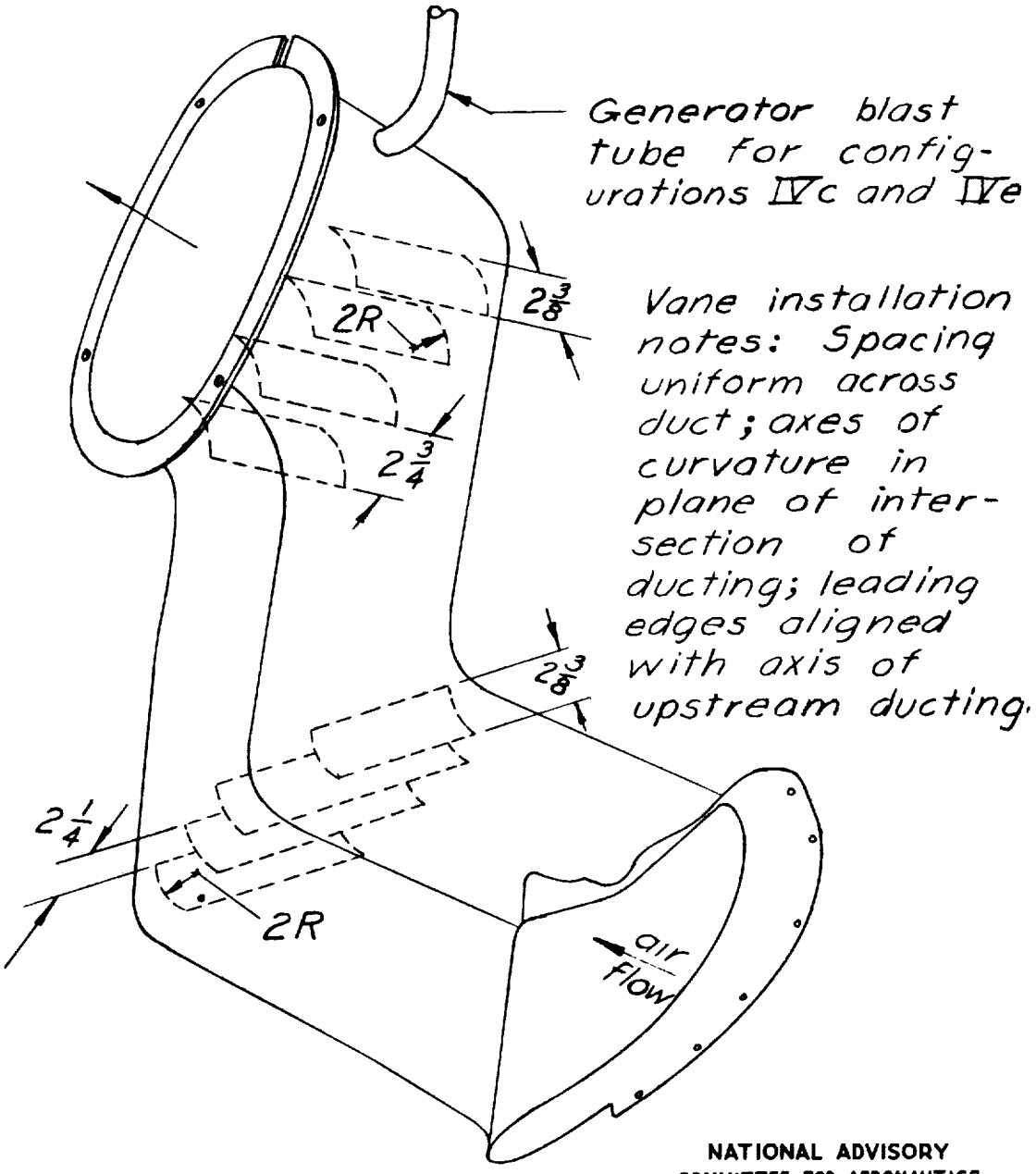

Figure 13. - Oil-cooler-inlet duct showing vanes and generator-blast-tube inlet.

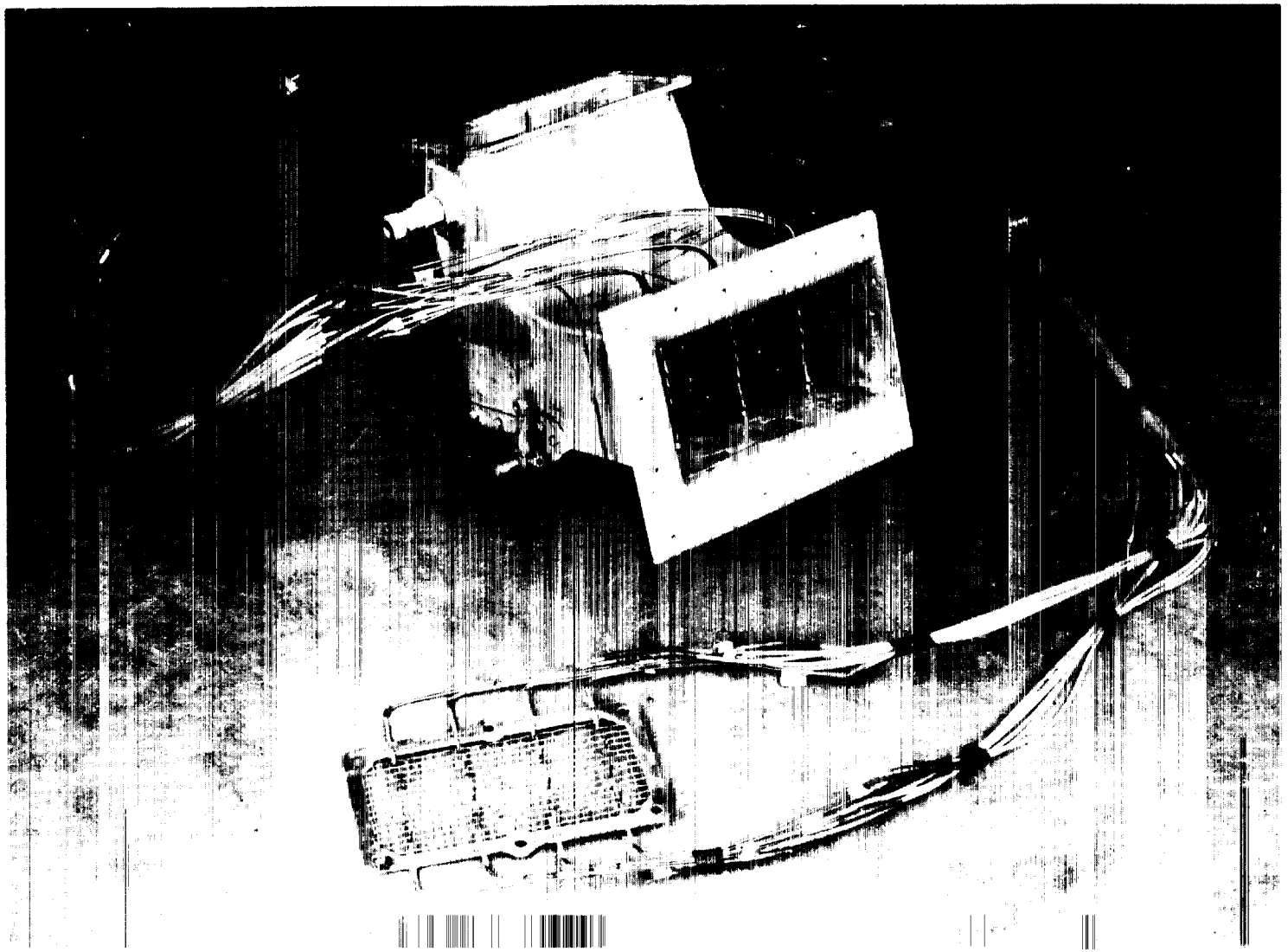

Figure 14.- Carburetor duct and screen.

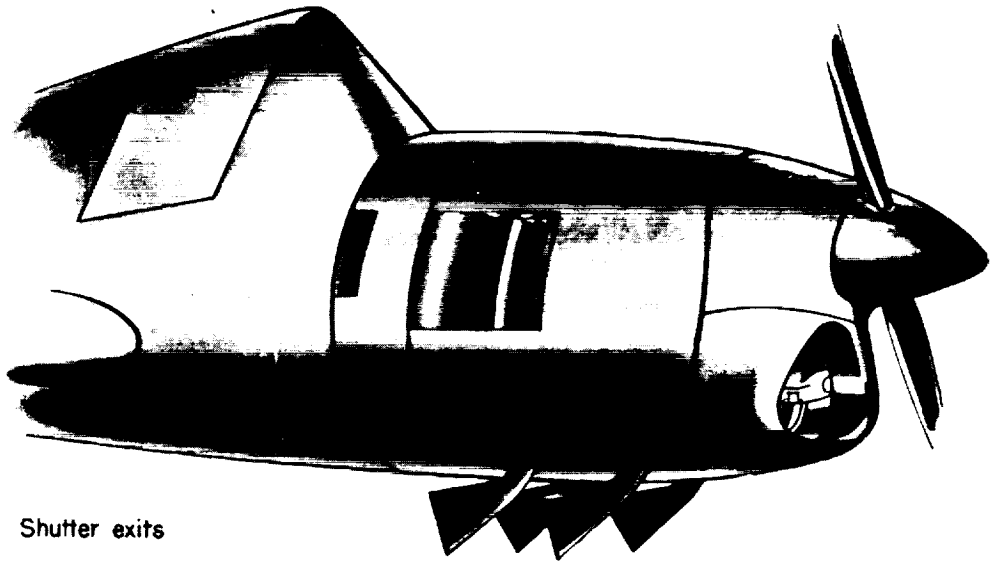

Shutter exits

(Configuration Ia)

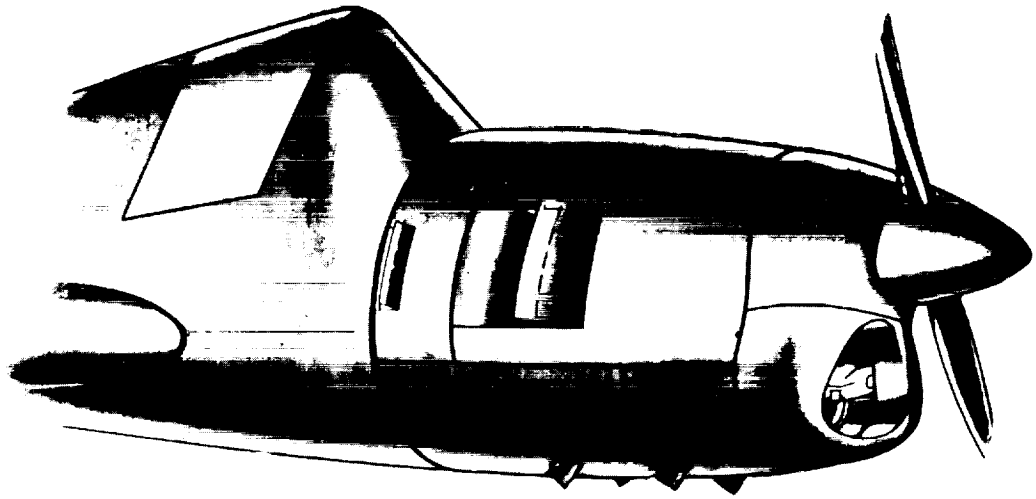

Flap exits

(Configuration IIc)

NATIONAL ADVISORY
COMMITTEE FOR AERONAUTICS

FIGURE 15.- COOLING-AIR-EXIT CONFIGURATIONS

L-562

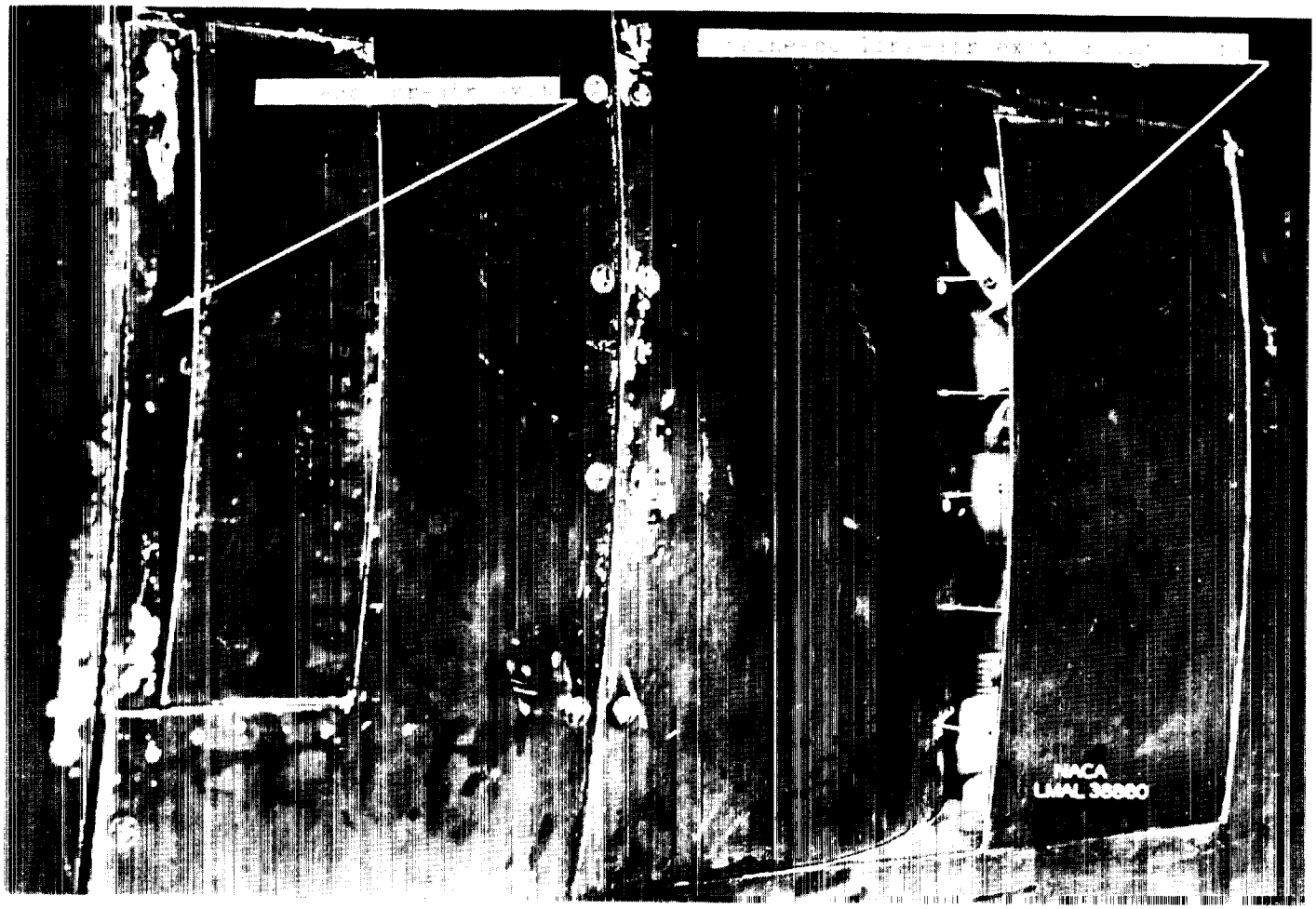

(a) Closed shutter exits.

Figure 16.- Cooling-air exits.

NATIONAL ADVISORY COMMITTEE FOR AERONAUTICS
LANGLEY MEMORIAL AERONAUTICAL LABORATORY - LANGLEY FIELD, VA.

MR No. L5I12b

(b) Closed flap exits.

Figure 16.- Continued.

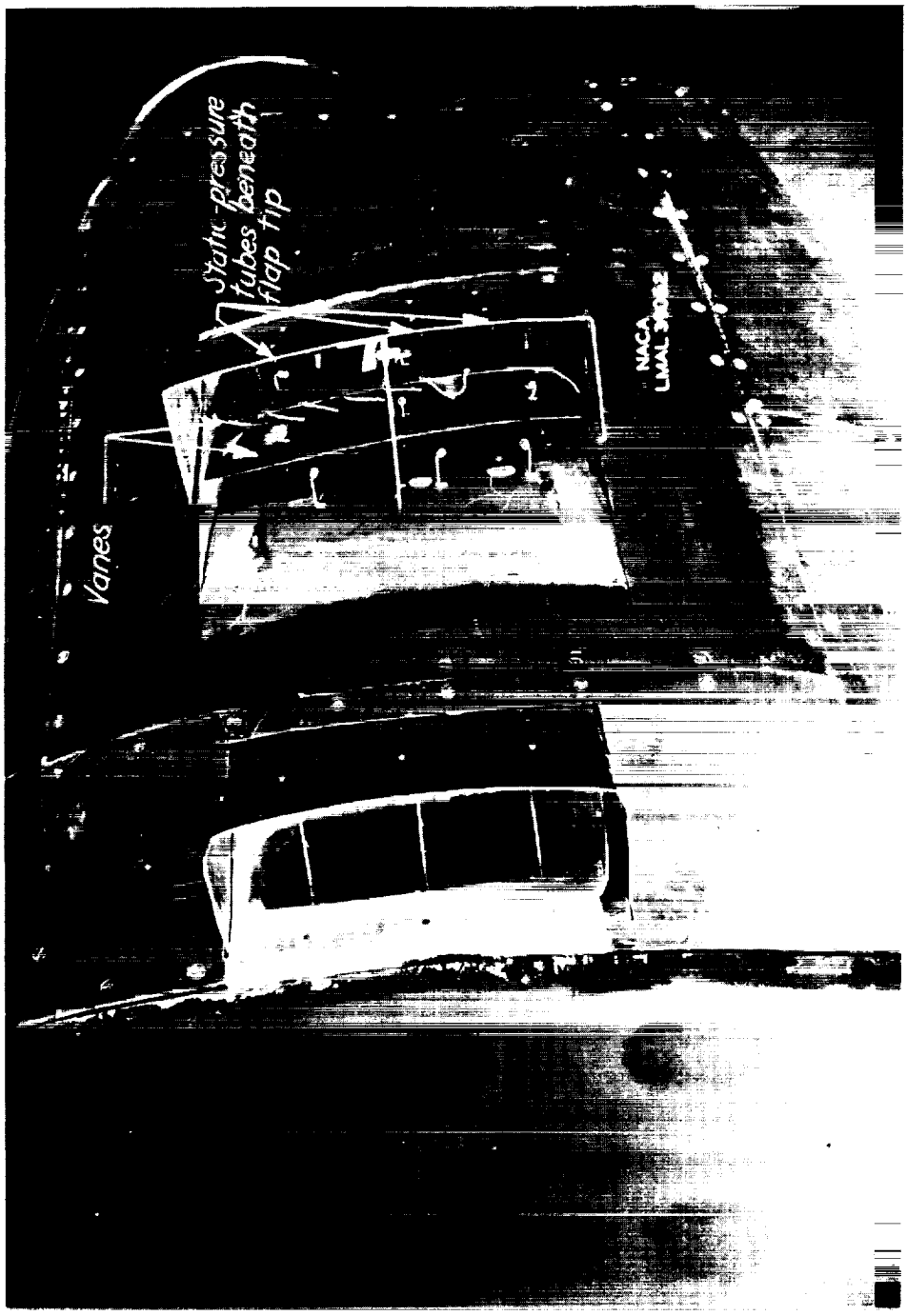

(c) Open flapped exits.

Figure 16.- Concluded.

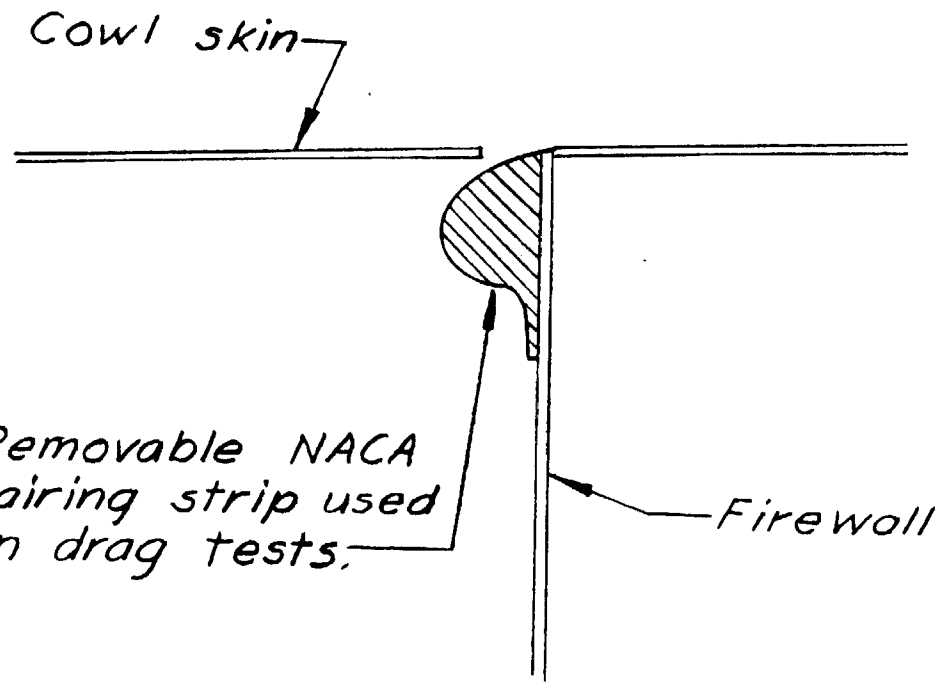

NATIONAL ADVISORY
COMMITTEE FOR AERONAUTICS

Figure 17.- Details of accessory-compartment exit gap at firewall.

MR No. L5112b

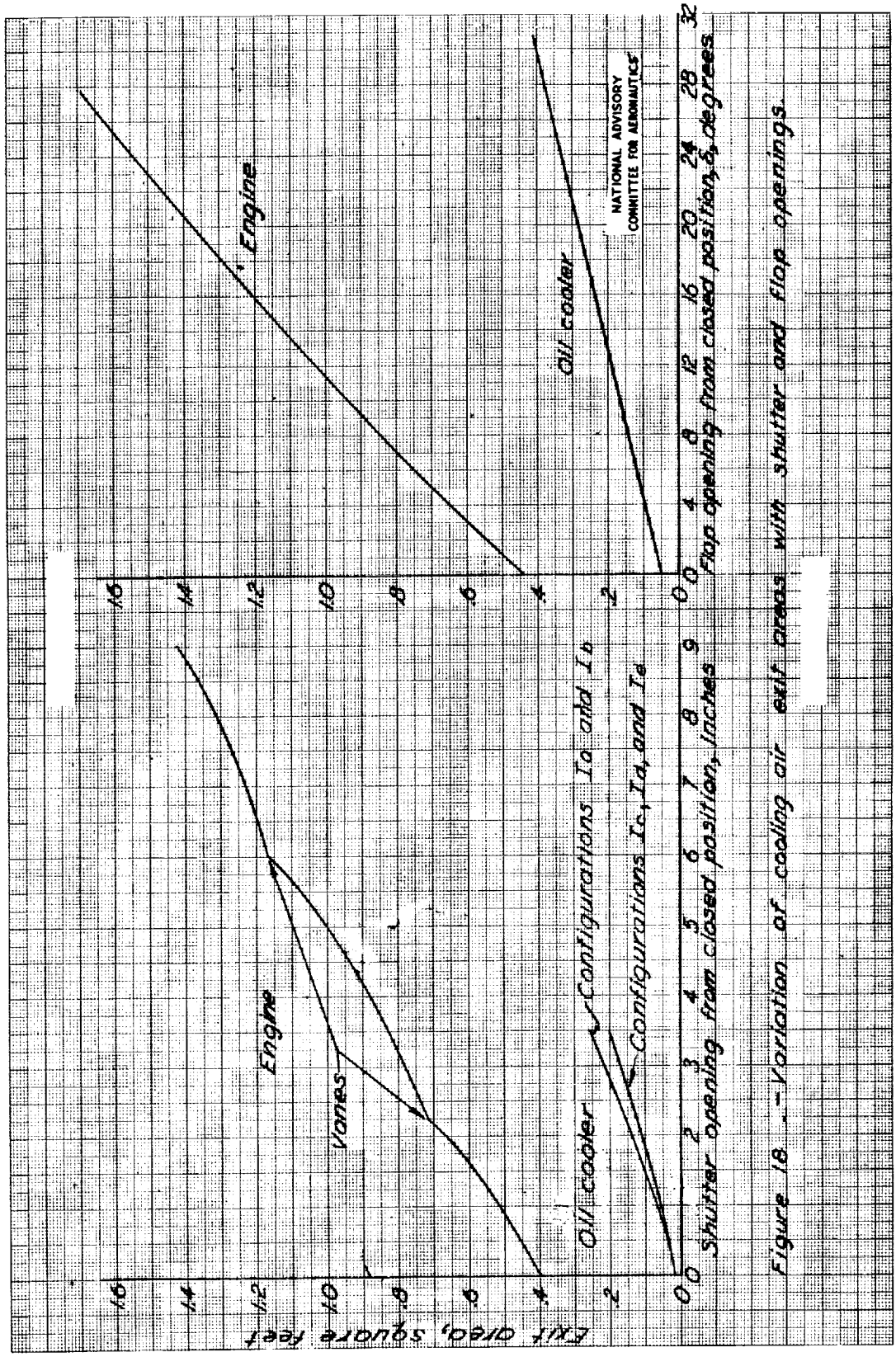

Figure 18.- Variation of cooling air exit areas with shutter and flap openings.

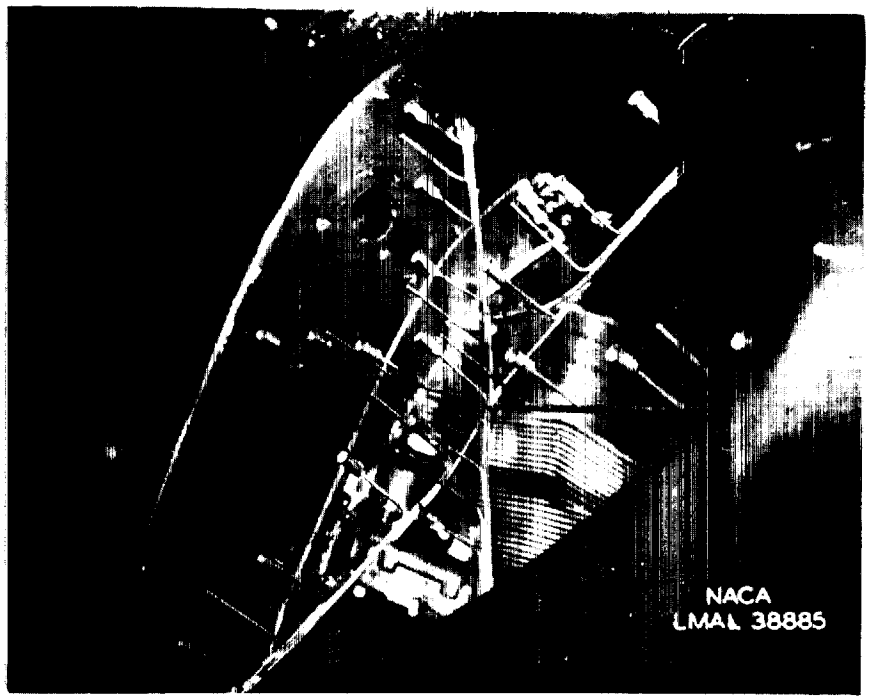

Figure 19.- Generator blast-tube inlet at top of cowl inlet; configuration Ia.

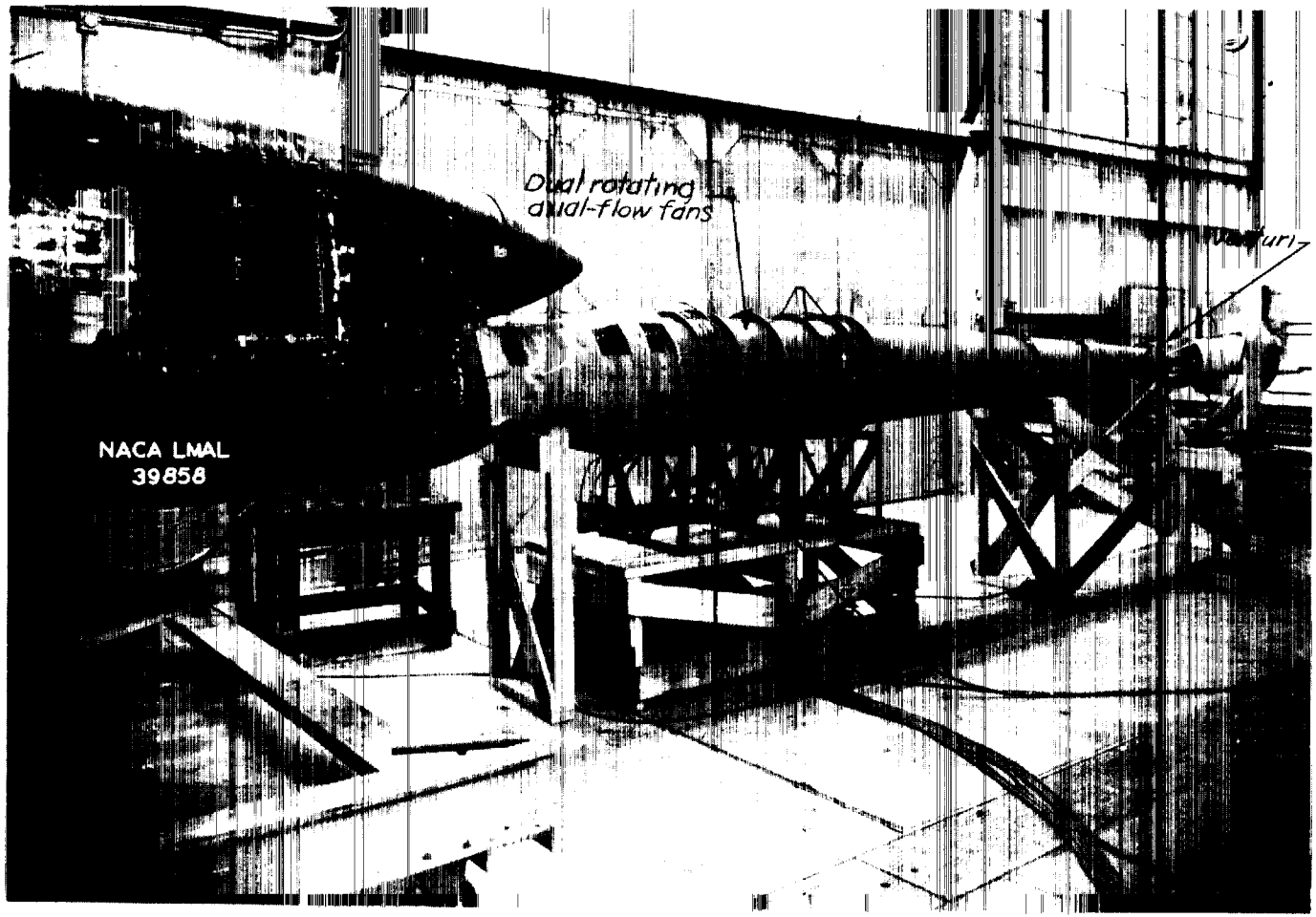

Figure 20.- Setup for air-flow calibration of engine, oil cooler, and cowl leakage areas.

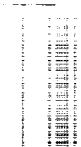

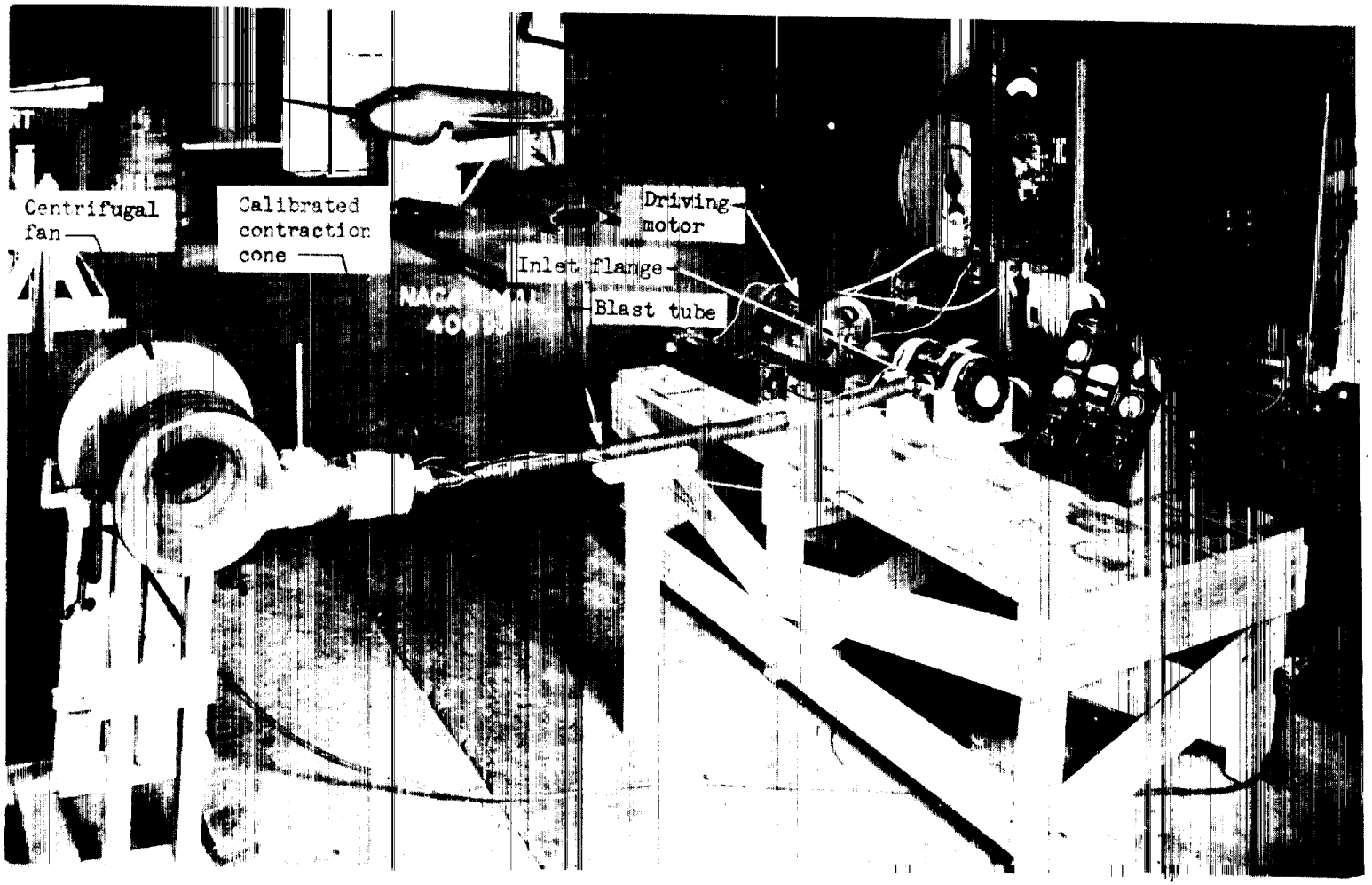

Figure 21.- Setup for air-flow calibrations of generator and blast tube.

MR No. L5I12b

$\Delta P_e = \overline{H_f} - \overline{p_r}$

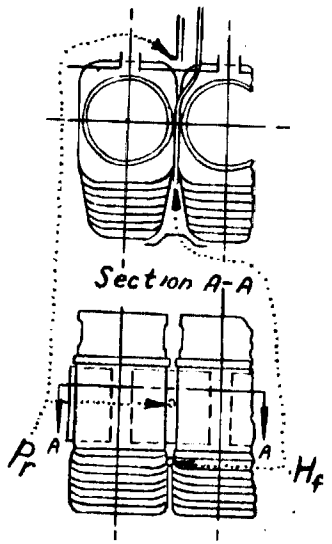

Location of engine pressure tubes

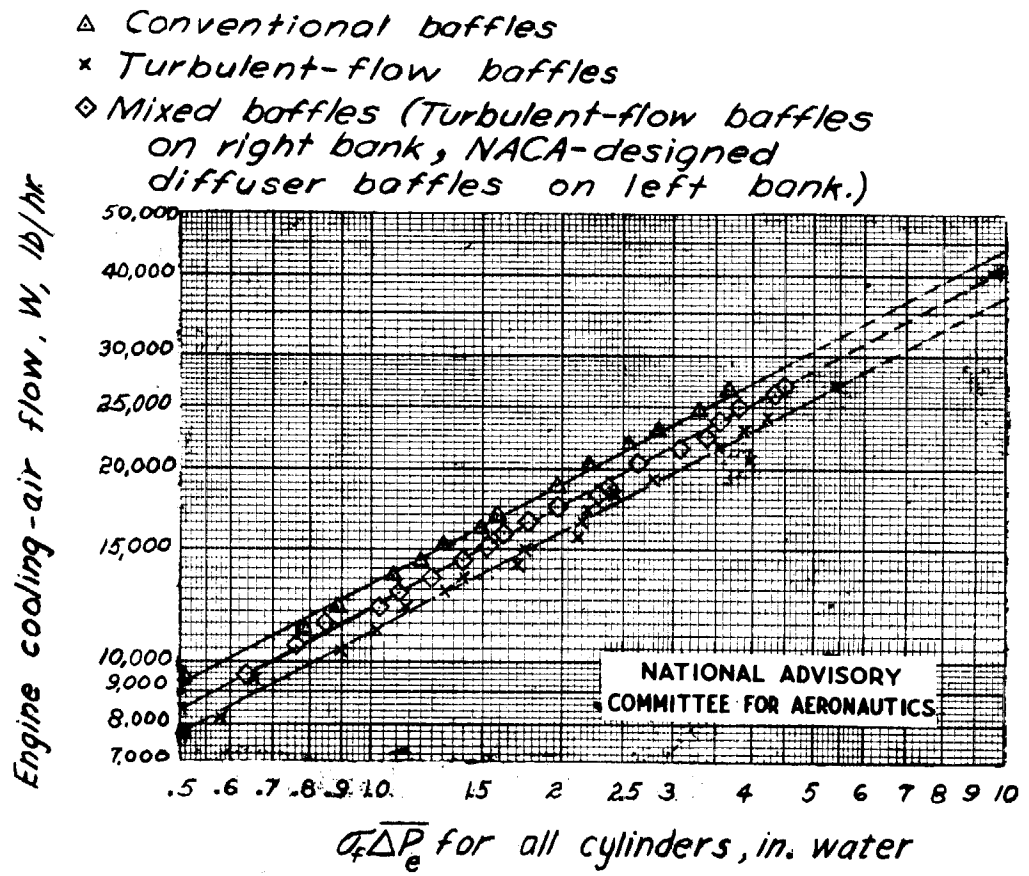

Figure 22.- Ground-stand calibration of cooling-air flow through engine.

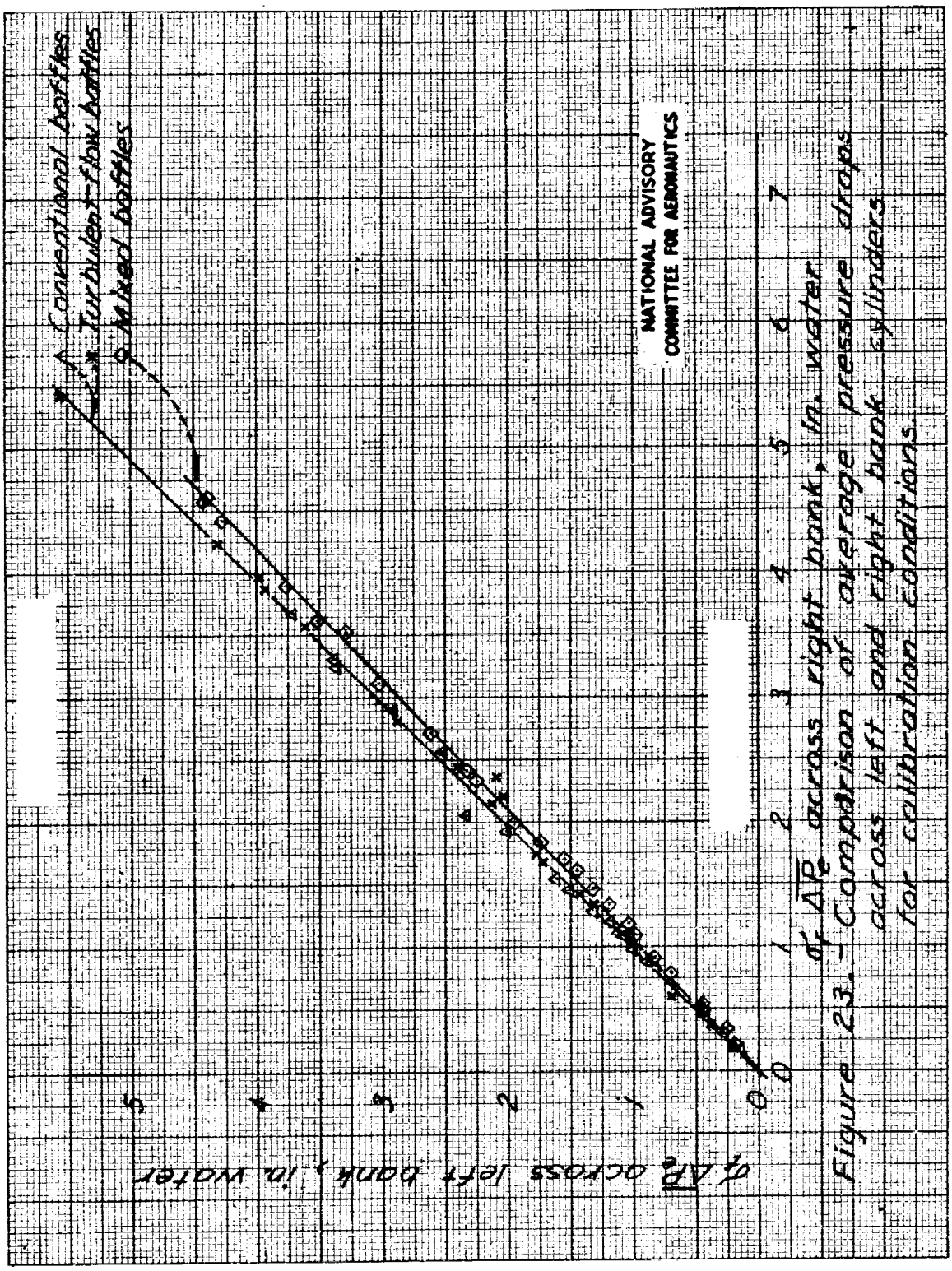

Figure 23.- Comparison of average pressure drops across left and right bank cylinders for calibration conditions.

L-562

L-562

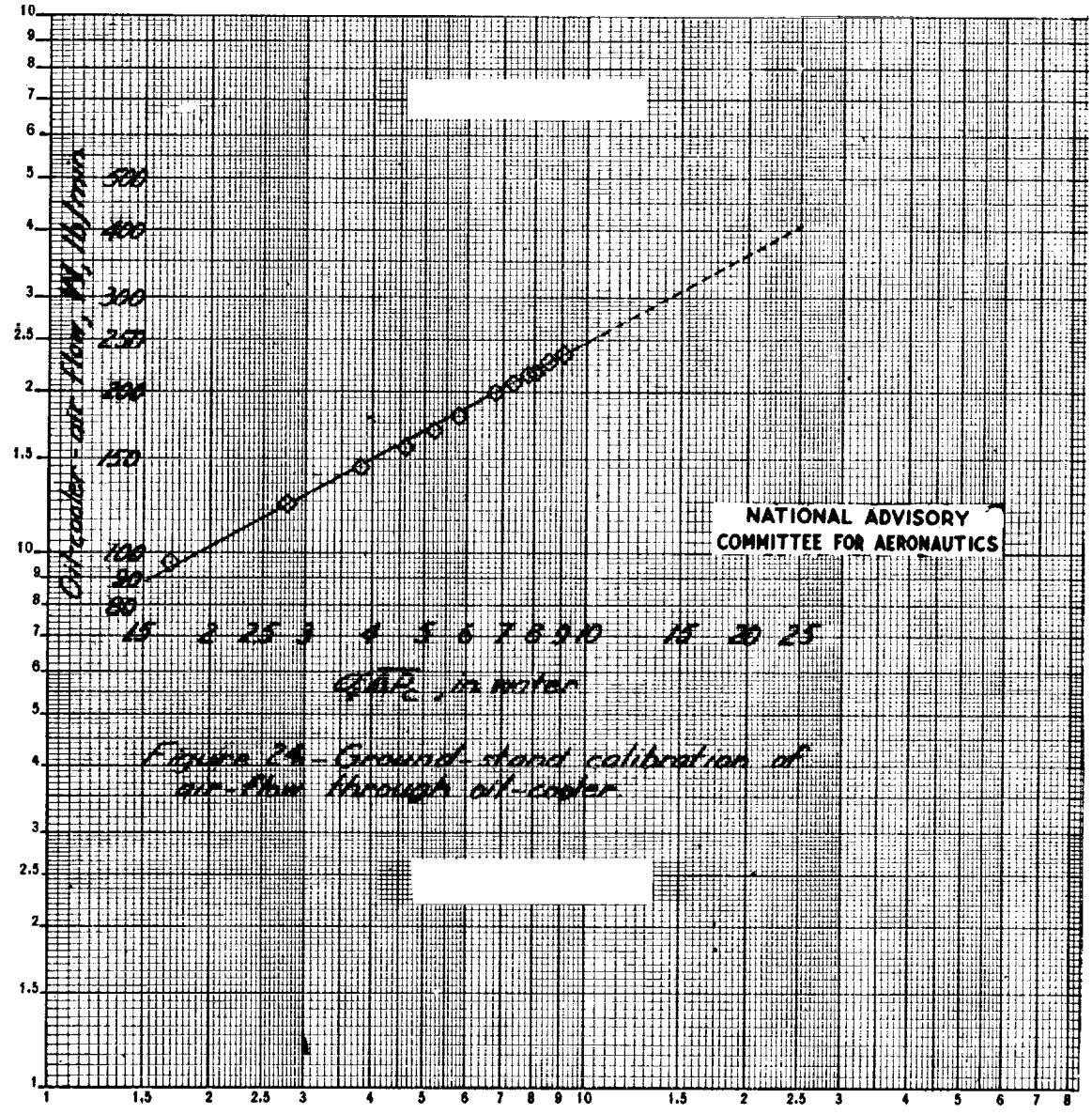

Figure 24.- Ground-stand calibration of air-flow through oil-cooler.

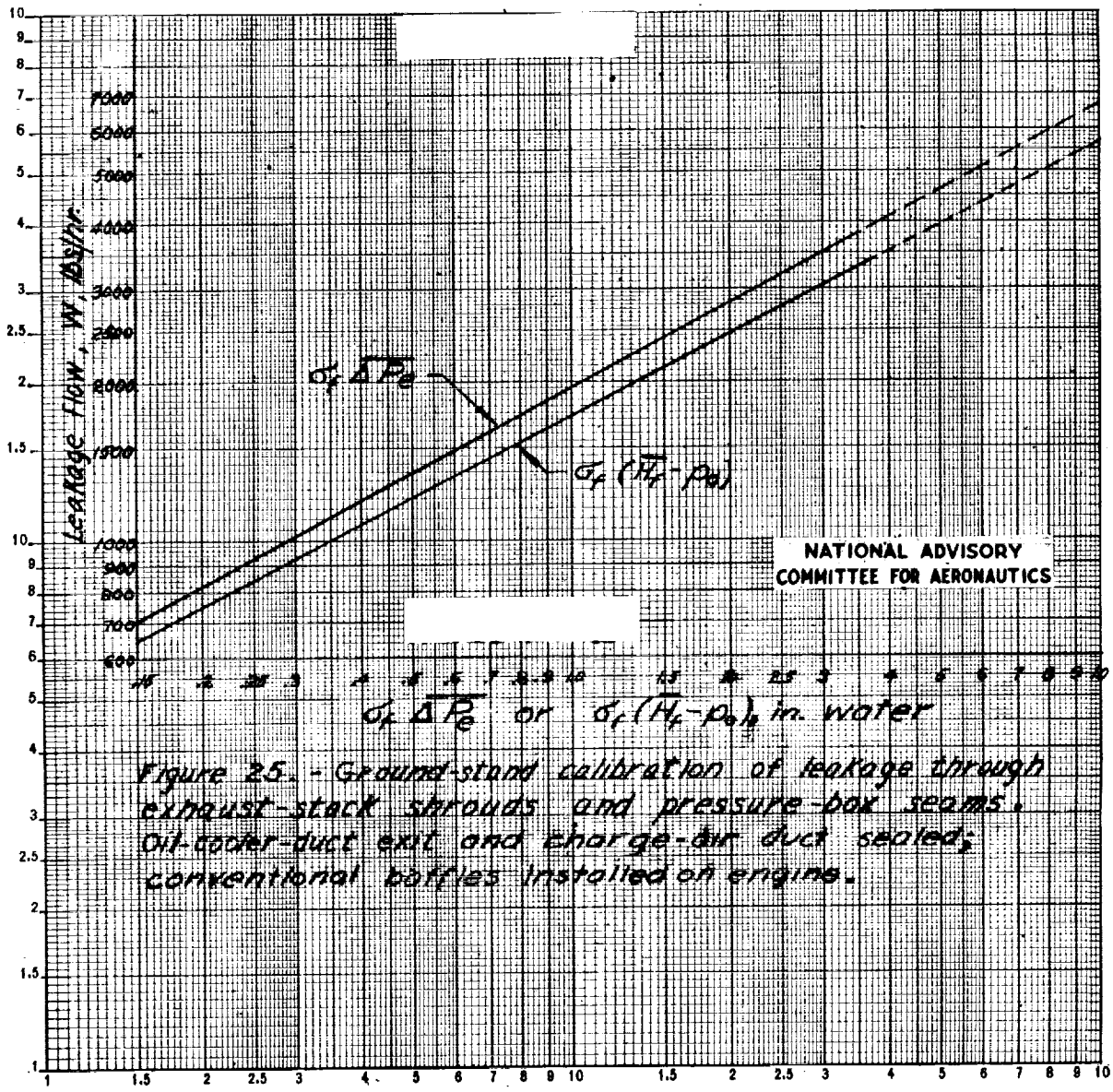

Figure 25. - Ground-stand calibration of leakage through exhaust-stack shrouds and pressure-box seams. Oil-cooler-duct exit and charge-air duct sealed; conventional baffles installed on engine.

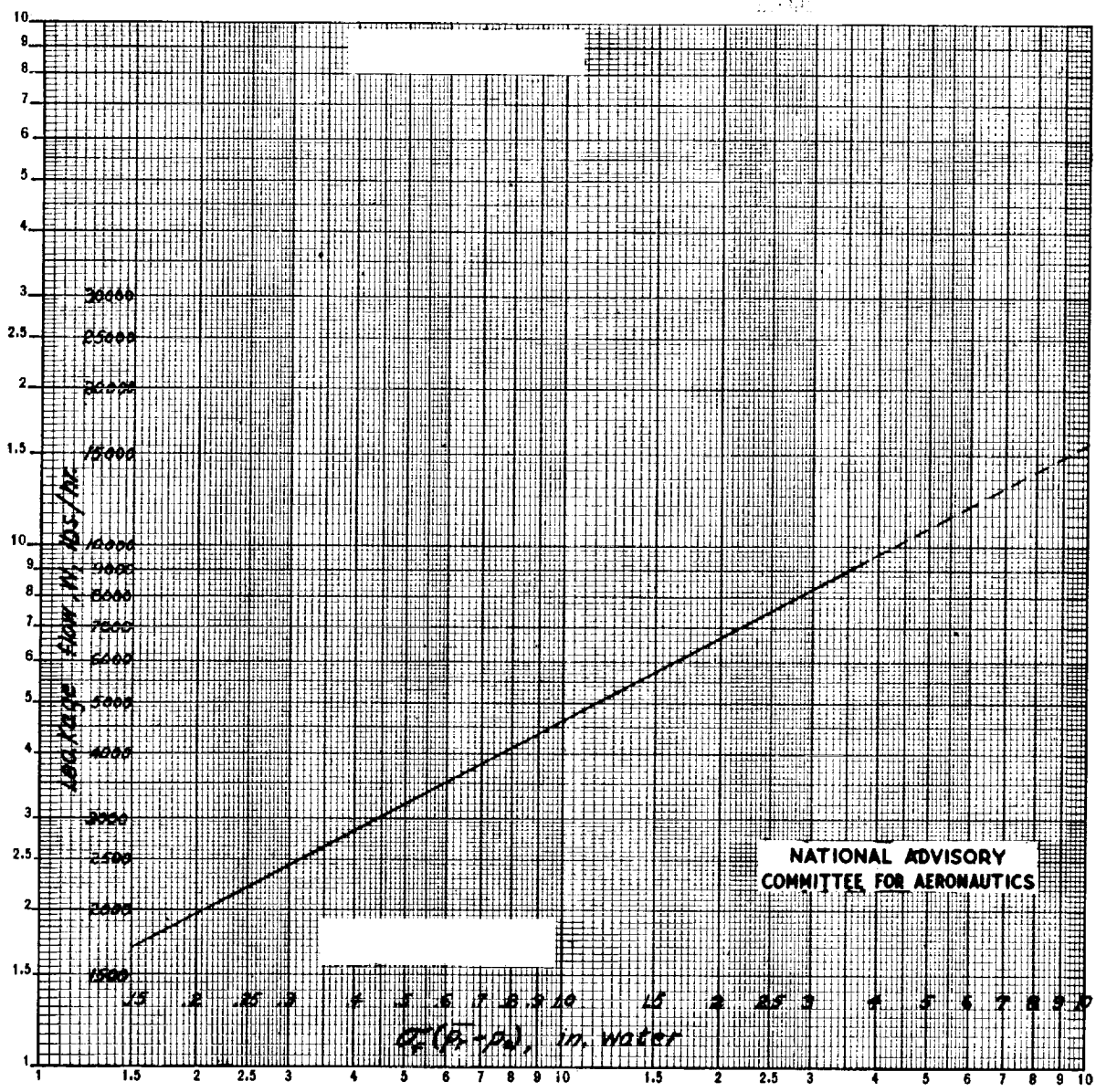

Figure 26.- Ground-stand calibration of leakage through cowl seams downstream of engine and from gap between cowl and firewall. Cowl flaps flush, fairing strip removed from accessory compartment exit.

MR No. L5I12b

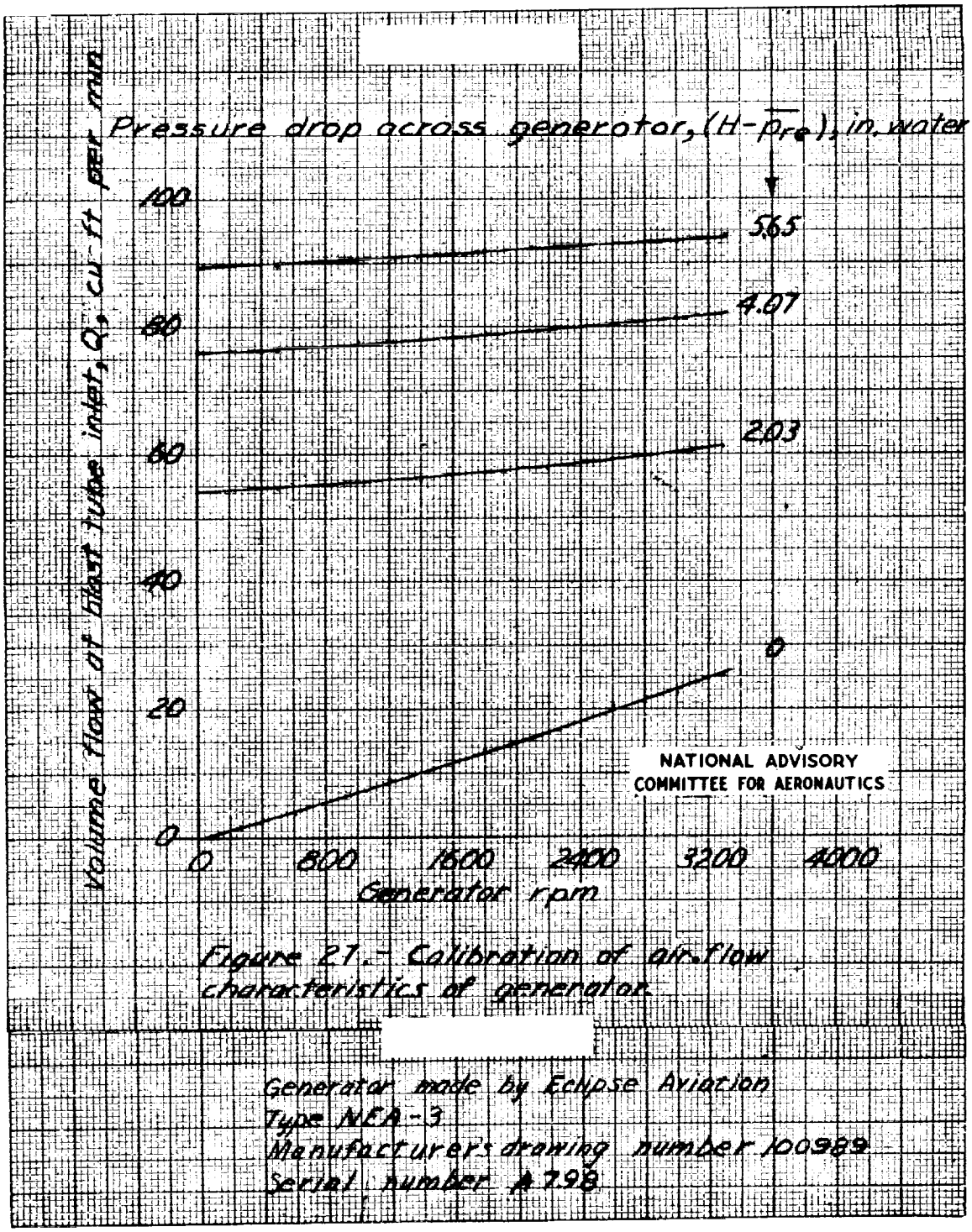

Figure 21.- Calibration of air-flow characteristics of generator.

Generator made by Eclipse Aviation
Type NEA-3
Manufacturer's drawing number 100989
Serial number A 298

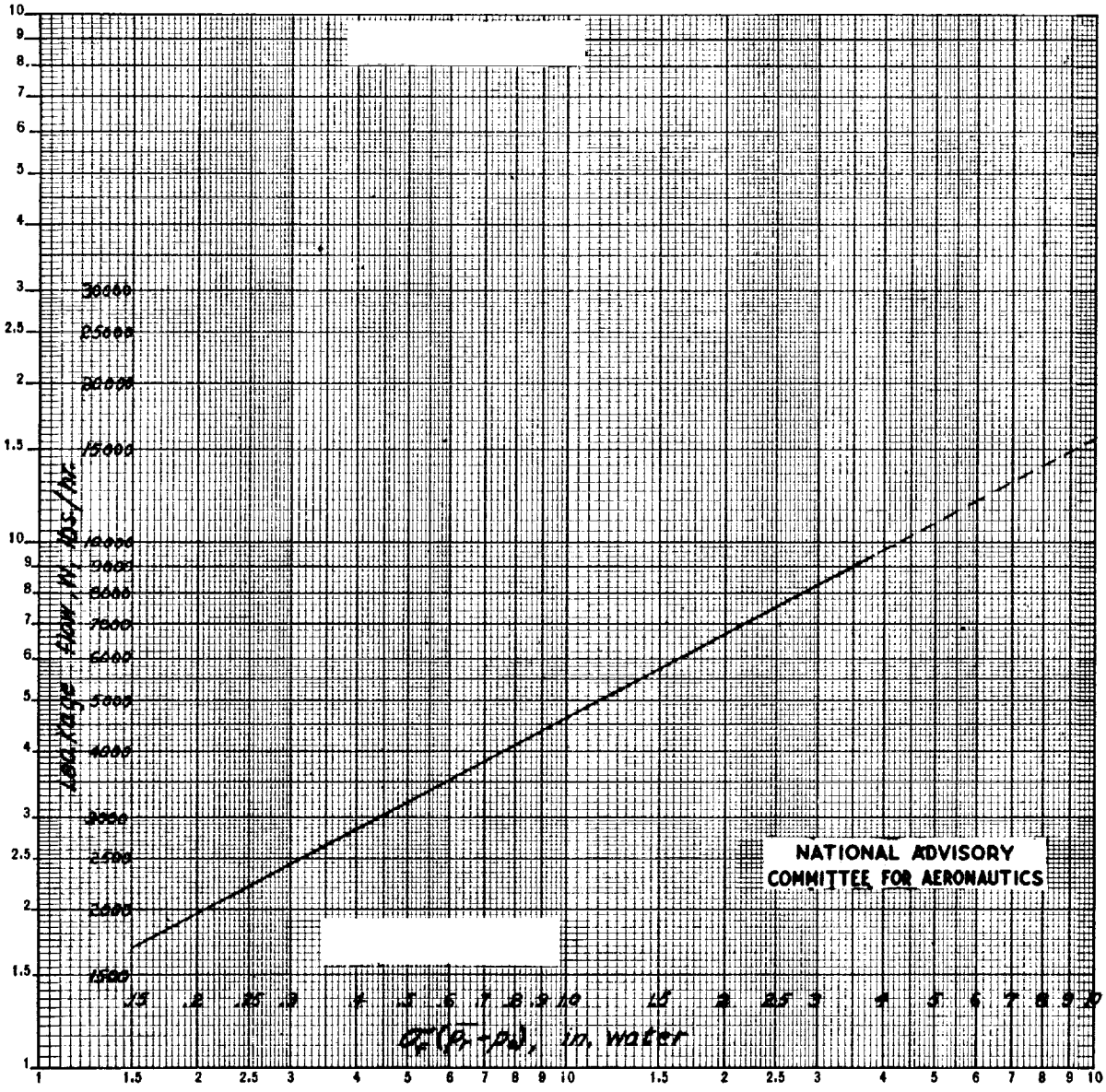

Figure 26.- Ground-stand calibration of leakage through cowl seams downstream of engine and from gap between cowl and firewall. Cowl flaps flush, fairing strip removed from accessory compartment exit.

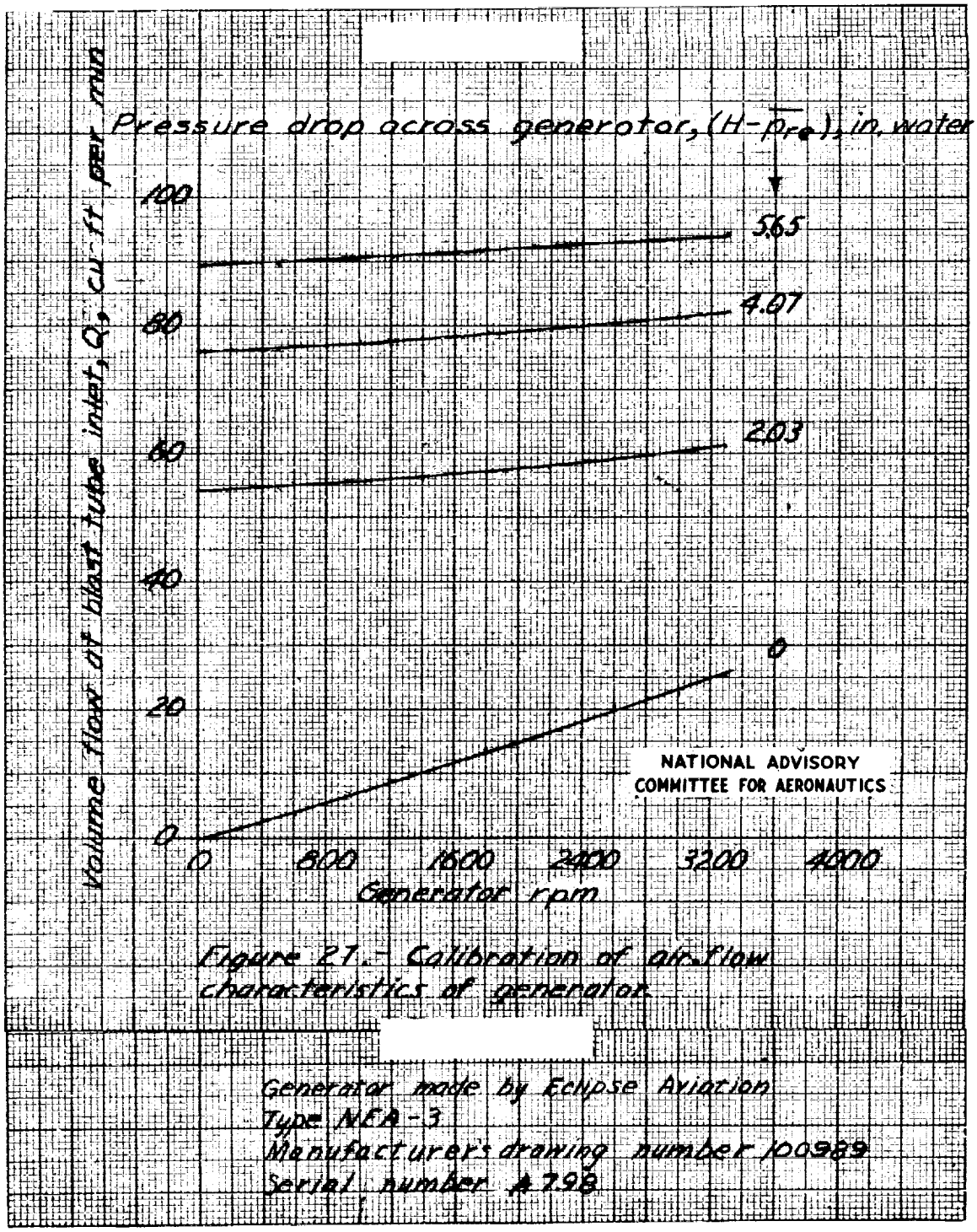

Figure 21.- Calibration of air-flow characteristics of generator.

Generator made by Eclipse Aviation
Type NCA-3
Manufacturer's drawing number 100989
Serial number A 798

L-562

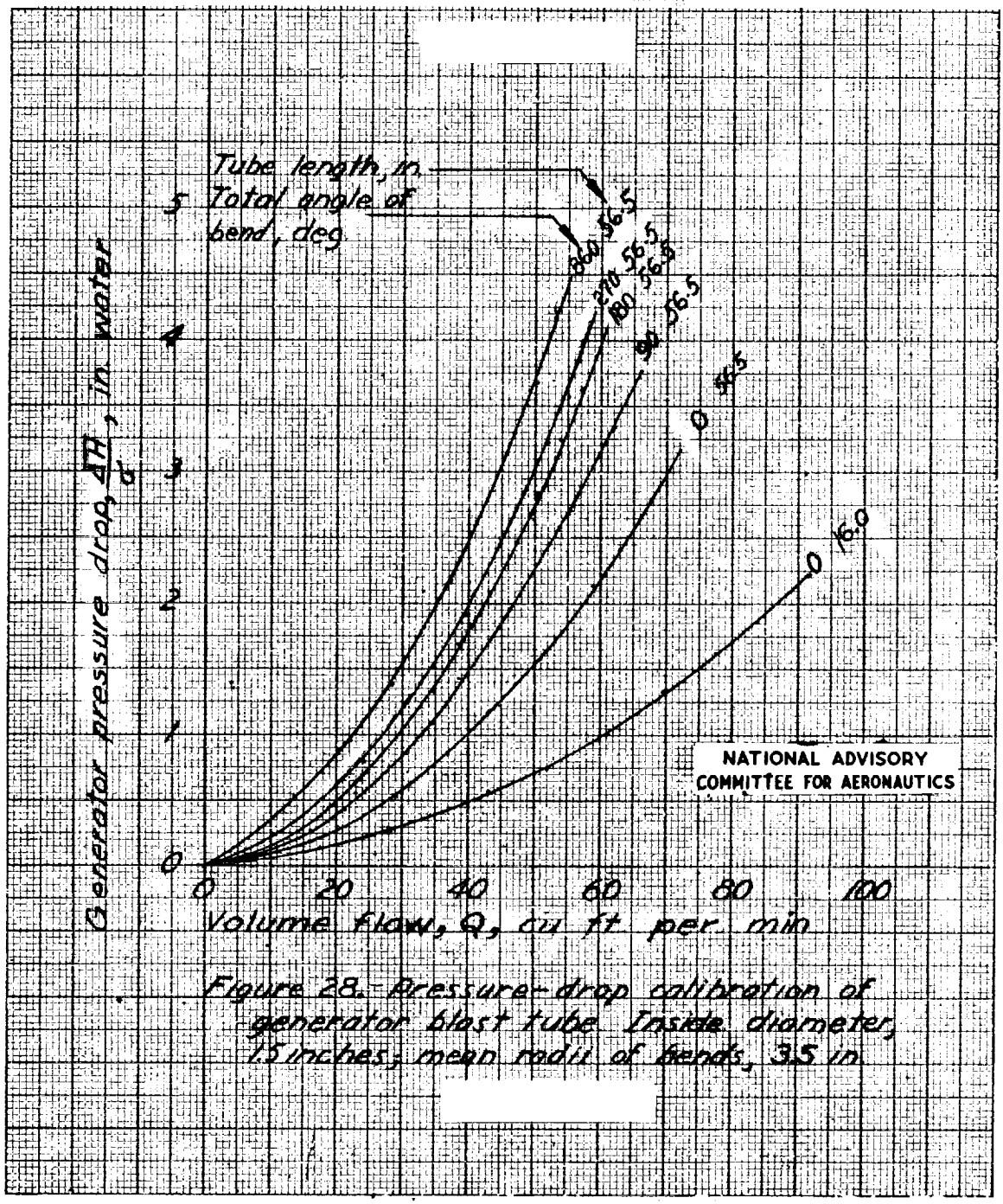

Figure 28. Pressure-drop calibration of generator blast tube. Inside diameter, 1.5 inches; mean radii of bends, 3.5 in.

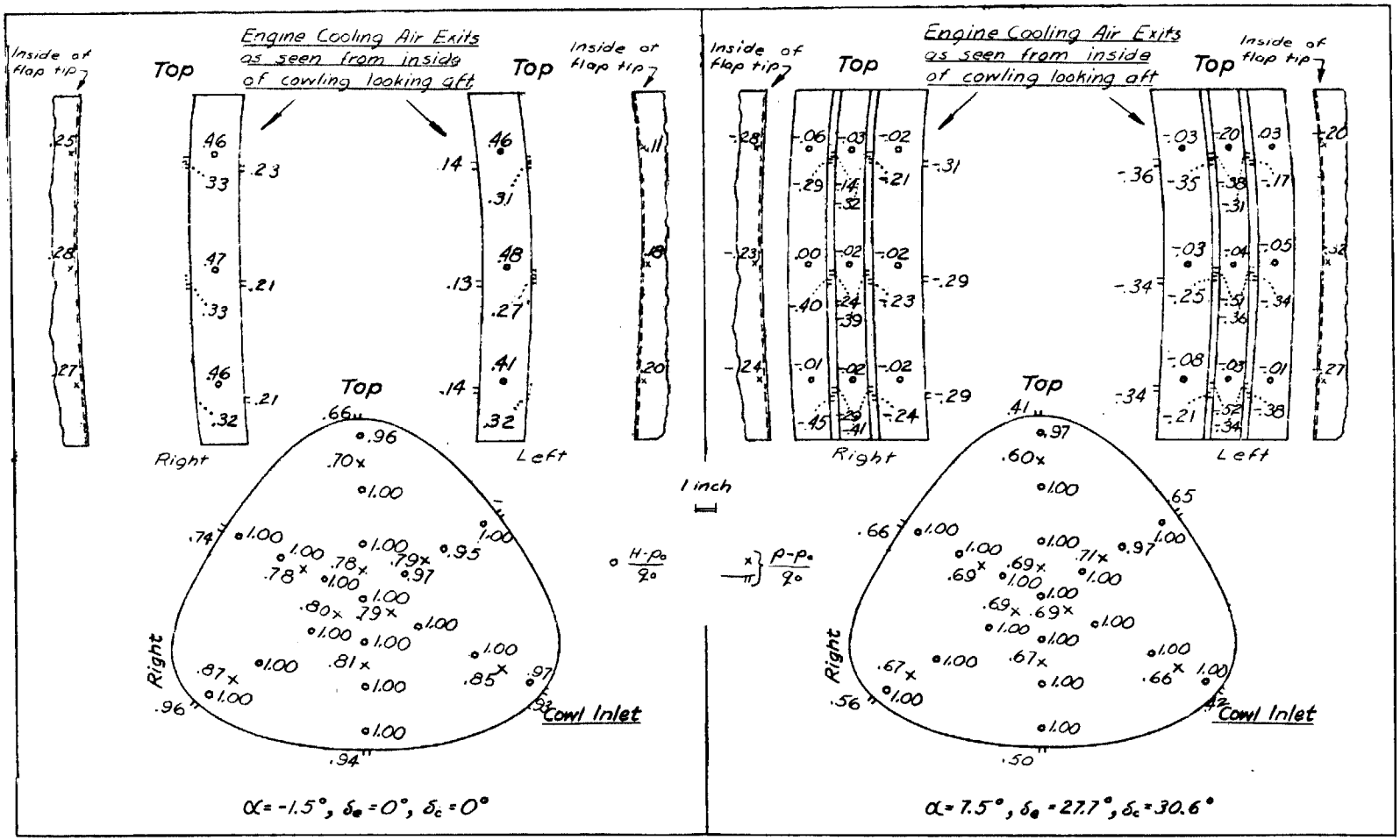

(a) Inlet and engine-cooling-air exits.

NATIONAL ADVISORY COMMITTEE FOR AERONAUTICS

Figure 29. - Typical pressure distributions in internal flow system for propeller-removed condition. Configuration IIa. All views are from points upstream with respect to cooling air flow unless otherwise noted.

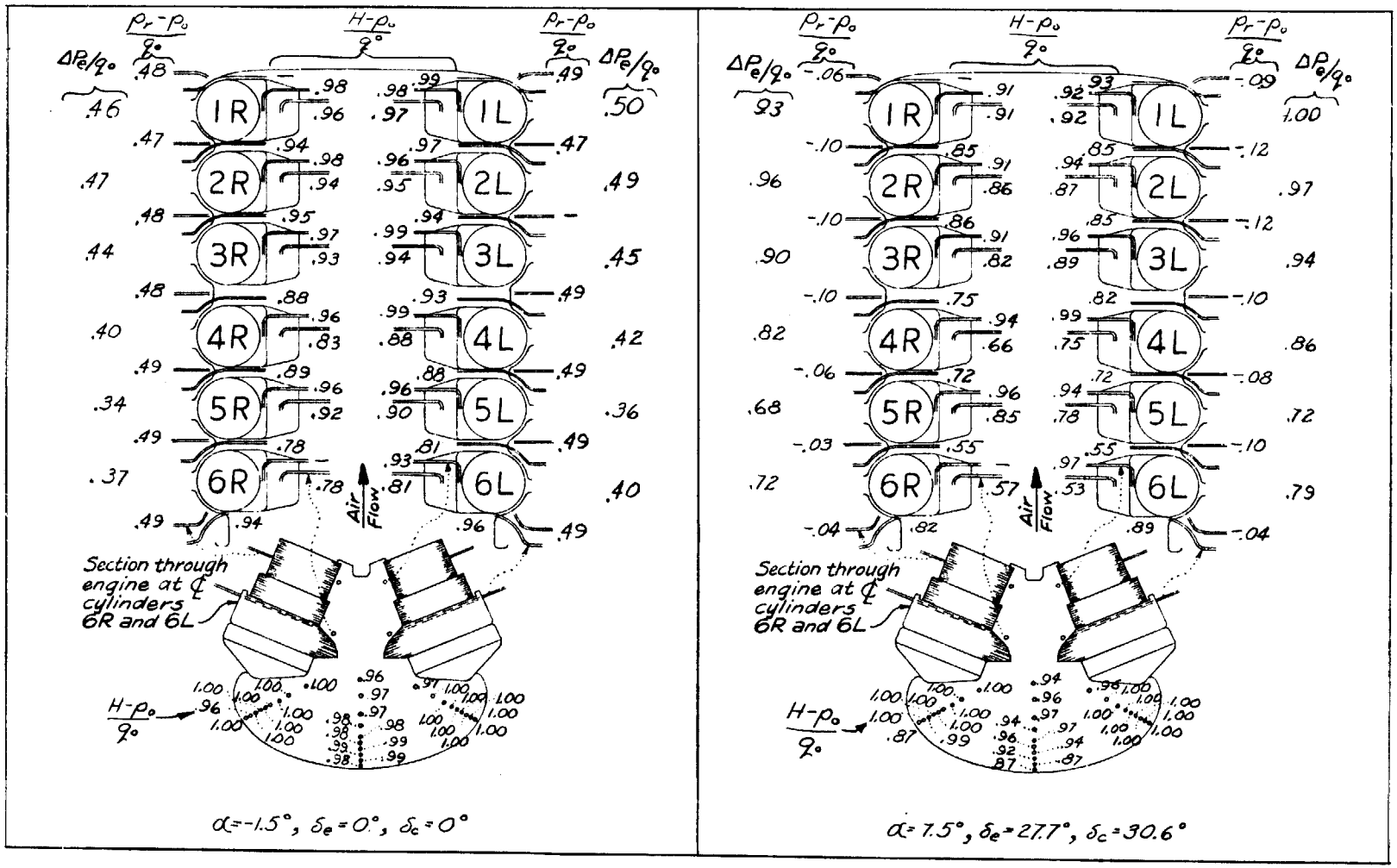

(b) Engine as viewed from above.

NATIONAL ADVISORY COMMITTEE FOR AERONAUTICS

Figure 29.- Continued.

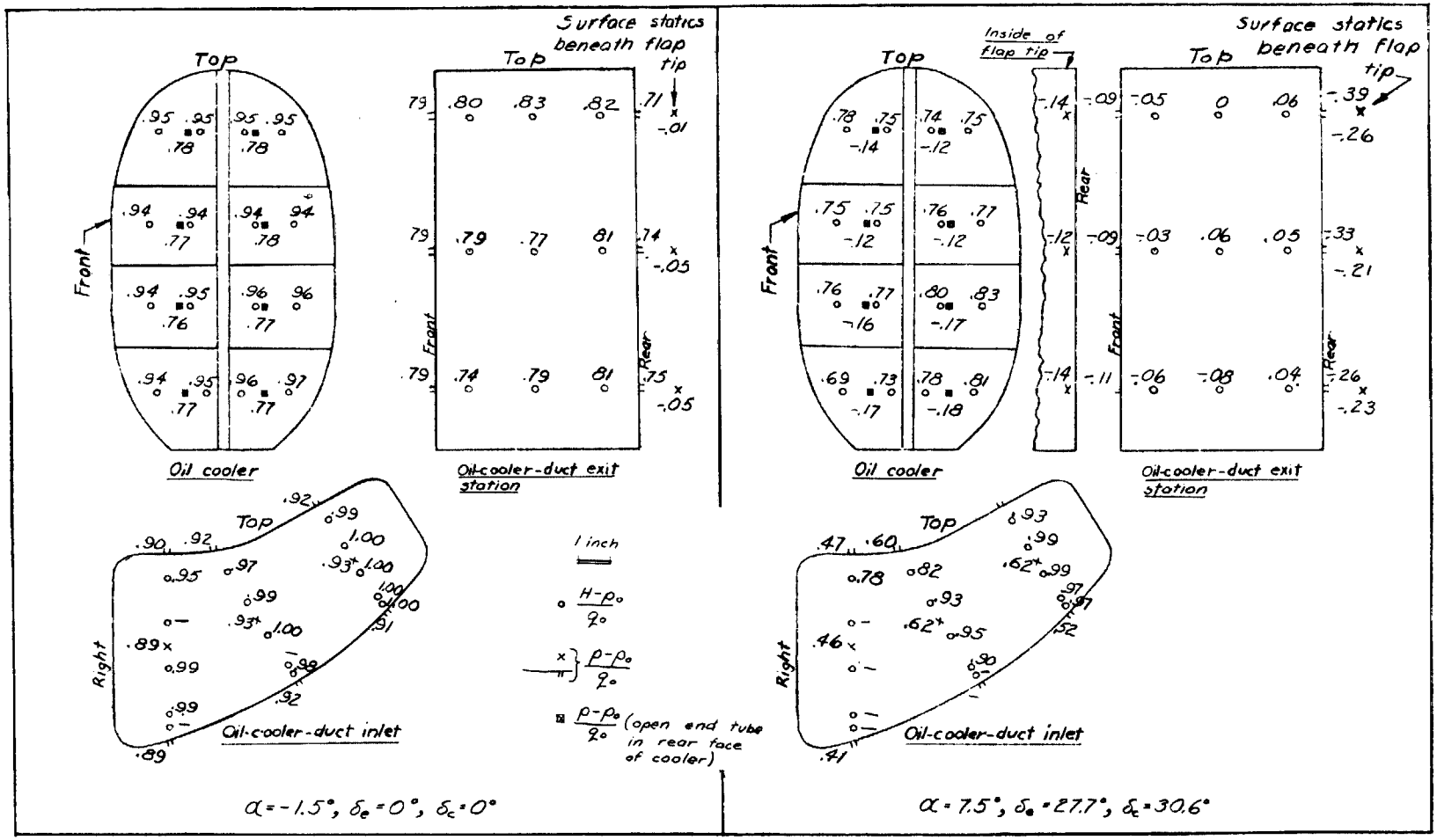

(c) Oil-cooler duct.

NATIONAL ADVISORY COMMITTEE FOR AERONAUTICS

Figure 29.- Concluded.

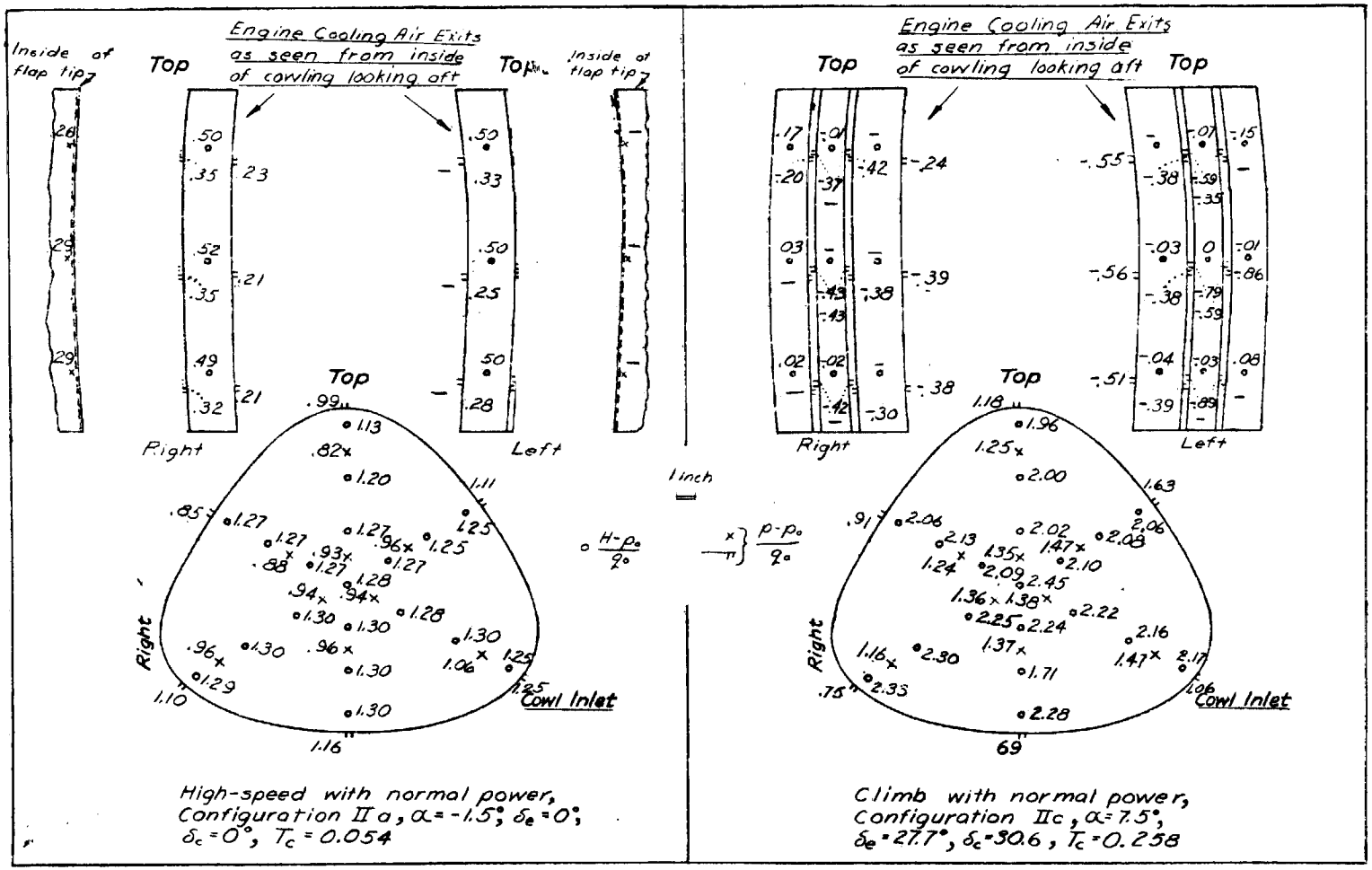

(a) Inlet and engine-cooling air exits.

NATIONAL ADVISORY COMMITTEE FOR AERONAUTICS

Figure 30.- Typical pressure distributions in internal flow system for two flight-simulation conditions. All views are from points upstream with respect to cooling air flow unless otherwise noted.

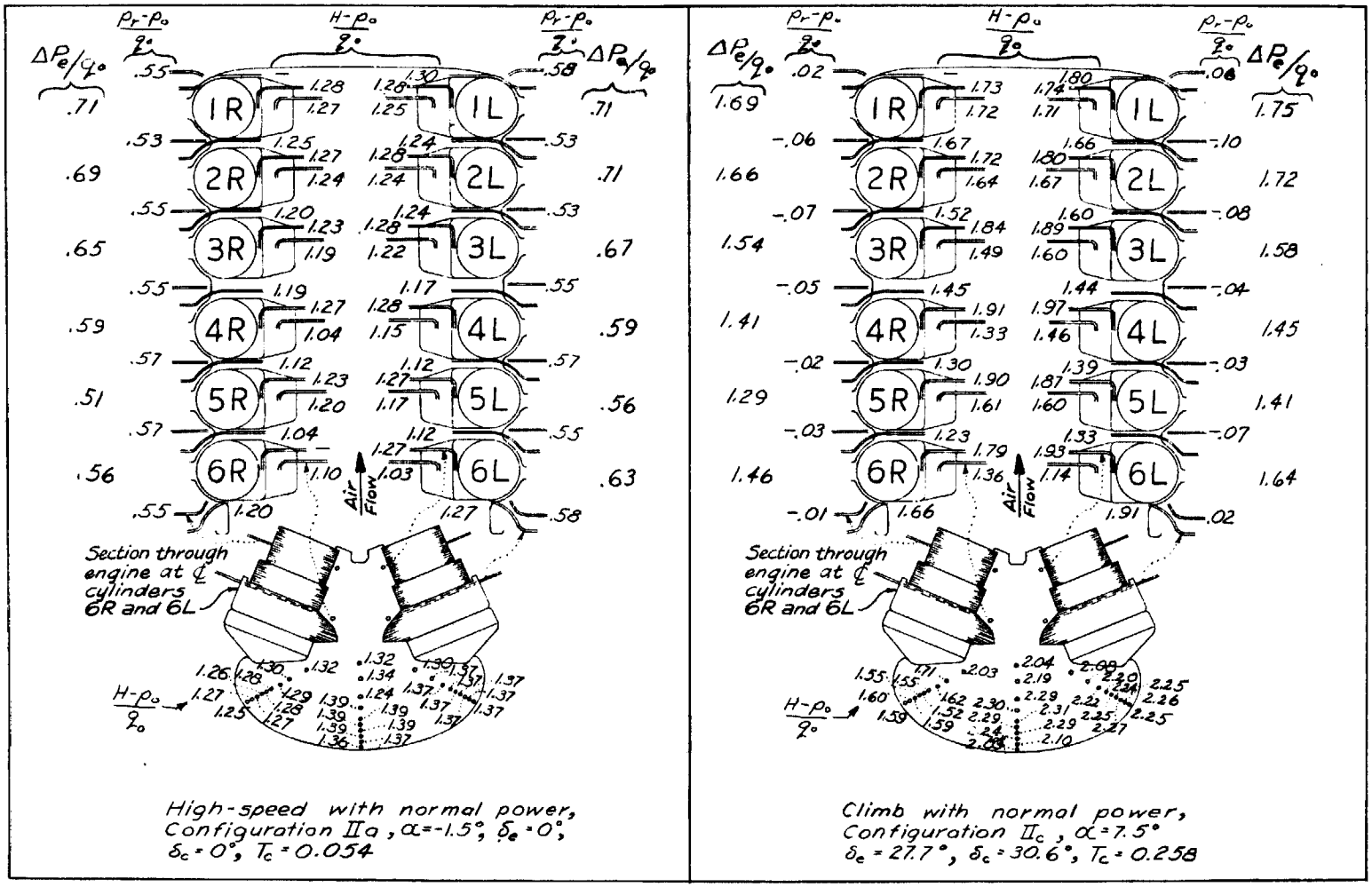

(b) Engine as viewed from above.

NATIONAL ADVISORY COMMITTEE FOR AERONAUTICS

Figure 30.- Continued.

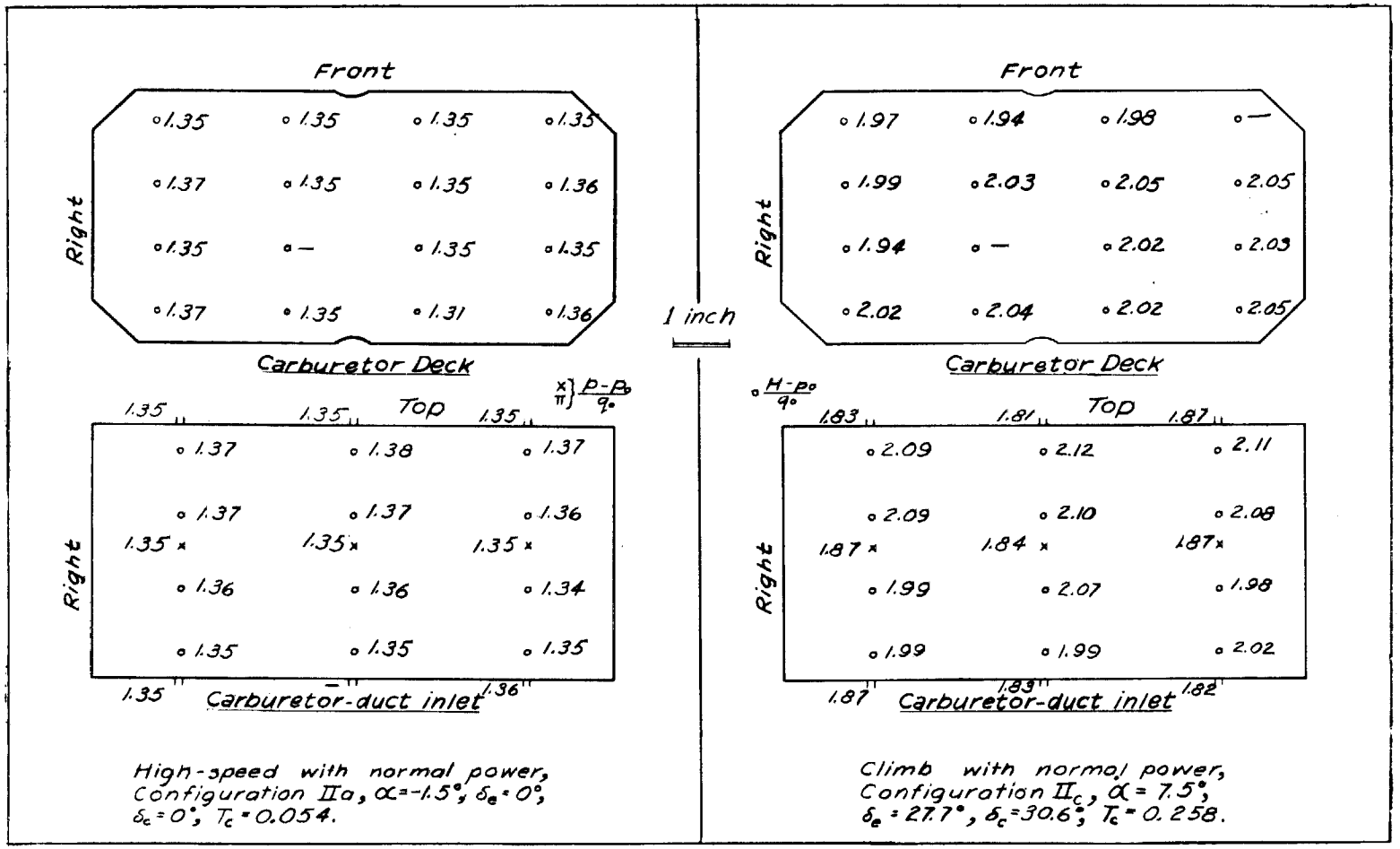

High-speed with normal power, Configuration IIa, $\alpha = -1.5°$, $\delta_e = 0°$, $\delta_c = 0°$, $T_c = 0.054$.

Climb with normal power, Configuration IIc, $\alpha = 7.5°$, $\delta_e = 27.7°$, $\delta_c = 30.6°$, $T_c = 0.258$.

NATIONAL ADVISORY COMMITTEE FOR AERONAUTICS

(c) Carburetor duct.

Figure 30.- Continued.

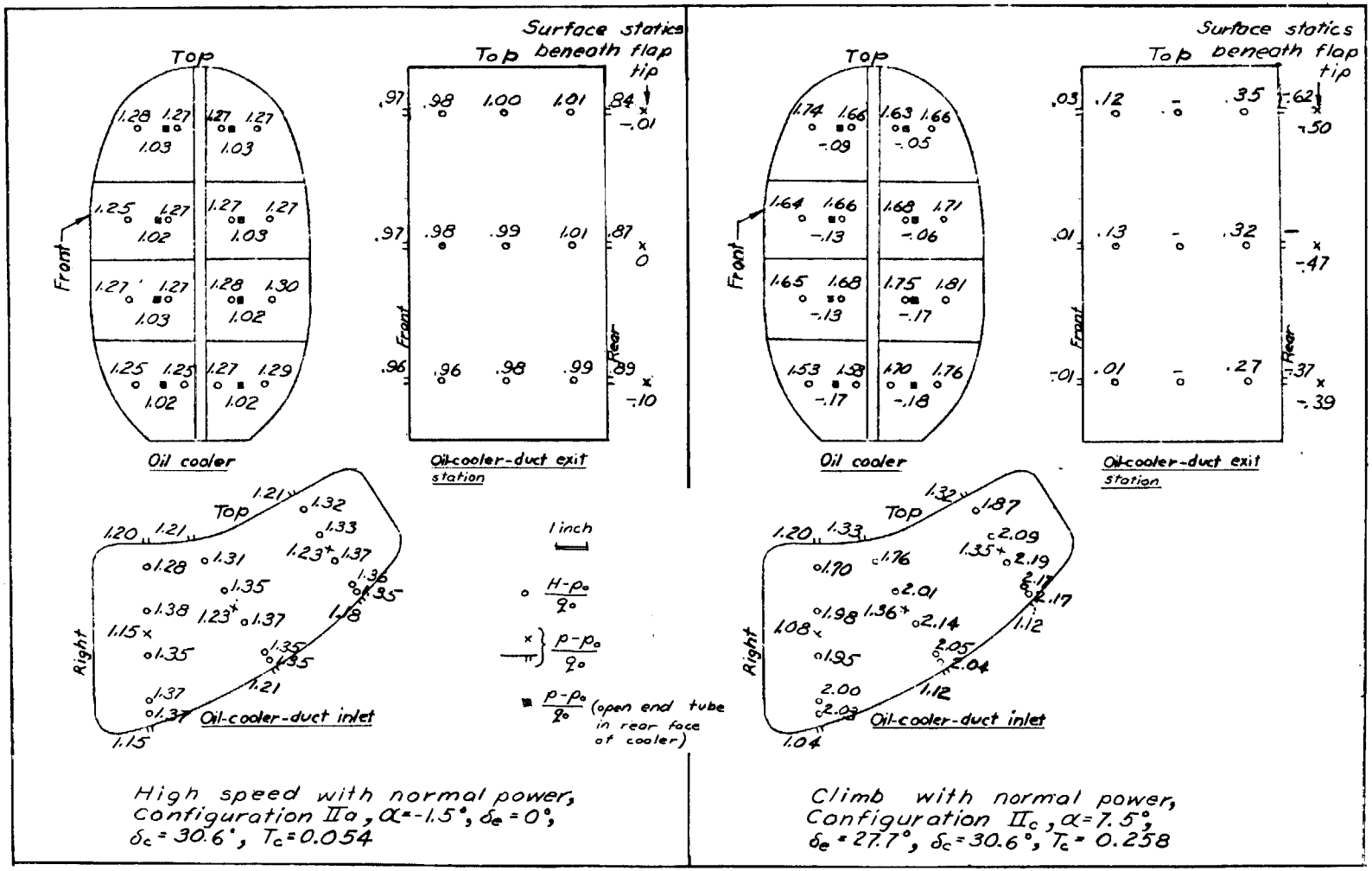

(d) Oil-cooler duct.

NATIONAL ADVISORY COMMITTEE FOR AERONAUTICS

Figure 30.- Concluded.

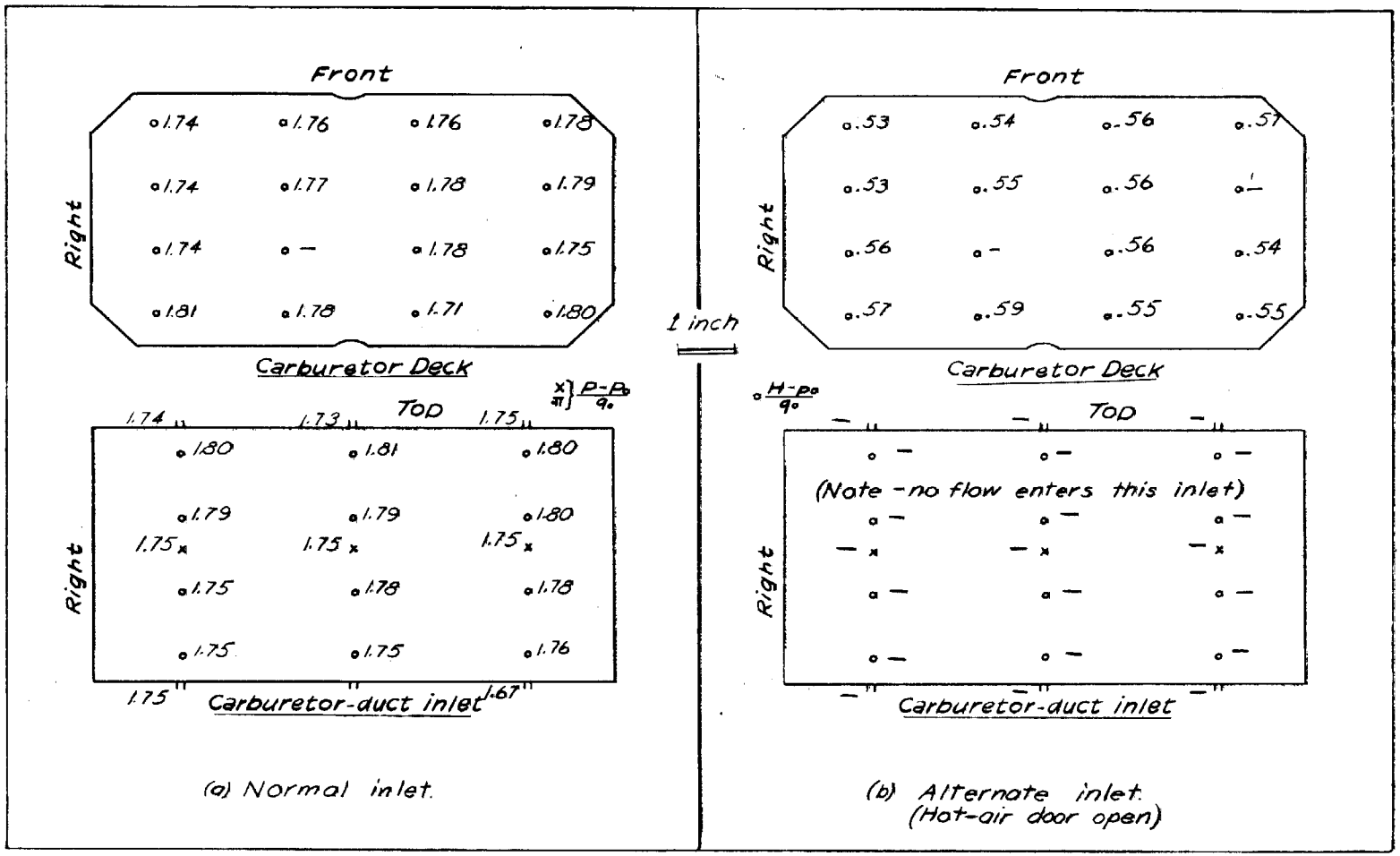

NATIONAL ADVISORY COMMITTEE FOR AERONAUTICS

Figure 31 .- Comparison of pressures in carburetor duct with normal and alternate inlets for maximum endurance cruise condition. Configuration II_c, $\alpha = 11.2°$, $\delta_e = 0°$, $\delta_c = 0°$, $T_c = 0.134$.

MR No. L5112b

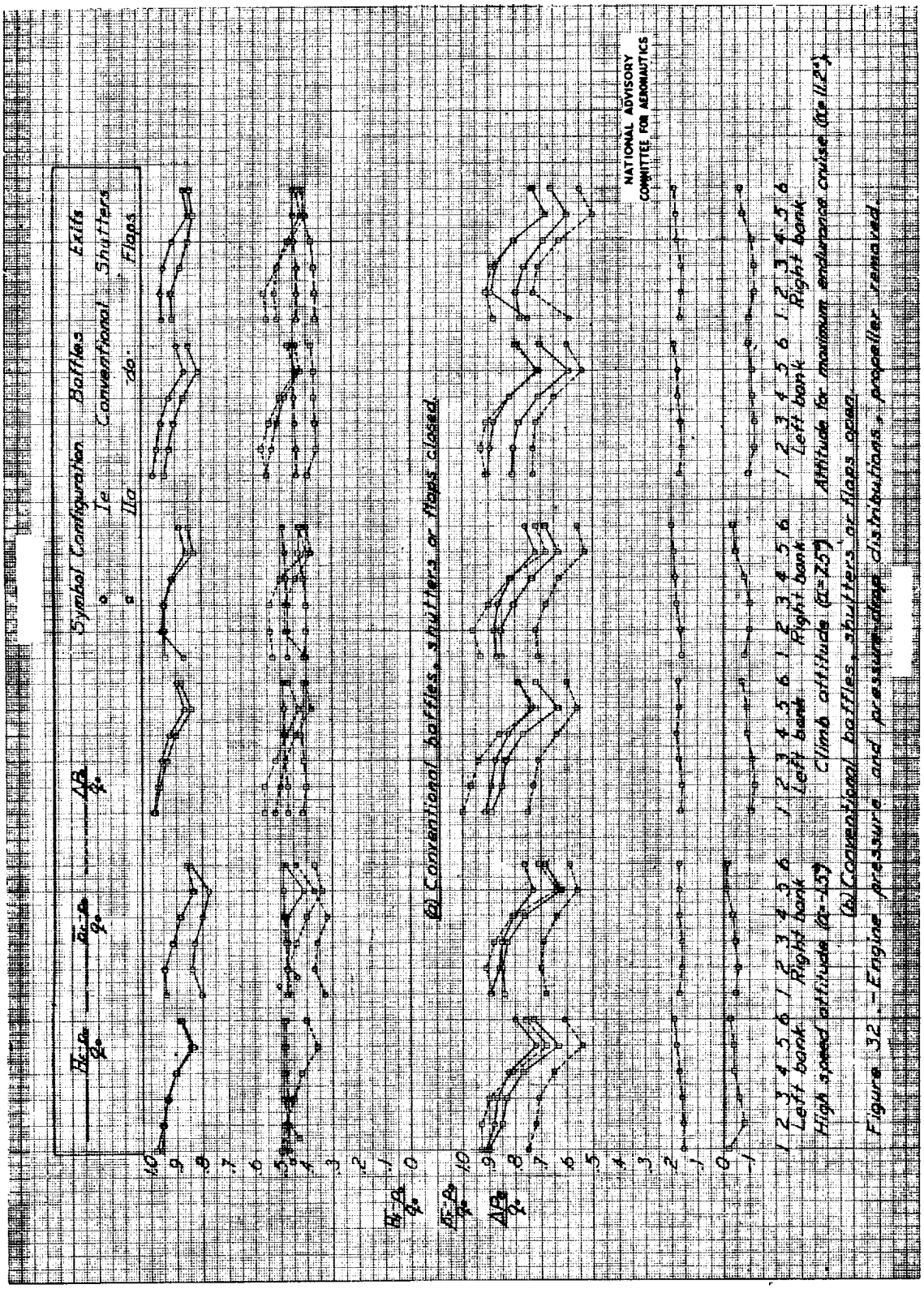

Figure 32.- Engine pressure and pressure-drop distributions - propeller removed.

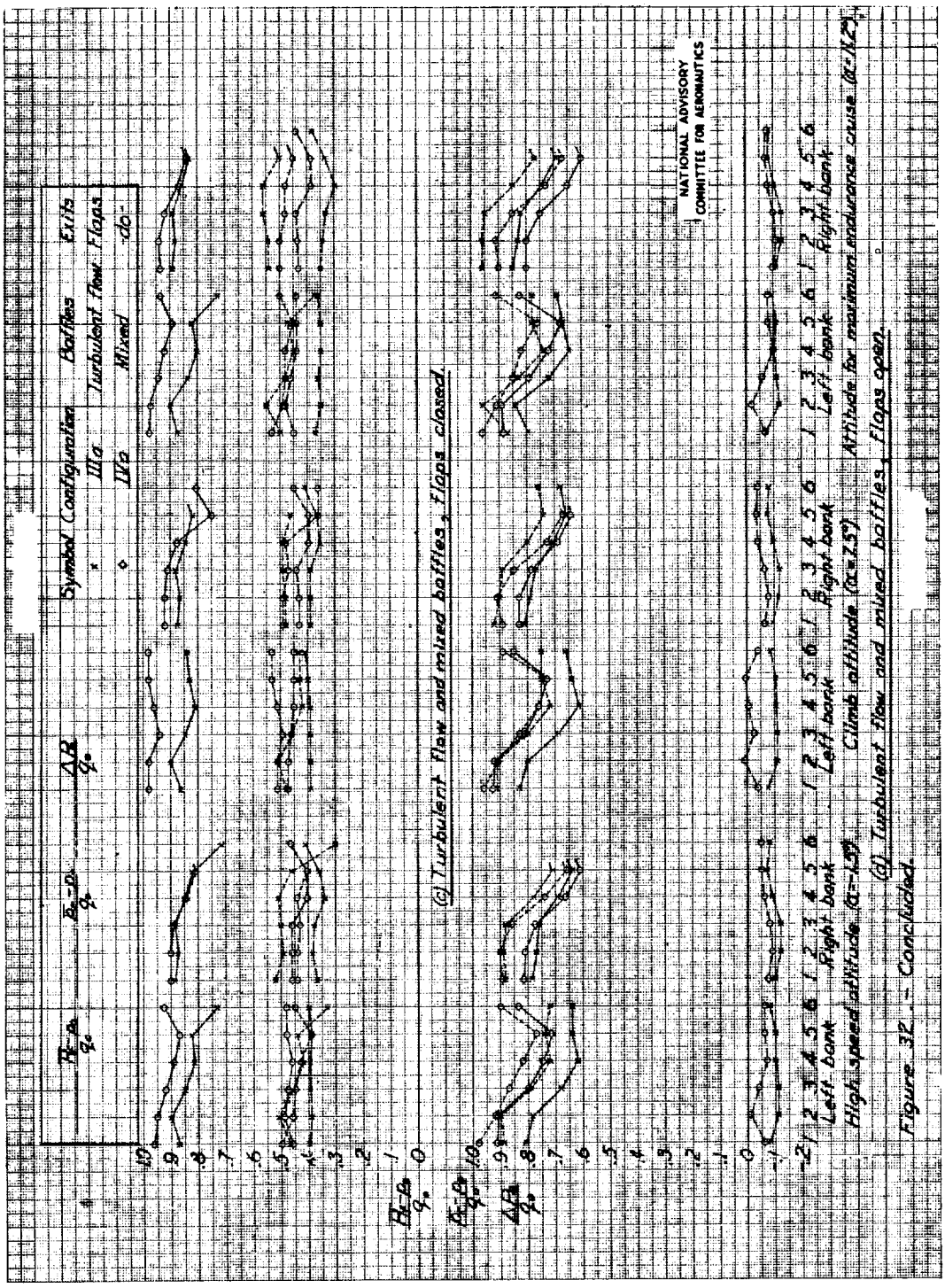

Figure 32.- Concluded.

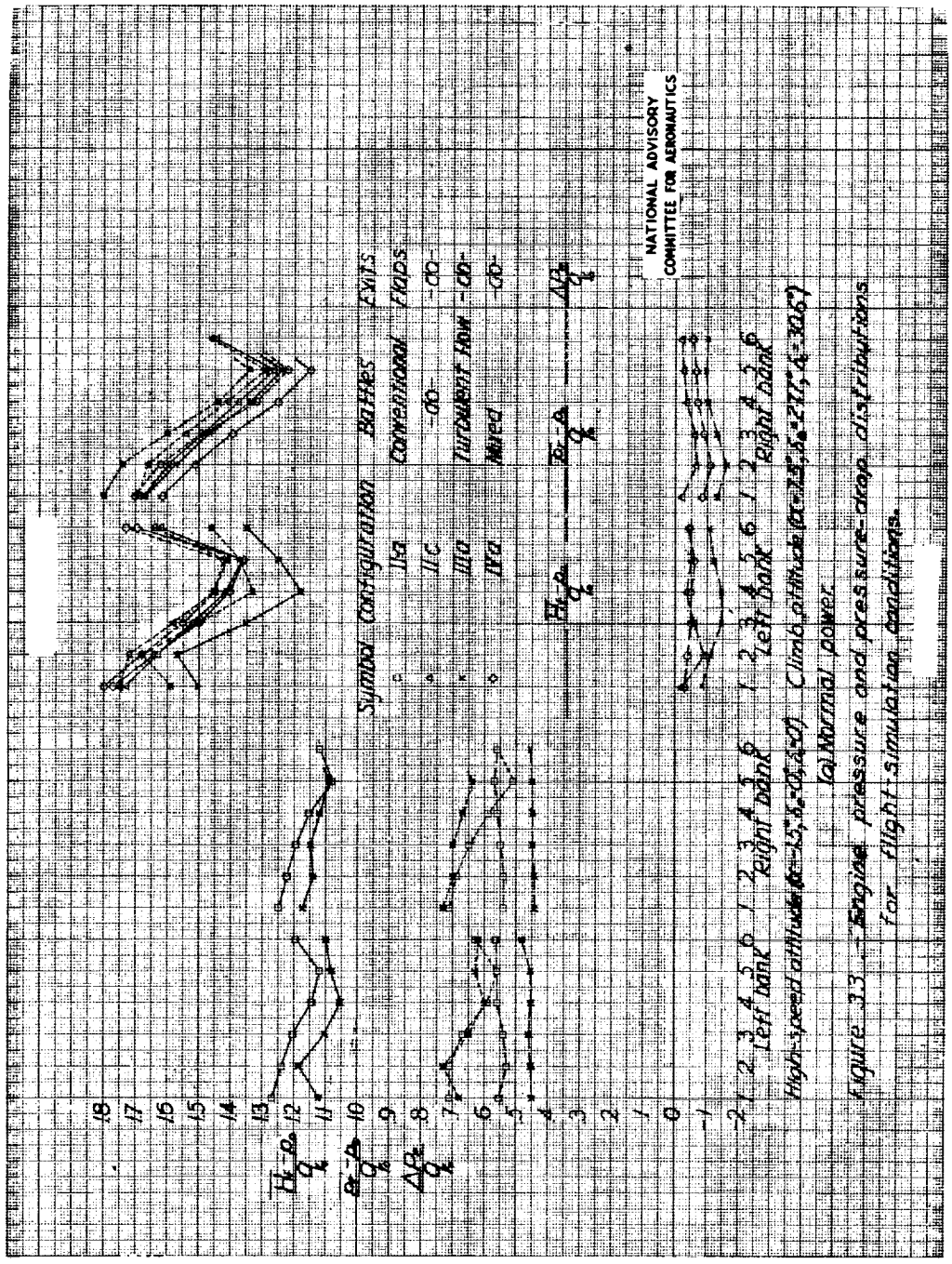

Figure 33.- Engine pressure and pressure-drop distributions for flight simulation conditions.

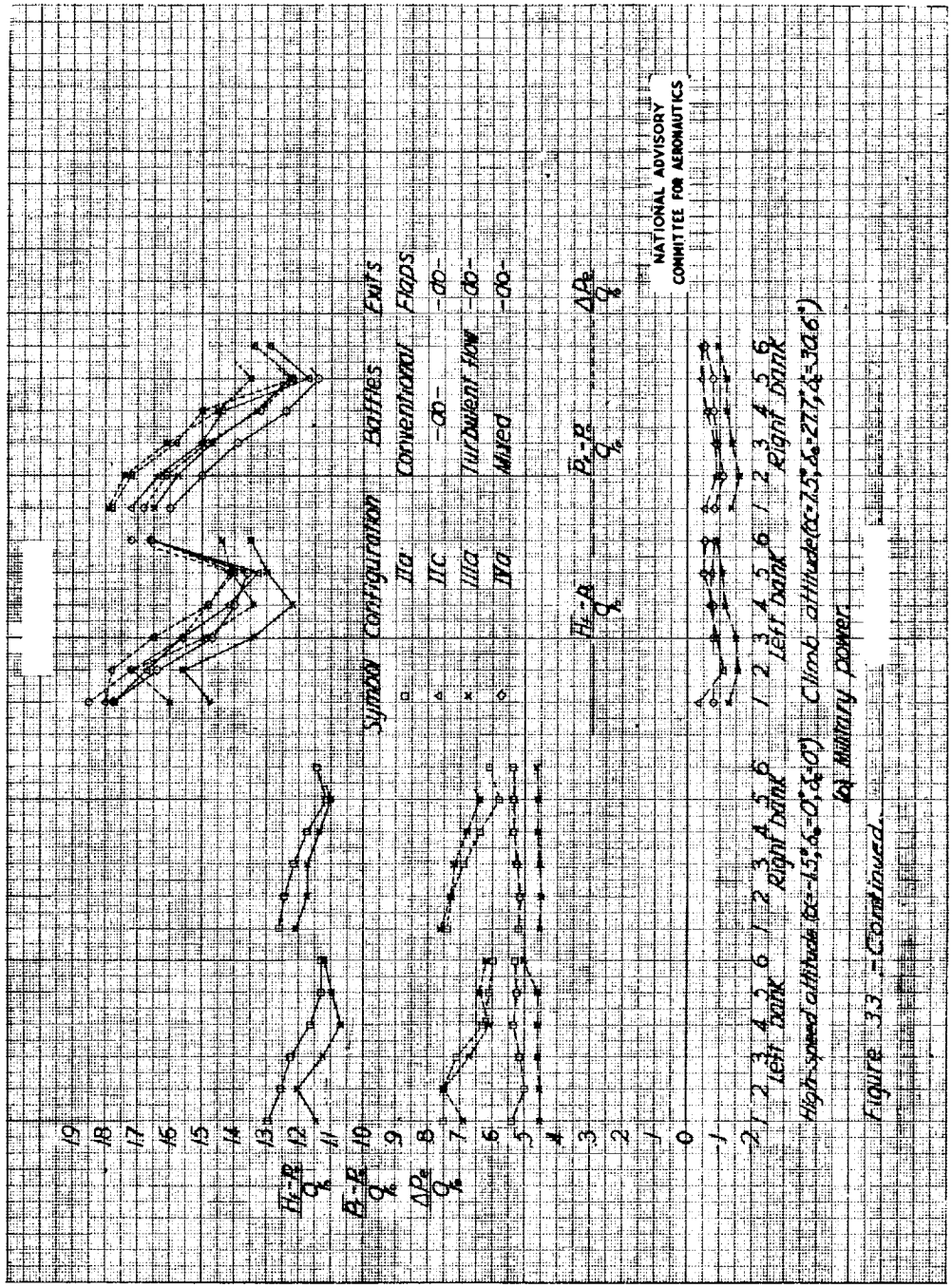

Figure 33.- Continued.

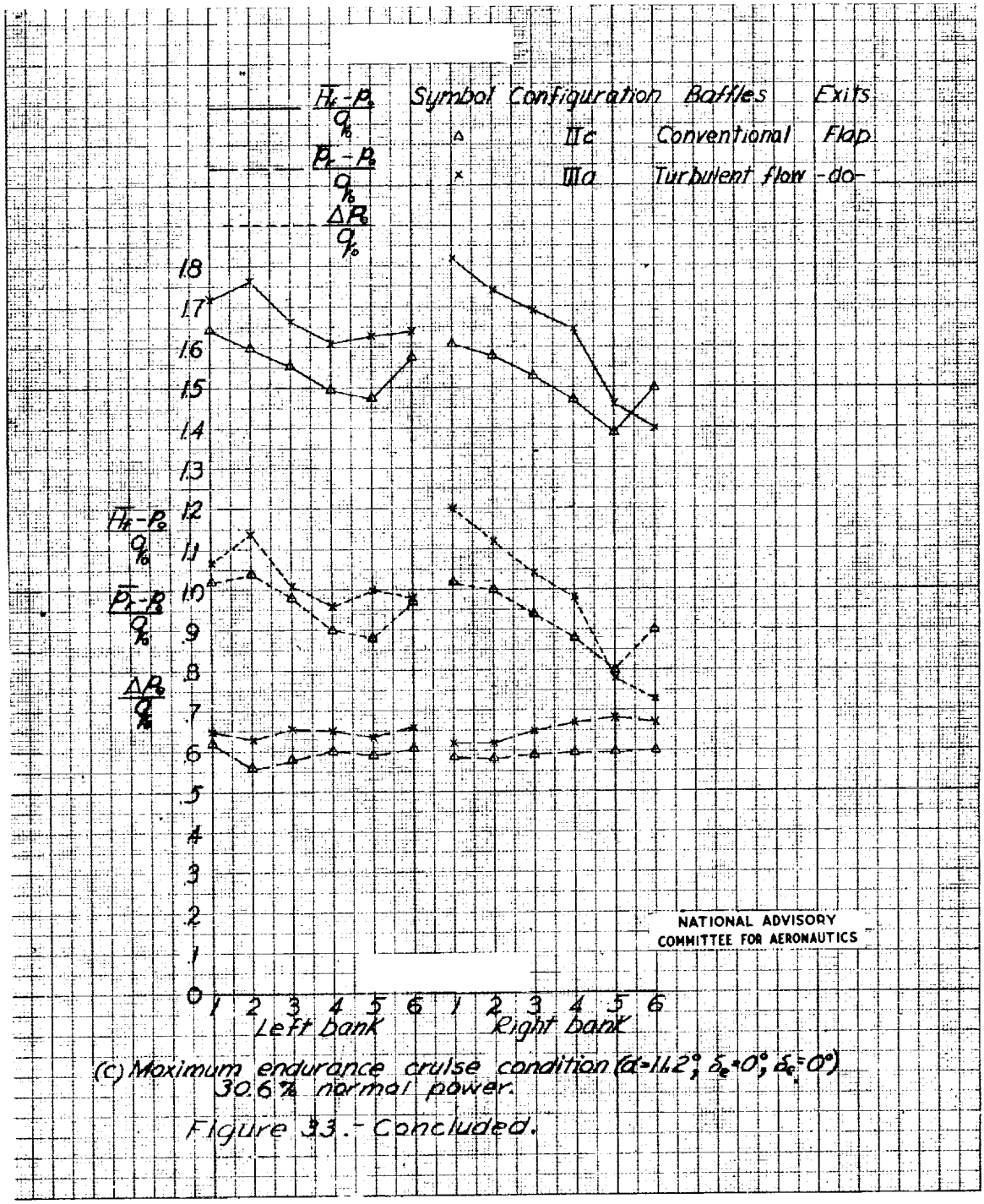

(c) Maximum endurance cruise condition (α=11.2°, δ_e=0°, δ_c=0°) 30.6% normal power.

Figure 33.- Concluded.

L-562

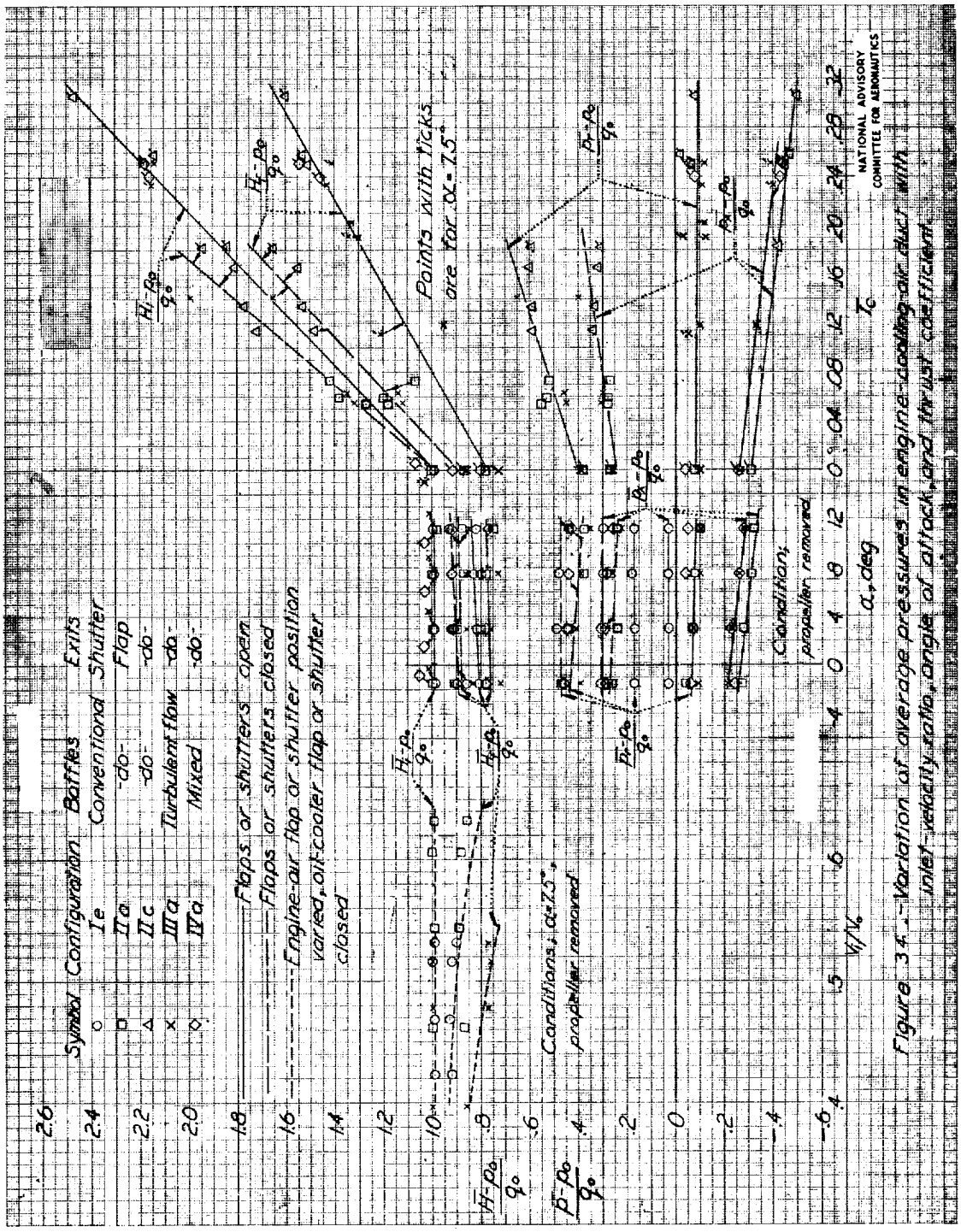

Figure 34.- Variation of average pressures in engine-cooling air duct with inlet-velocity ratio, angle of attack, and thrust coefficient.

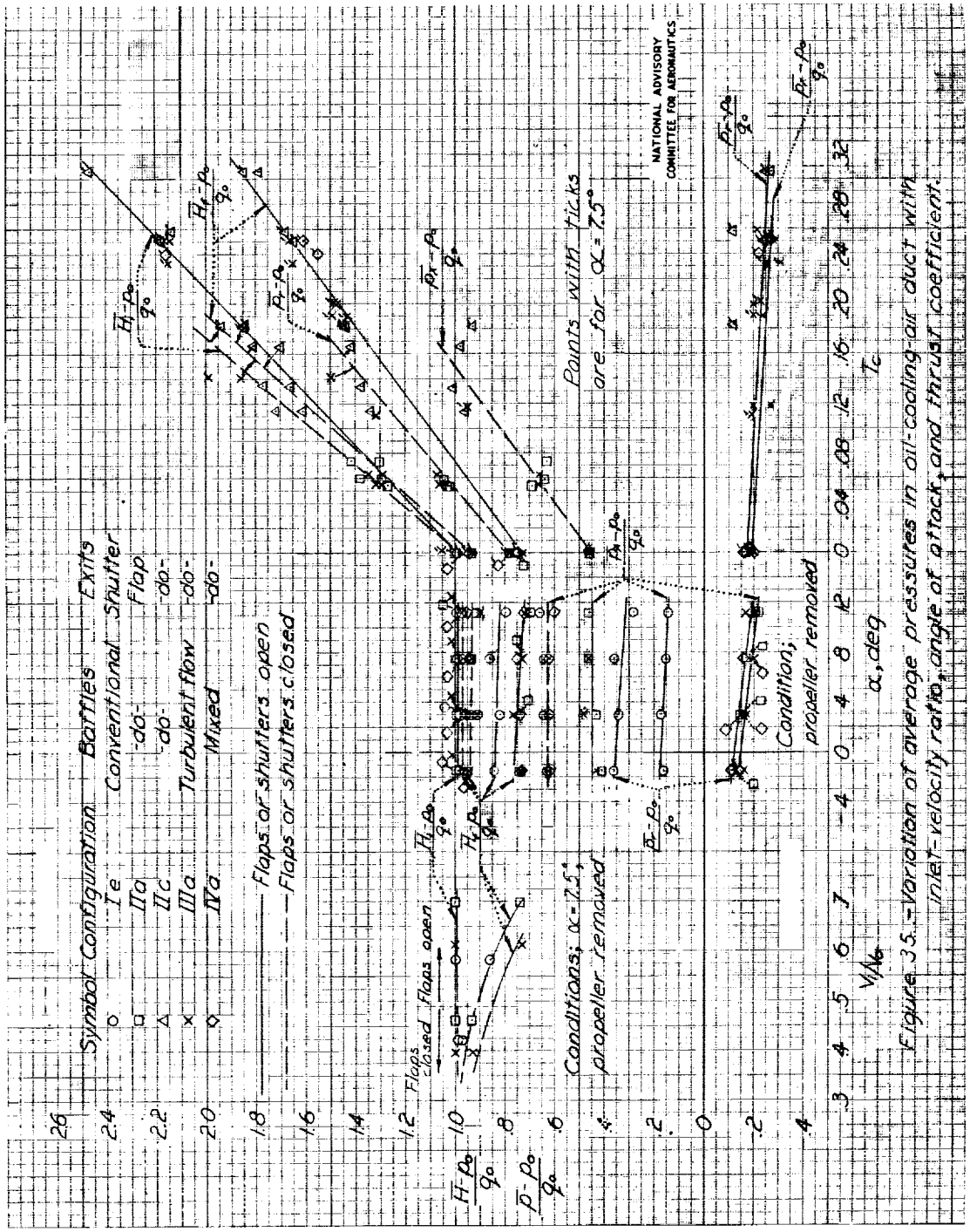

Figure 35.-Variation of average pressures in oil-cooling-air duct with inlet-velocity ratio, angle of attack, and thrust coefficient.

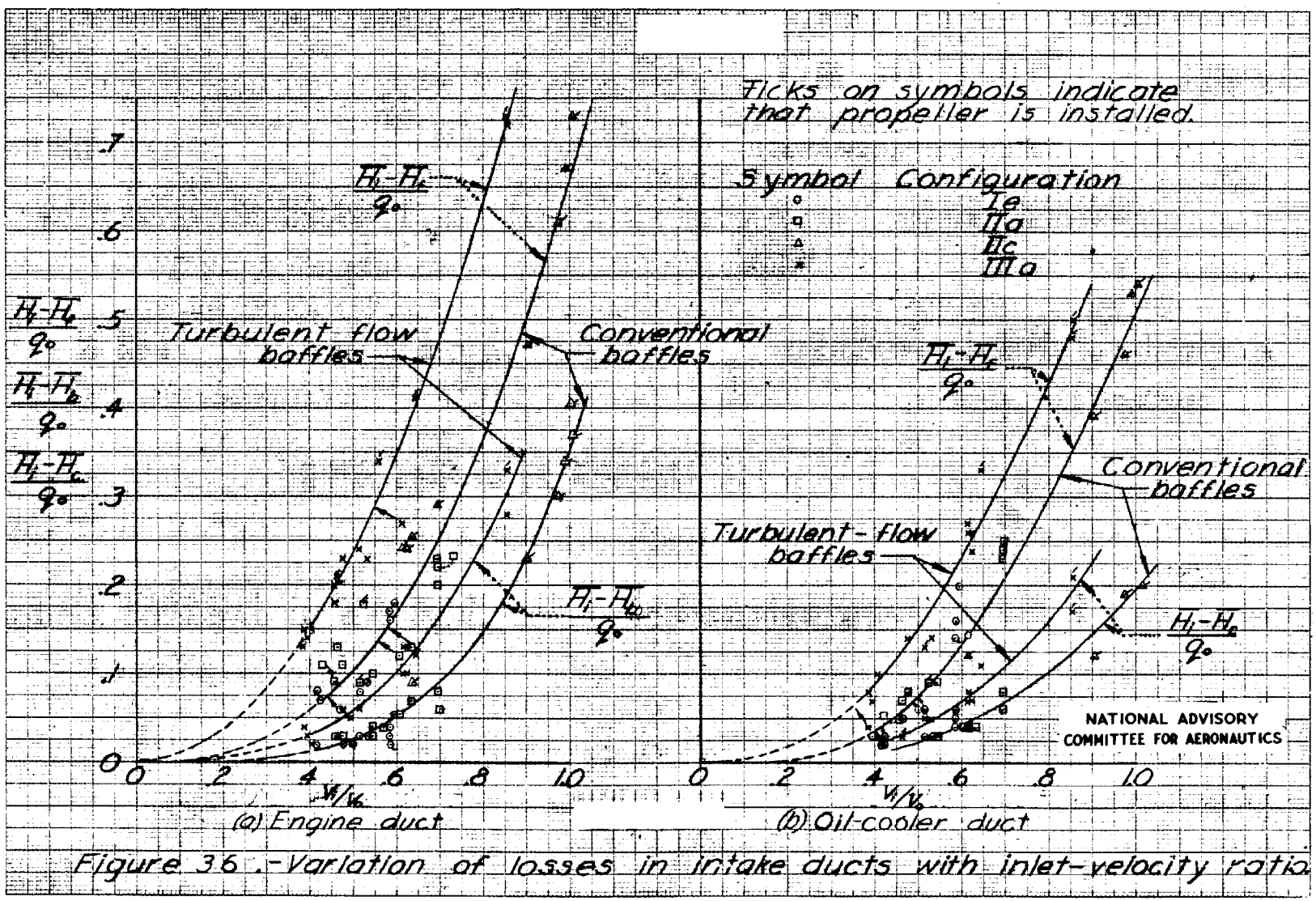

Figure 36.- Variation of losses in intake ducts with inlet-velocity ratio

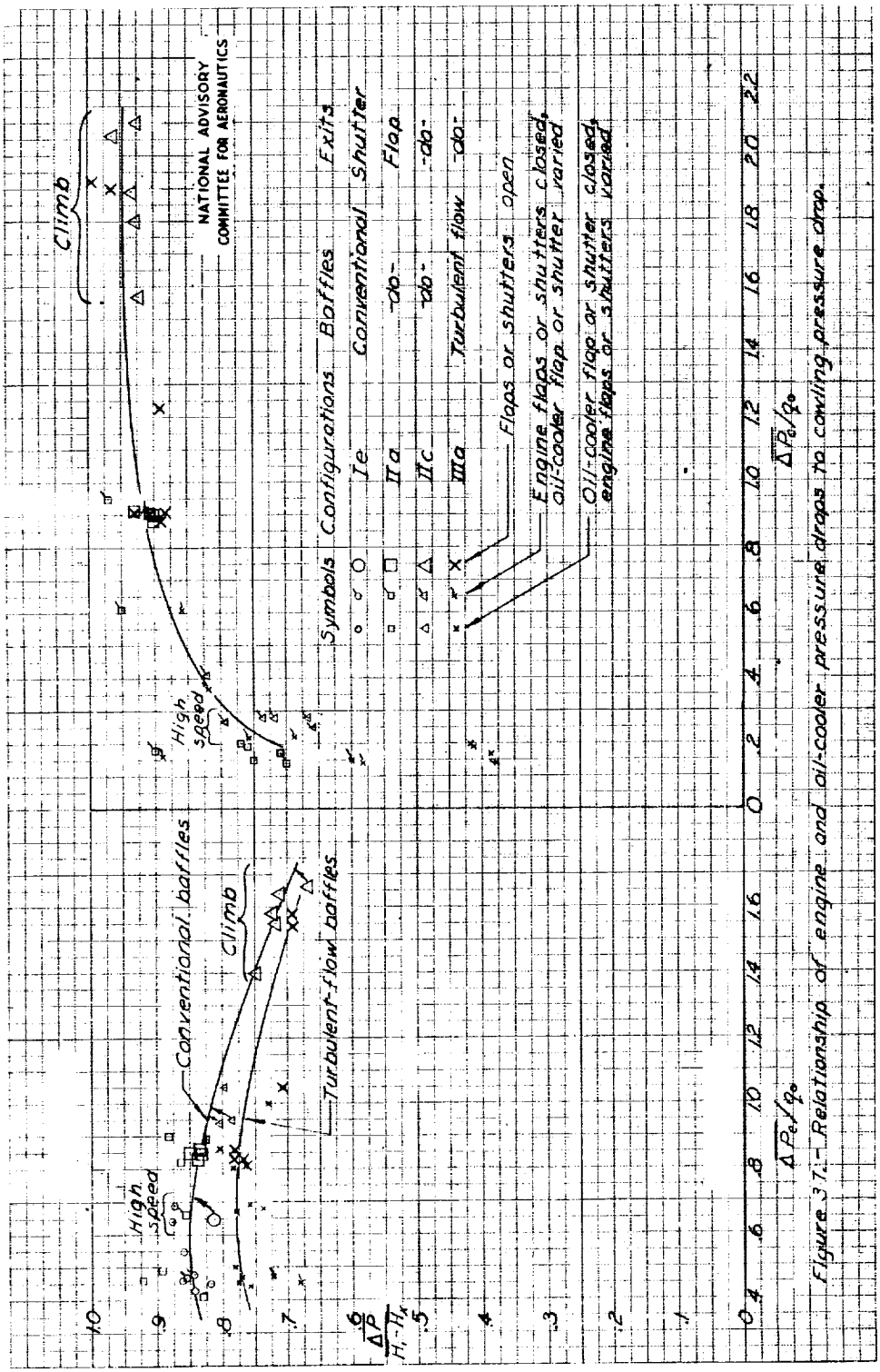

Figure 7.- Relationship of engine and oil-cooler pressure drops to cowling pressure drop.

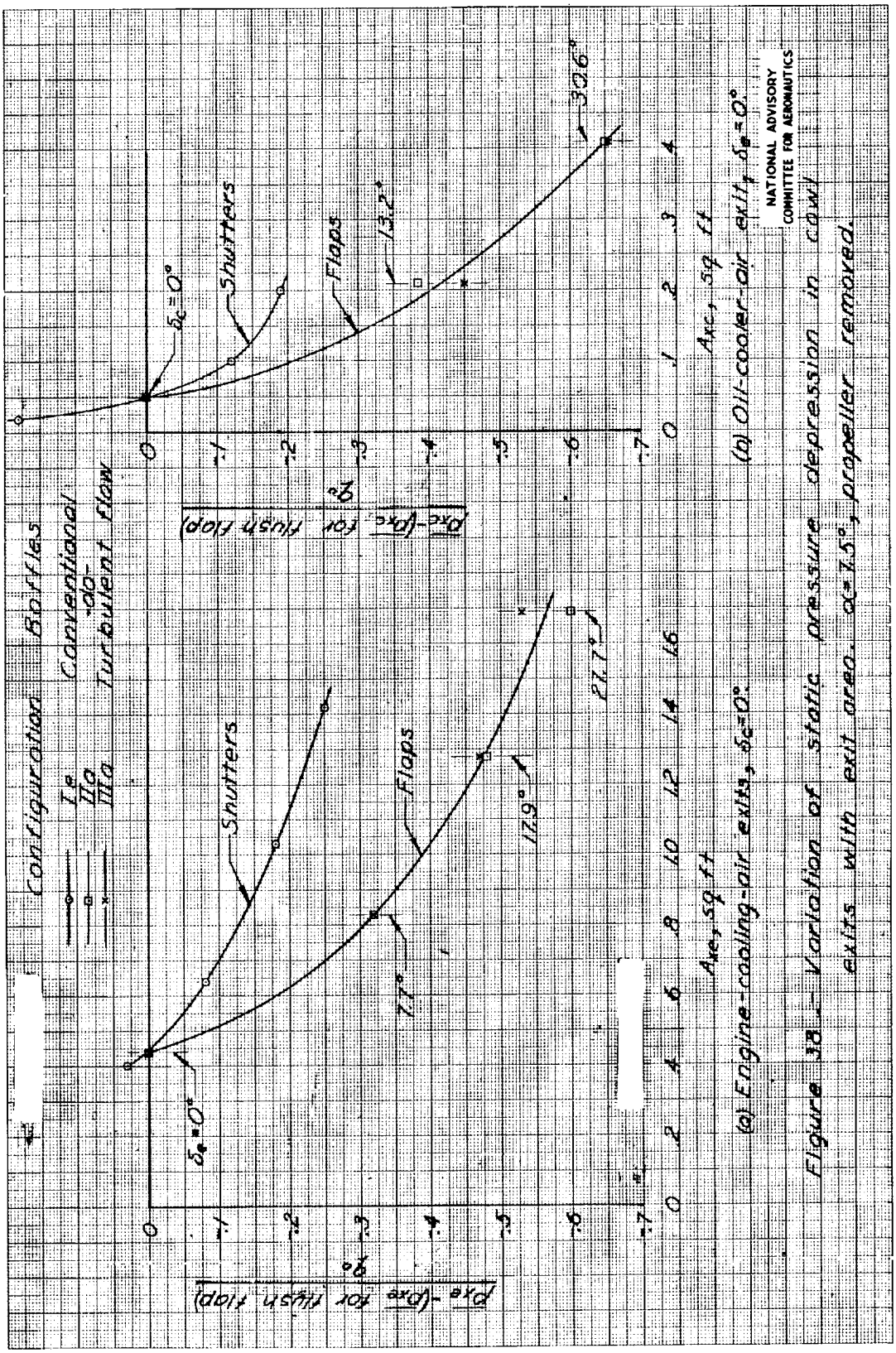

Figure 38.- Variation of static pressure depression in cowl exits with exit area. $\alpha = 2.5°$, propeller removed.

(a) Engine-cooling-air exits, $\delta_c = 0°$.

(b) Oil-cooler-air exit, $\delta_s = 0°$.

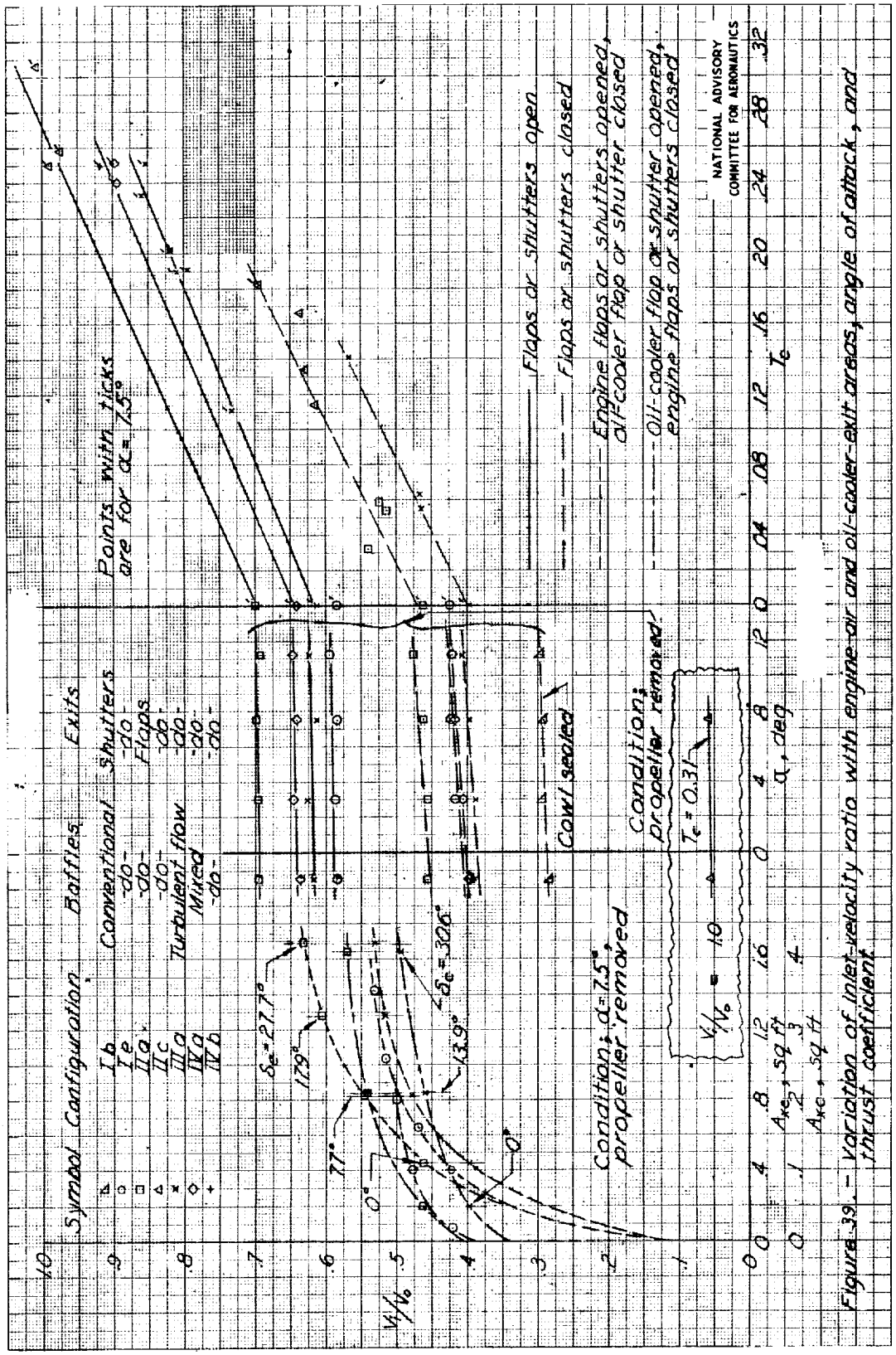

Figure 39. - Variation of inlet-velocity ratio with engine-air and oil-cooler-exit areas, angle of attack, and thrust coefficient.

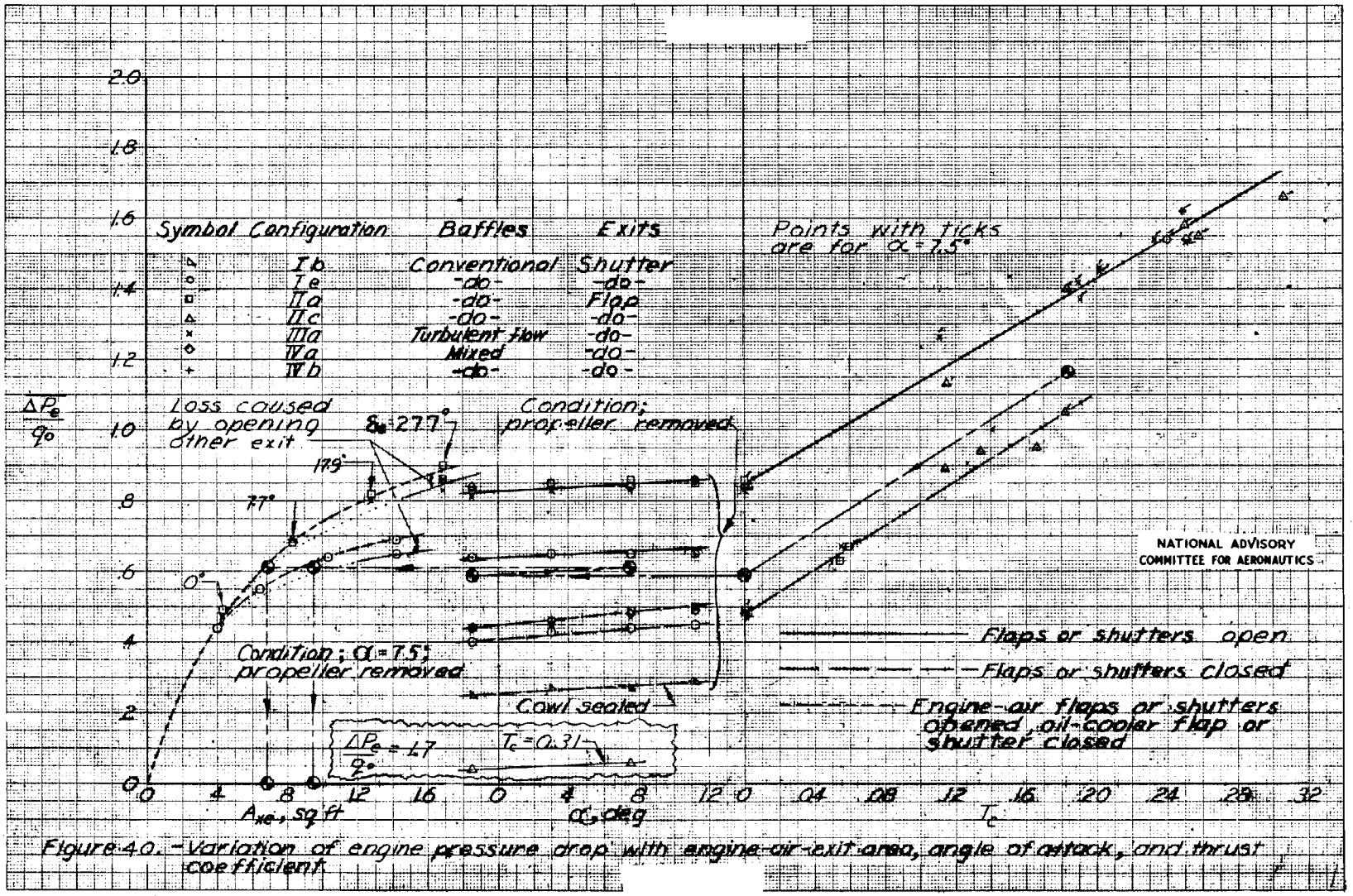

Figure 40.- Variation of engine pressure drop with engine-air-exit area, angle of attack, and thrust coefficient.

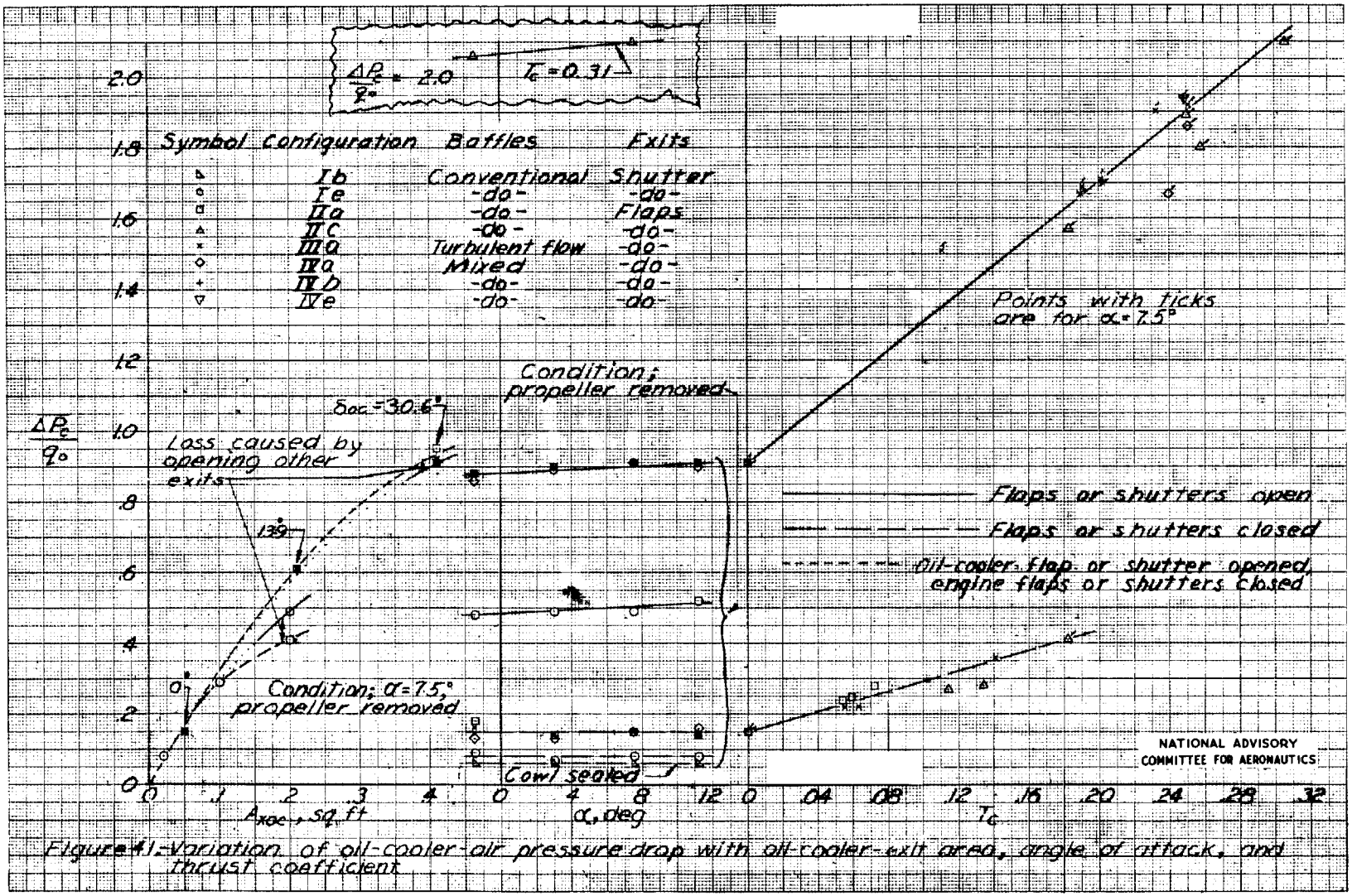

Figure 11.- Variation of oil-cooler-air pressure drop with oil-cooler-exit area, angle of attack, and thrust coefficient.

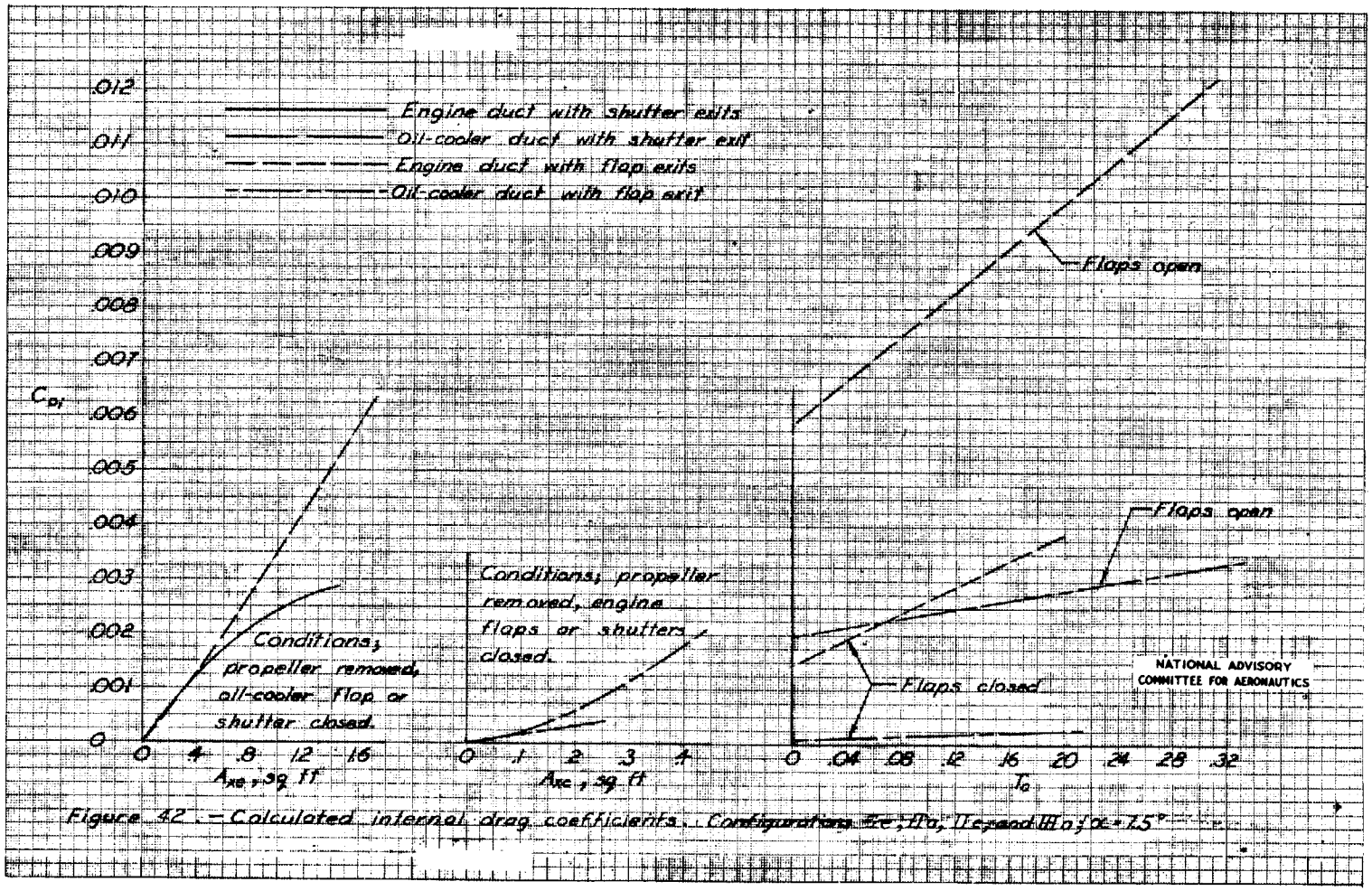

Figure 42.—Calculated internal drag coefficients. Configurations Ie, IIa, IIc, and IIIa; $\alpha = 7.5°$.

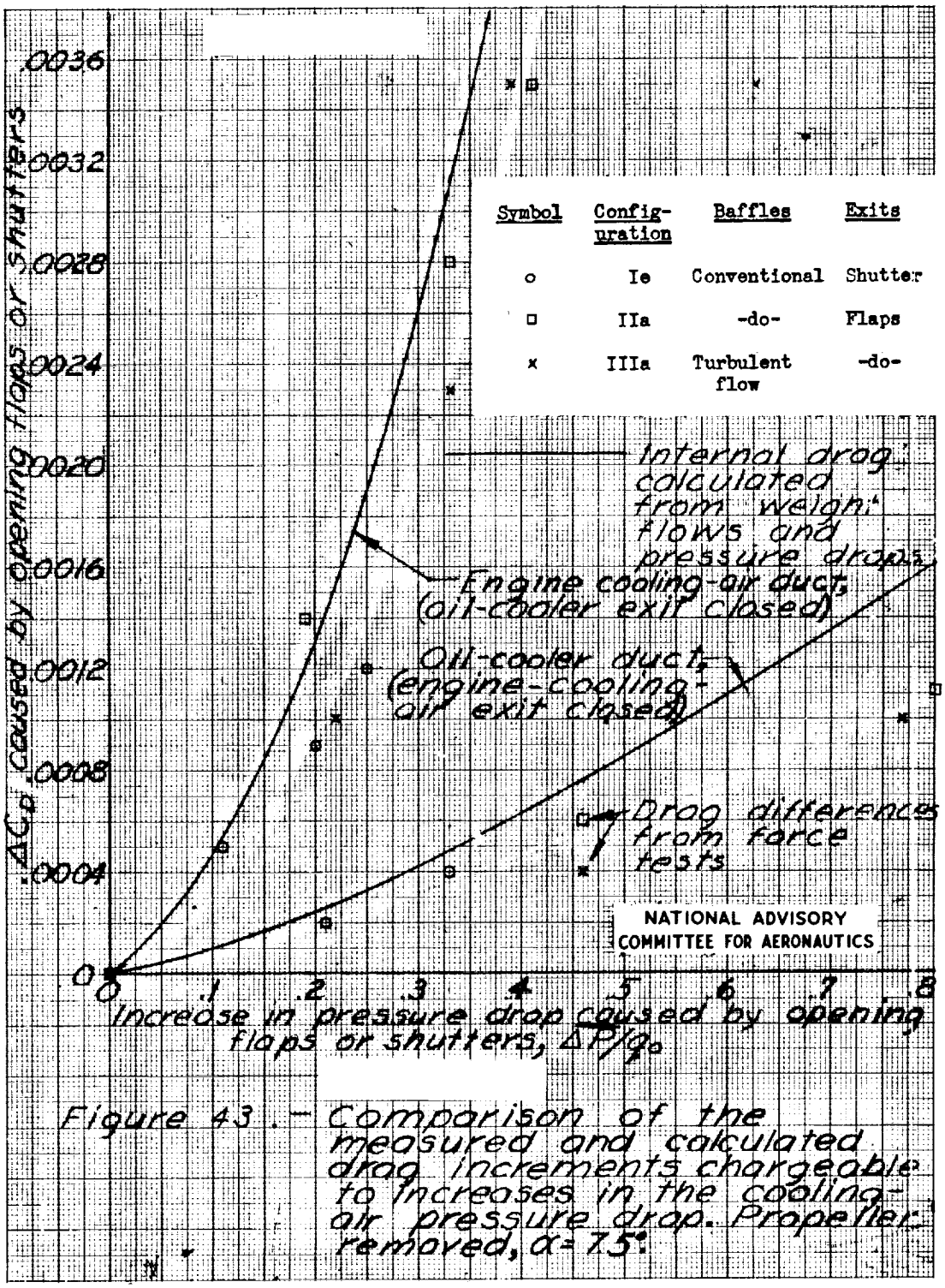

Figure 43.- Comparison of the measured and calculated drag increments chargeable to increases in the cooling-air pressure drop. Propeller removed, $\alpha = 7.5°$.

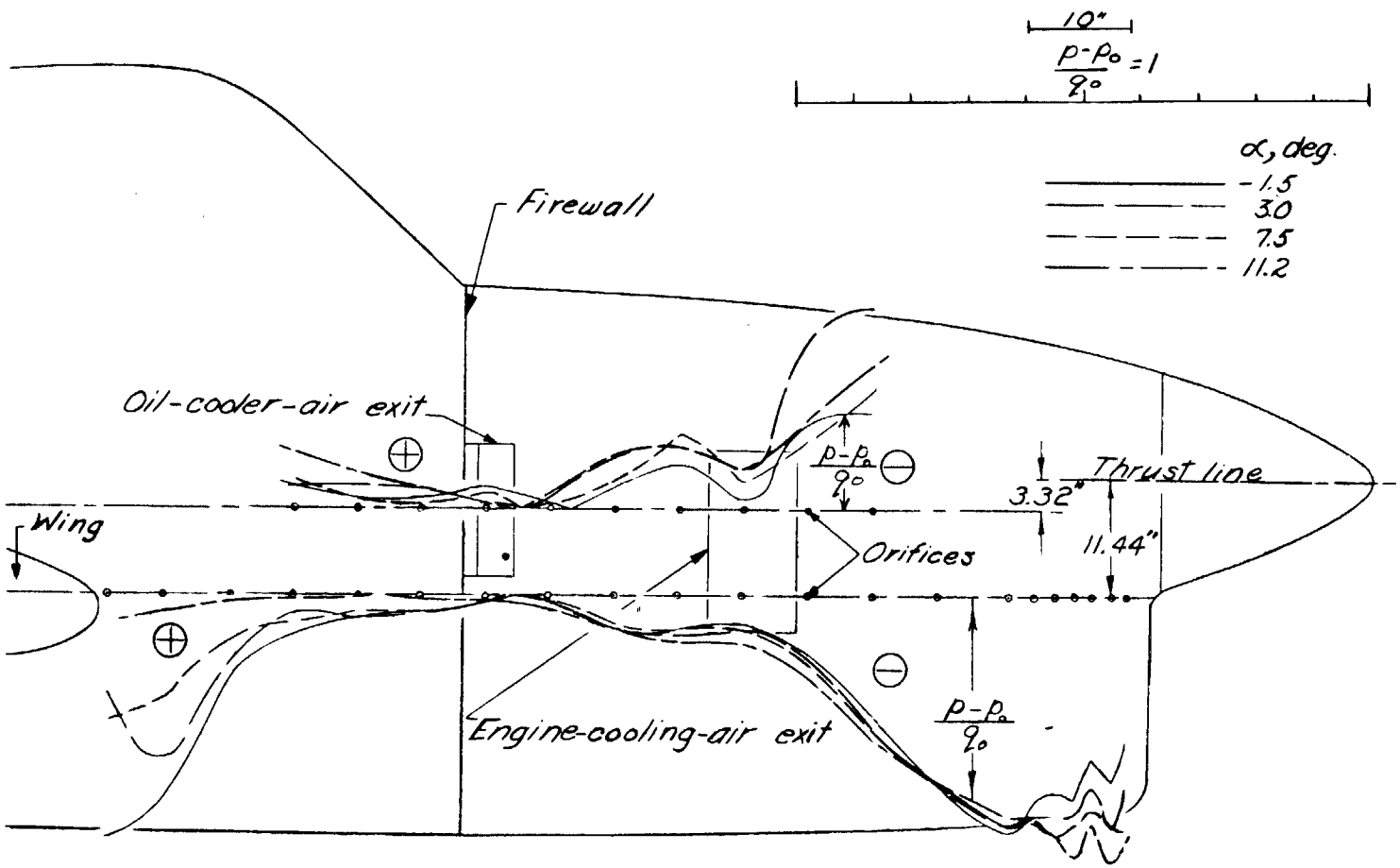

Figure 44.—Pressure distribution along side of cowling. Propeller removed, inlet and exits sealed and faired.

NATIONAL ADVISORY COMMITTEE FOR AERONAUTICS

MR No. L5I12b

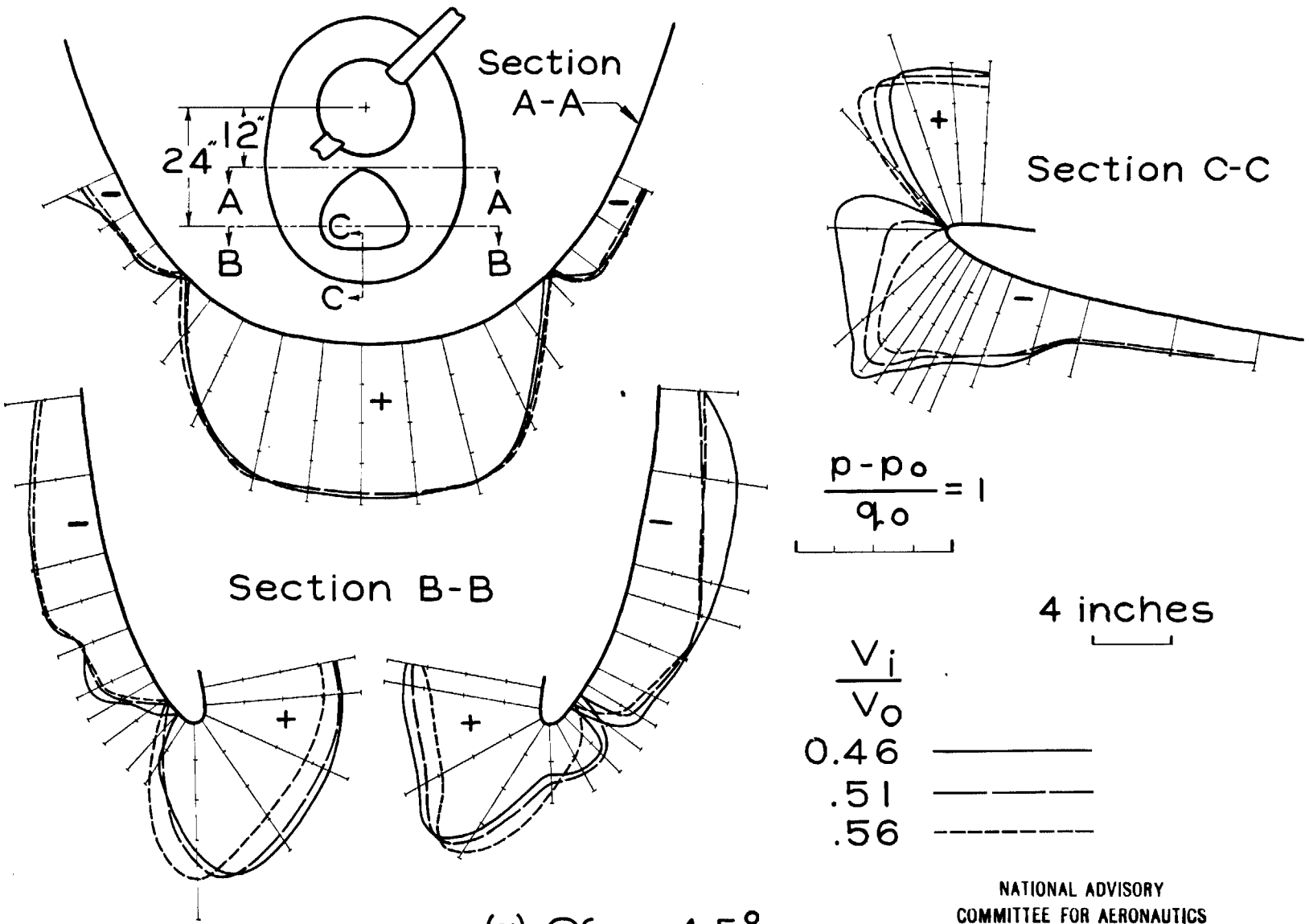

(a) $\alpha = -4.5°$

Figure 45.- Surface pressure distributions at cowl inlet. Propeller removed.

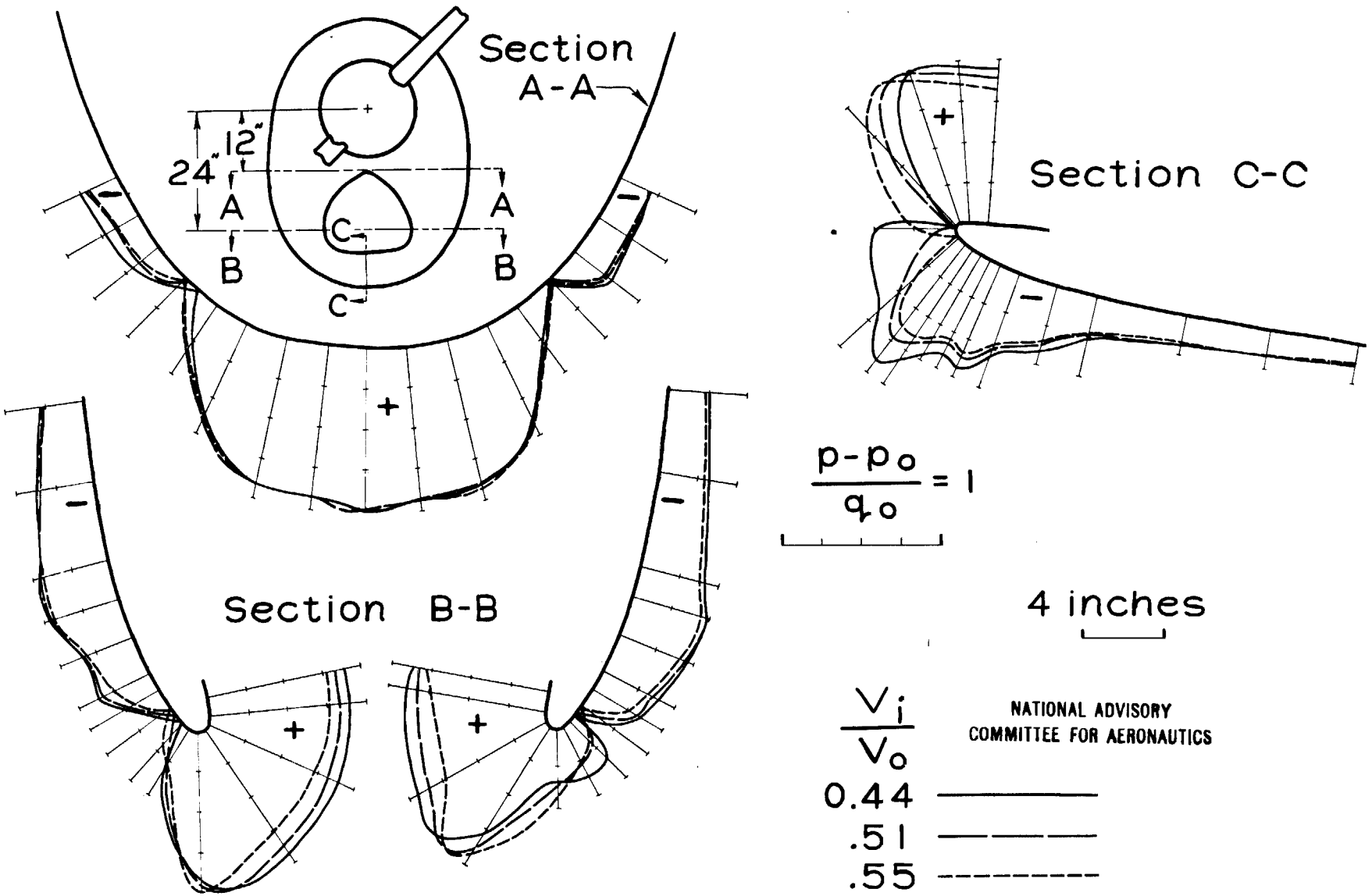

(b) $\alpha = -3°$

Figure 45 .- Continued.

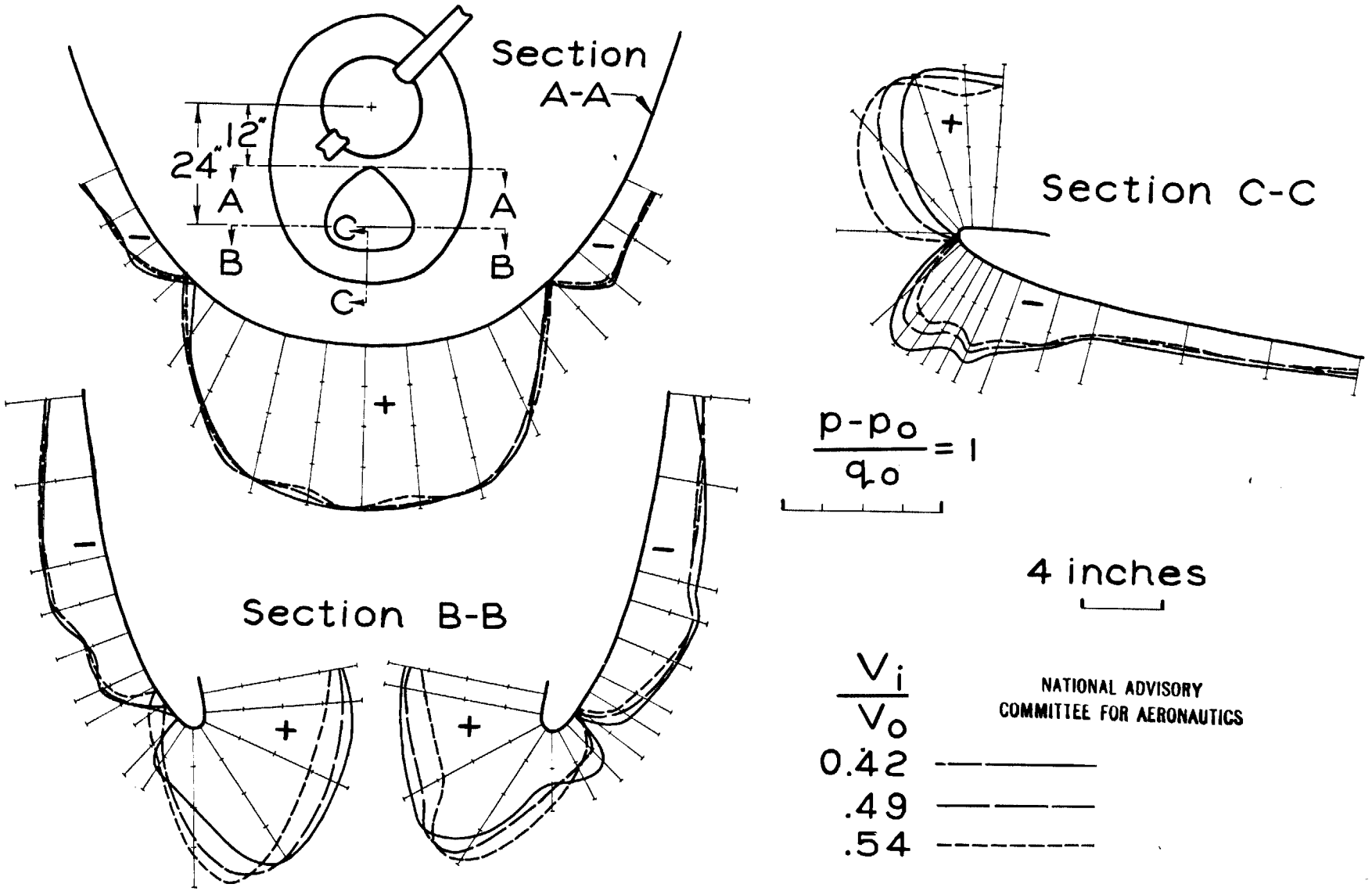

(C) $\alpha = -1.5°$

Figure 45.- Continued.

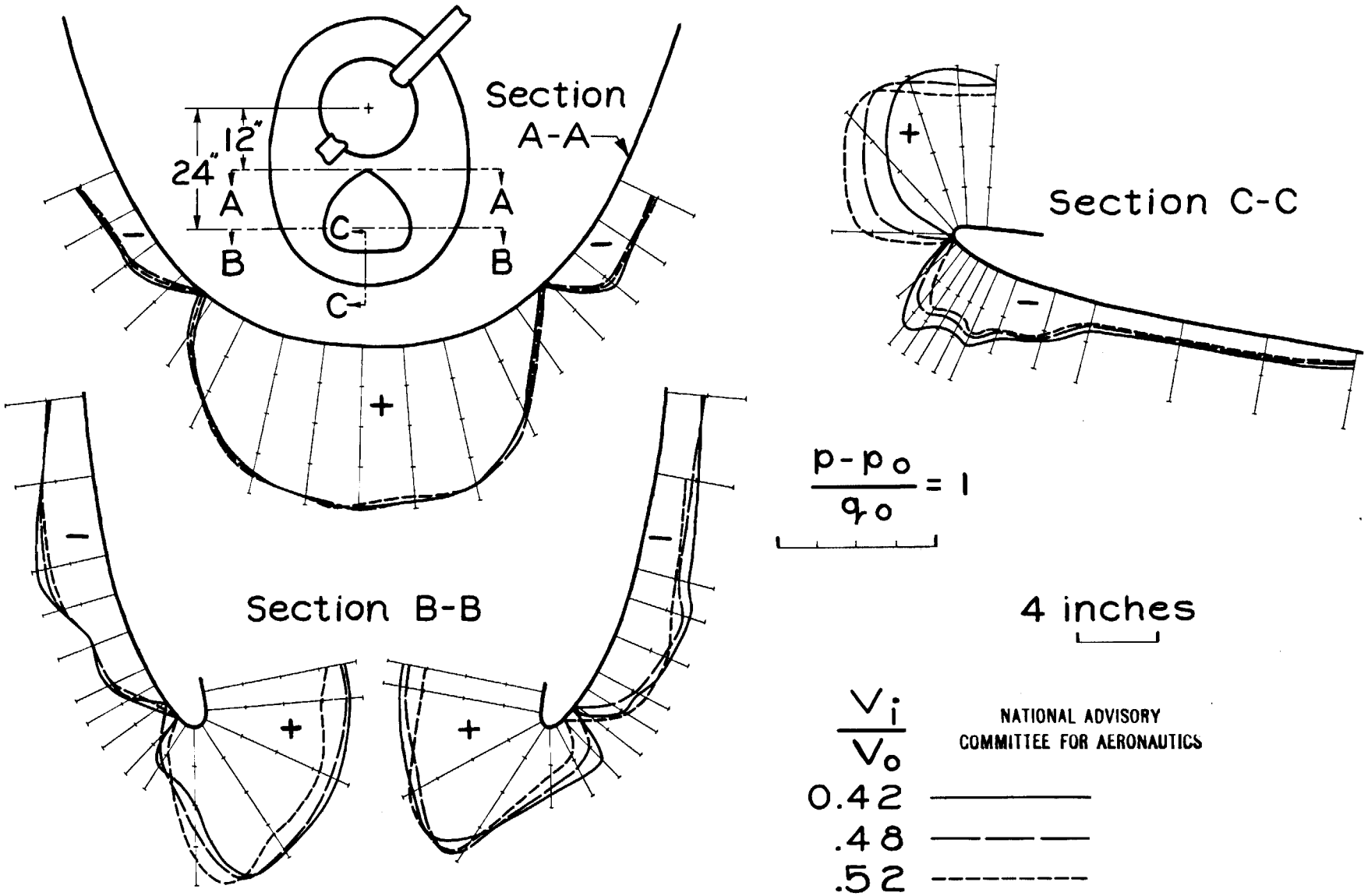

(d) $\alpha = 0°$

Figure 45.- Continued.

MR No. L5I12b

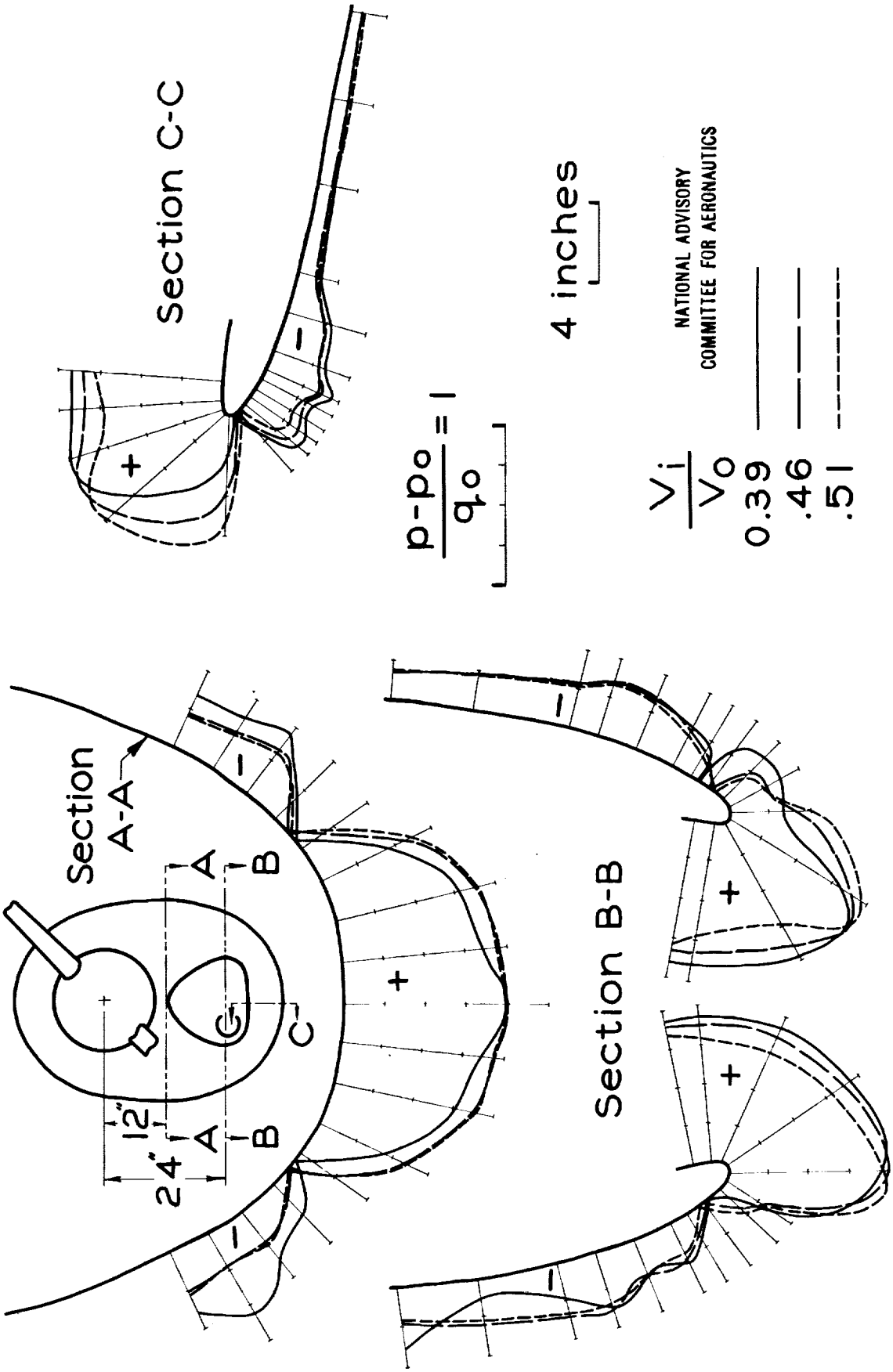

(e) $\alpha = 1.5°$

Figure 45.- Concluded.

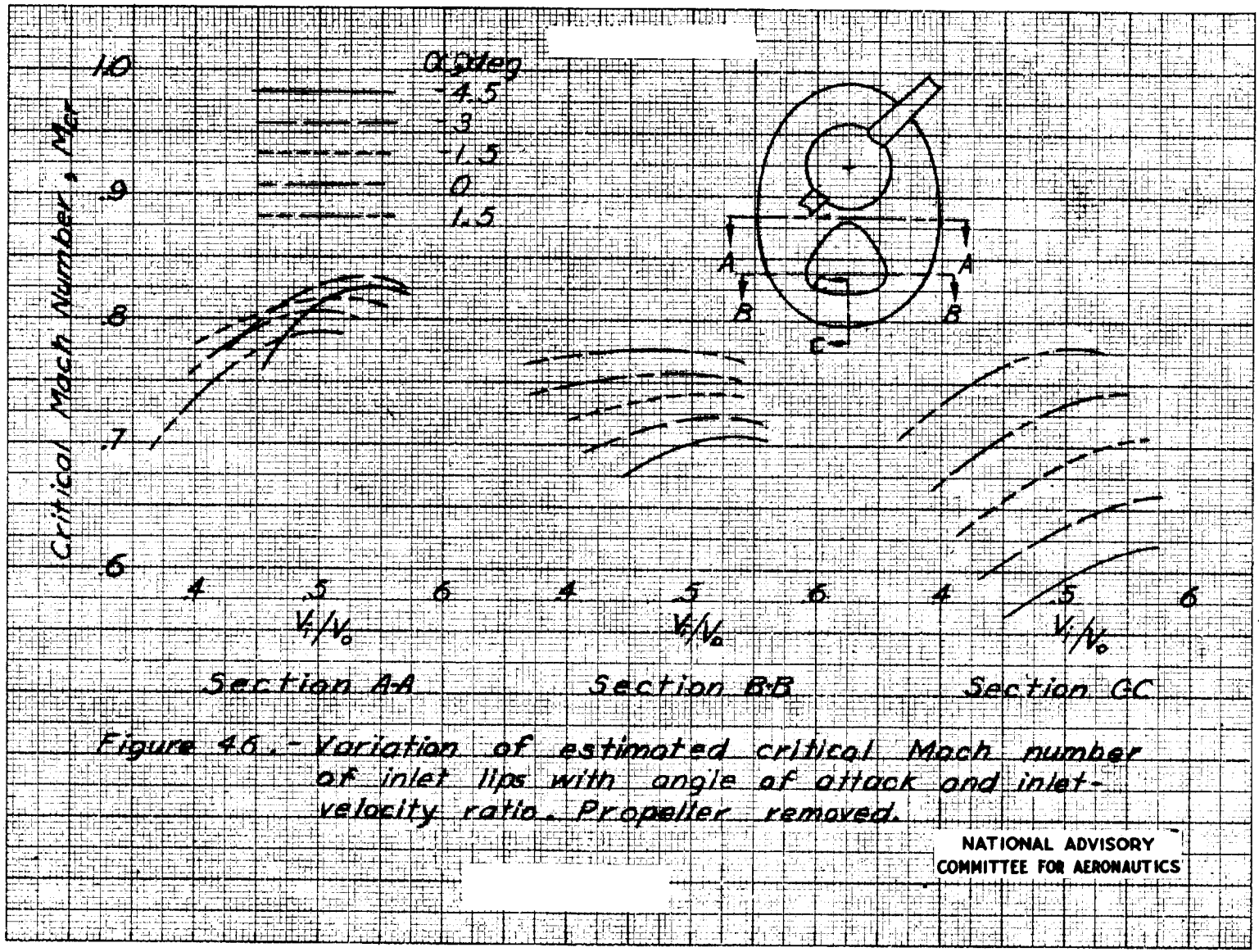

Figure 46.- Variation of estimated critical Mach number of inlet lips with angle of attack and inlet-velocity ratio. Propeller removed.

NATIONAL ADVISORY COMMITTEE FOR AERONAUTICS

NR No. L5I12b

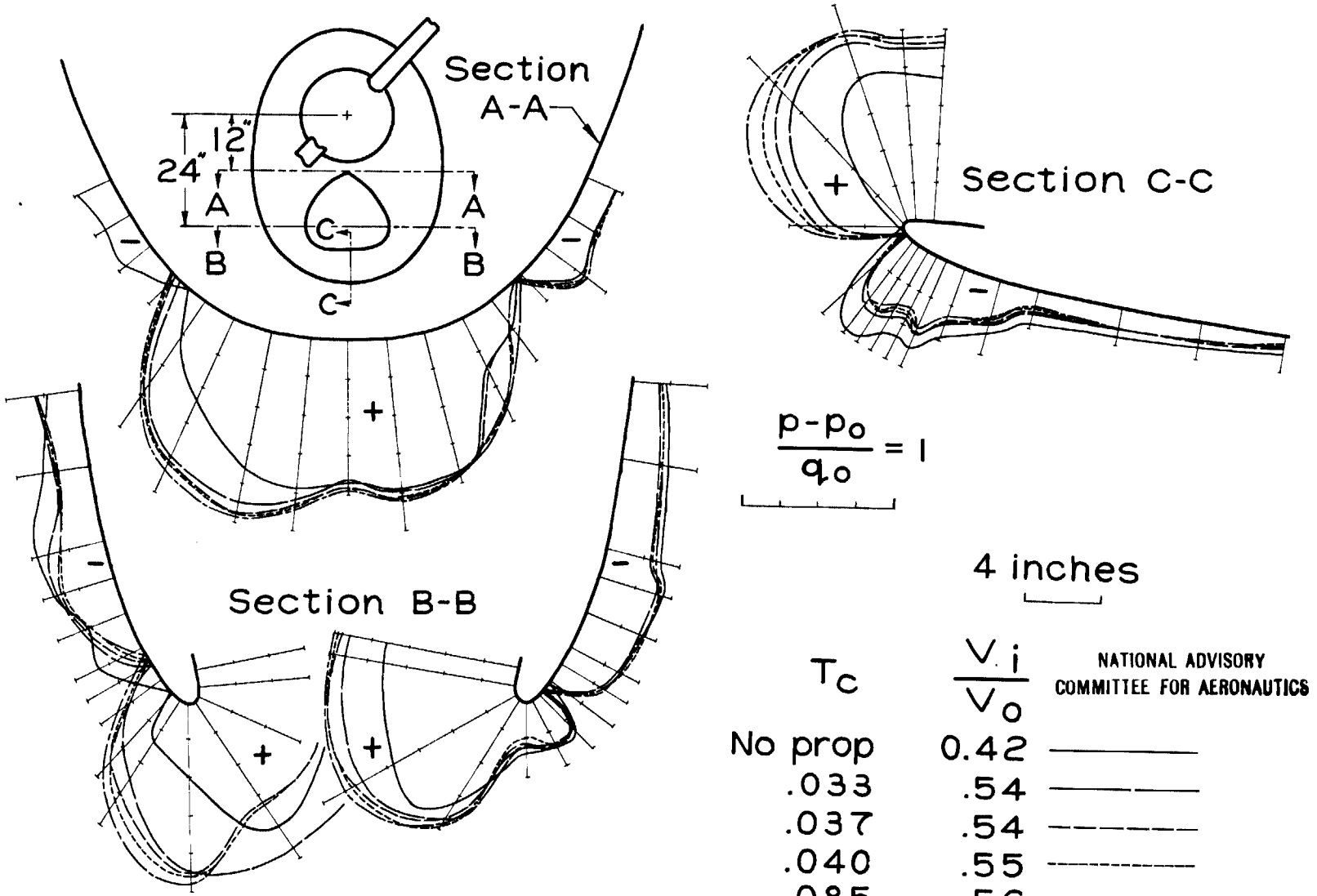

T_c	$\frac{V_i}{V_o}$	
No prop	0.42	———
.033	.54	— — —
.037	.54	— — — —
.040	.55	————
.085	.56	— — — —

Figure 47.- Effect of propeller operation on surface pressures at cowl inlet. $\alpha = -1.5°$. $\beta = 22°$, shutters closed.